1-1-2012

Neuropathologic Role of Inositol (1,4,5)-Trisphosphate Receptor Proteolysis

Catherine M. Kopil
University of Pennsylvania, kopil@mail.med.upenn.edu

Neuropathologic Role of Inositol (1,4,5)-Trisphosphate Receptor Proteolysis

Abstract
Ischemic brain injury represents a major cause of death and disability. Developing targeted therapies for neuroprotection requires increased understanding of the molecular mechanisms of neuronal injury following ischemia. Both disruption of Ca^{2+} homeostasis and pathological activation of proteases are believed to play causal roles in delayed neuronal death after ischemia-reperfusion. Presented here are data supporting a novel role for proteolysis of an intracellular Ca^{2+} release channel, inositol 1,4,5-trisphosphate receptor ($InsP_3R$), in ischemic brain injury. We identified a unique calpain cleavage site in the type 1 $InsP_3R$ ($InsP_3R1$) and utilized a recombinant truncated form of the channel (capn-$InsP_3R1$) to investigate the functional consequences of $InsP_3R1$ proteolysis. Using a combination of single-channel electrophysiology and single-cell Ca^{2+} imaging, we determined that capn-$InsP_3R1$ has $InsP_3$-independent gating and constitutive channel activity. This constitutive channel activity decreased Ca^{2+} content of intracellular stores in Neuro-2A cells by increasing endoplasmic reticulum (ER) Ca^{2+} leak. Additionally, capn-$InsP_3R1$ compromised ER Ca^{2+} buffering capacity in primary cortical cultures, leading to decreased neuronal viability and enhanced sensitivity to excitotoxic injury. Using stereotaxic intracerebral injection of viral vectors, we transduced neurons *in vivo* with capn-$InsP_3R1$ and observed spontaneous degeneration of subpopulations of neurons in the hippocampus. Together, these results reveal a previously unknown role of calpain-cleaved $InsP_3R1$ in disruption of intracellular Ca^{2+} homeostasis and neuronal death. Importantly, we also provide evidence of calpain-mediated proteolysis of $InsP_3R1$ in neurons in the cerebellum after ischemic brain injury. The findings presented here provide the first functional studies of calpain-cleaved $InsP_3R1$, and advance our understanding of the pathological role of the cleaved channel in neurodegeneration. Inhibiting Ca^{2+} release through calpain-cleaved $InsP_3R1$ may emerge as a novel therapeutic strategy for intervention in ischemic brain injury and other neurodegenerative diseases associated with disruption of Ca^{2+} homeostasis.

Degree Type
Dissertation

Degree Name
Doctor of Philosophy (PhD)

Graduate Group
Neuroscience

First Advisor
Robert W. Neumar

Keywords
calcium, calpain, endoplasmic reticulum, inositol (1,4,5)-trisphosphate receptor, ischemia, neuron

NEUROPATHOLOGIC ROLE OF INOSITOL (1,4,5)-TRISPHOSPHATE RECEPTOR PROTEOLYSIS

Catherine M. Kopil

A DISSERTATION

in

Neuroscience

Presented to the Faculties of the University of Pennsylvania

in

Partial Fulfillment of the Requirements for the

Degree of Doctor of Philosophy

2012

SUPERVISOR OF DISSERTATION

Signature _____

Dr. Robert W. Neumar

Associate Professor, Department of Emergency Medicine, School of Medicine

GRADUATE GROUP CHAIRPERSON

*Signature*_____

Dr. Joshua I. Gold, Associate Professor, Department of Neuroscience, School of Medicine

DISSERTATION COMMITTEE

Dr. Kelly Jordan-Sciutto (Chair), Associate Professor, Department of Pathology, School of Dental Medicine

Dr. J. Kevin Foskett, Professor of Physiology, School of Medicine

Dr. David R. Lynch, Professor of Neurology, Children's Hospital of Philadelphia

Dr. Gregory C. Carlson, Assistant Professor of Neuroscience in Psychiatry, School of Medicine

Dr. Grace E. Stutzmann, Assistant Professor of Neuroscience, Rosalind Franklin University of Medicine and Science

ACKNOWLEDGEMENTS

My nearly six years in graduate school have been an immensely rewarding learning experience and I have many people to thank for that. Foremost, thank you to my mentor, Bob Neumar, for his expertise and thoughtful guidance throughout my graduate training. He viewed all of my data equally, whether a failure or success, always challenging me to think of what the next steps should be. For that, I am extremely grateful. Bob's passion for truly translational research in addition to his exceptional ability to craft compelling scientific stories will have a lasting impact on my career.

I would like to thank all members of the Neumar lab, past and present, for sharing in our common research goals. Many thanks to Matt Bevers, Marek Ma, and Michael Paine, my fellow graduate students, who made every scientific disappointment more bearable. Thanks also to the skilled surgeons who enabled my *in vivo* research in cardiac arrest—Lori Ingelton, Javier Urbano, Dongfang Che, and Luchuan Li.

I am tremendously grateful for the rich collaboration I shared with the Foskett lab. Thank you to Kevin Foskett for thinking deeply about my project, being constantly available to discuss data and ideas, and wholly welcoming me into his lab. I am indebted to Horia Vais and King-Ho Cheung for their technical and scientific expertise in electrophysiology, which laid the groundwork for understanding how proteolyzed $InsP_3$ receptors function. Thanks to Jun Yang for teaching me the mysteries of cloning, and to Daniel Mak for his exceedingly helpful explanations and discussion. Thank you to Dustin Shilling, Marioly Muller, and Adam Siebert for making every long day in lab a

pleasure. Further and special thanks to Adam—my confidant, sympathizer, and celebrator—for his counsel on every subject and unconditional support. Adam's endless encouragement and confidence in me has completely transformed my journey through graduate school, and I feel extremely fortunate to have shared this process with him.

I also thank the many other collaborators I have worked with on this project. My thanks and appreciation to Margaret Maronski for providing me with a limitless supply of primary neurons. Thanks also to Shu-Jen Chen and Arbansjit Sandhu for their excellent technical expertise in viral vector generation. To the members of the Jordan-Scuitto lab, particularly Ying Wang, Cagla Akay and Matthew Krey, thank you for the helpful reagents, technical advice, and intellectual input. I am moreover deeply appreciative of the mentorship of Kelly Jordan-Sciutto, which I have enjoyed from the moment I interviewed at Penn. Kelly has helped me grow both scientifically and personally, and I am thankful for her invaluable role in my development.

Thank you to the other members of my thesis committee—Greg Carlson, Dave Lynch, and Beth Stutzmann—their enthusiastic interest in my project and support of my scientific growth have helped make my time in graduate school so productive.

I am also very grateful for the support of the Neuroscience Graduate Group and countless faculty mentors I have met through the program. Together, they have provided me with an incredibly strong foundation in research, scholarship, and teaching.

Thank you to Elizabeth Gould, David Solit, and all my previous scientific mentors and teachers who encouraged me to pursue this path.

Finally, I would like to thank my other friends and family for their constant enthusiasm, understanding, and diversions during my time in graduate school. My

deepest and fullest thank you to my parents, Tom and Carol, and sister, Jenny. Their enduring love, support, and encouragement have always kept me going. I move forward with confidence knowing that they will continue to stand behind me.

Training during my thesis work was supported by American Heart Association grant 0815440D, and National Institutes of Health grant NS071828.

ABSTRACT

NEUROPATHOLOGIC ROLE OF INOSITOL (1,4,5)-TRISPHOSPHATE RECEPTOR PROTEOLYSIS

Catherine M. Kopil

Robert W. Neumar

Ischemic brain injury represents a major cause of death and disability. Developing targeted therapies for neuroprotection requires increased understanding of the molecular mechanisms of neuronal injury following ischemia. Both disruption of Ca^{2+} homeostasis and pathological activation of proteases are believed to play causal roles in delayed neuronal death after ischemia-reperfusion. Presented here are data supporting a novel role for proteolysis of an intracellular Ca^{2+} release channel, inositol 1,4,5-trisphosphate receptor ($InsP_3R$), in ischemic brain injury. We identified a unique calpain cleavage site in the type 1 $InsP_3R$ ($InsP_3R1$) and utilized a recombinant truncated form of the channel (capn-$InsP_3R1$) to investigate the functional consequences of $InsP_3R1$ proteolysis. Using a combination of single-channel electrophysiology and single-cell Ca^{2+} imaging, we determined that capn-$InsP_3R1$ has $InsP_3$-independent gating and constitutive channel activity. This constitutive channel activity decreased Ca^{2+} content of intracellular stores in Neuro-2A cells by increasing endoplasmic reticulum (ER) Ca^{2+} leak. Additionally, capn-$InsP_3R1$ compromised ER Ca^{2+} buffering capacity in primary cortical cultures,

leading to decreased neuronal viability and enhanced sensitivity to excitotoxic injury. Using stereotaxic intracerebral injection of viral vectors, we transduced neurons *in vivo* with capn-InsP_3R1 and observed spontaneous degeneration of subpopulations of neurons in the hippocampus. Together, these results reveal a previously unknown role of calpain-cleaved InsP_3R1 in disruption of intracellular Ca^{2+} homeostasis and neuronal death. Importantly, we also provide evidence of calpain-mediated proteolysis of InsP_3R1 in neurons in the cerebellum after ischemic brain injury. The findings presented here provide the first functional studies of calpain-cleaved InsP_3R1, and advance our understanding of the pathological role of the cleaved channel in neurodegeneration. Inhibiting Ca^{2+} release through calpain-cleaved InsP_3R1 may emerge as a novel therapeutic strategy for intervention in ischemic brain injury and other neurodegenerative diseases associated with disruption of Ca^{2+} homeostasis.

TABLE OF CONTENTS

LIST OF TABLES

CHAPTER 1

LIST OF FIGURES

CHAPTER 1

CHAPTER 2

CHAPTER 3

INTRODUCTION

The long-term goal of this project is to understand the mechanisms of neuronal Ca^{2+} dysregulation that contribute to delayed neuronal death after ischemic brain injury. Ca^{2+} homeostasis in post-ischemic neurons is potentially disrupted by proteolytic modification of Ca^{2+} regulatory proteins. This dissertation focuses on calpain-mediated cleavage of the endoplasmic reticulum (ER) Ca^{2+} release channel inositol (1,4,5)-trisphosphate receptor ($InsP_3R$). Previously published studies and data presented in this dissertation suggest that type 1 $InsP_3R$ ($InsP_3R1$) is a target for proteolysis following ischemia, and that the cleaved channel has dysregulated gating and leaks Ca^{2+} from ER stores. Based on these findings, we hypothesize that calpain proteolysis of $InsP_3R1$ plays a causal role in Ca^{2+} dysregulation and neuronal death following ischemic brain injury. The results presented in this thesis provide fundamental understanding of the mechanisms by which calpain proteolysis of $InsP_3R1$ could cause neurodegeneration through pathological disruption of intracellular Ca^{2+} homeostasis.

Ischemic Brain Injury

Each year, more than 300,000 people in the United States suffer global brain ischemia due to cardiac arrest (Lloyd-Jones et al., 2010), often resulting in death or severe, long-term disability (CDC, 2001). Despite extensive clinical and basic science research in ischemic brain injury, the prognosis for patients remains poor. Treatment for

cardiac arrest targets early reperfusion and restoration of blood flow, as the severity of neurological injury depends on the duration of ischemia. Periods of ischemia that are sufficient to trigger depolarization of neuronal plasma membranes are widely known to activate molecular injury mechanisms leading to neuronal death (Kristian and Siesjo, 1998; Neumar, 2000; Szydlowska and Tymianski, 2010). In global brain ischemia, as occurs with cardiac arrest, ischemia-induced membrane depolarization occurs within 1 or 2 min of cessation of blood flow (Nakashima et al., 1995). Resuscitation and survival after prolonged cardiac arrest is uncommon. Thus, nearly all patients who are successfully resuscitated experience brief to intermediate durations of ischemic depolarization (5 to 30 min) followed by reperfusion (Neumar, 2000). Reperfusion after these durations of global ischemia typically results in initial restoration of adenosine trisphosphate (ATP) synthesis (Sims, 1992) and neuronal membrane repolarization (Silver and Erecinska, 1992). Despite this apparent return of physiological function however, subpopulations of neurons eventually undergo delayed cell death following ischemia-reperfusion.

Interestingly, transient global brain ischemia results in selective neurodegeneration. Vulnerable neuron populations include CA1 pyramidal neurons in hippocampus, Purkinje cells in cerebellum, small and medium spiny neurons in the dorsolateral striatum, and neurons in layers 3 and 5 of cortex (Pulsinelli et al., 1982; Smith et al., 1984; Pulsinelli, 1985; Katz et al., 1995; Yamashima et al., 2003; Hara et al., 2007). Cells outside of these selectively vulnerable areas are usually unaffected by brief durations of ischemia experienced by most cardiac arrest survivors. Within the vulnerable brain regions, neuronal death is delayed hours to days after the initial ischemic

event (Kirino, 1982; Pulsinelli et al., 1982; Kirino et al., 1984; Smith et al., 1984; Yamashima et al., 2003). Therefore, there is a potentially wide therapeutic window for neuroprotective interventions following cardiac arrest and ischemic brain injury.

Identifying the molecular events that cause delayed post-ischemic neuronal death is essential to developing innovative, targeted therapies. However, nearly 3 decades after delayed neuronal death was first documented, the precise mechanisms responsible are not yet fully understood. Impaired Ca^{2+} homeostasis, pathological protease activation, mitochondrial dysfunction, activation of the unfolded protein response, altered gene expression, and inflammation have all been identified as molecular mechanisms of post-ischemic neuronal injury (Kristian and Siesjo, 1998; Fiskum et al., 1999; Neumar, 2000; Paschen and Mengesdorf, 2005; Zipp and Aktas, 2006; Bevers and Neumar, 2008; Szydlowska and Tymianski, 2010). Cross-talk between these pathways has been well established, and may play a critical role in the ultimate execution of cell death following ischemia-reperfusion. Particularly relevant to this dissertation, protease-mediated cleavage of Ca^{2+} regulatory proteins has emerged as a novel mechanism that links pathological activation of proteases to irreversible disruption of neuronal Ca^{2+} homeostasis (Bevers and Neumar, 2008). Proteolytically modified Ca^{2+} channels that become dysregulated following cleavage could represent novel therapeutic targets for reducing neuronal pathology and degeneration after ischemic brain injury.

Disruption of Neuronal Ca^{2+} Homeostasis during Ischemia and Reperfusion

Calcium is a universal intracellular messenger, essential to proper neuronal function and survival. A diverse array of ion channels, buffers, pumps and exchangers

work in concert to allow for dynamic and tight regulation of neuronal Ca^{2+} signaling (Berridge et al., 2000; Berridge et al., 2003). Disruption of these molecular Ca^{2+}-homeostatic mechanisms can serve as a trigger for cell death (Berridge et al., 2000; Berridge et al., 2003; Orrenius et al., 2003; Mattson, 2007; Zhivotovsky and Orrenius, 2011). Brain ischemia and reperfusion dramatically disrupts neuronal Ca^{2+} homeostasis, and there is compelling evidence for a causal role of Ca^{2+} overload in post-ischemic neuronal death.

Ischemic Depolarization

Brain ischemia initiates a number of cellular events that dramatically increase cytoplasmic free Ca^{2+} concentration ($[Ca^{2+}]_i$) in neurons. Loss of blood flow to the brain results in oxygen and glucose deprivation, which depletes neuronal energy stores (Dirnagl et al., 1999). Without ATP, neurons are unable to maintain the electrochemical gradients across their plasma membrane. This ischemic depolarization activates voltage-gated Ca^{2+} channels, leading to Ca^{2+} influx from the extracellular space. Depolarization and elevated presynaptic $[Ca^{2+}]_i$ stimulate release of neurotransmitters, including the excitatory amino acid glutamate. Glutamate, in turn, acts to further increase $[Ca^{2+}]_i$ through activation of its postsynaptic ionotropic and metabotropic receptors (Michaelis, 1998). Glutamate binding to *N*-methyl-D-aspartate (NMDA) receptors enhances neuronal Ca^{2+} influx, where as binding to G-protein coupled receptors releases Ca^{2+} from intracellular stores via $InsP_3$ signaling. In addition to ATP depletion and membrane depolarization, changes in cellular pH and production of reactive oxygen species (ROS) associated with ischemia increase $[Ca^{2+}]_i$ through activation of Ca^{2+}-permeable transient

receptor potential channels (Aarts et al., 2003) and acid-sensing ion channels (Allen and Attwell, 2002; Xiong et al., 2004).

Ischemia also impairs normal cellular mechanisms for removing Ca^{2+} from the cytoplasm. Sustained depolarization and loss of the Na^+ gradient changes the direction of the Na^+/Ca^{2+} exchanger (NCX), transporting Na^+ out of the cell and Ca^{2+} into the cell (Jeffs et al., 2007). Additionally, depleted energy stores during ischemia prevent energy-dependent Ca^{2+} pumps, located on intracellular stores and the plasma membrane, from removing Ca^{2+} from the cytoplasm. In global ischemia, these aberrant Ca^{2+} signaling events and the resulting elevation in $[Ca^{2+}]_i$ can occur to varying degrees in all neurons throughout the brain.

Changes in $[Ca^{2+}]_i$ with Ischemia-Reperfusion

In selectively vulnerable neurons, ischemia-induced disruption of neuronal Ca^{2+} homeostasis generates a 100- to 1,000-fold transient increase in $[Ca^{2+}]_i$. Intracellular microelectrode measurements from CA1 hippocampal neurons *in vivo* have demonstrated an increase in $[Ca^{2+}]_i$ from a baseline of 60-90 nM to a peak of 20-200 μM with 8 min of low-flow ischemia (Silver and Erecinska, 1990; Erecinska and Silver, 1992; Silver and Erecinska, 1992). Interestingly, measurements from CA3 hippocampal neurons in the same animals revealed changes in $[Ca^{2+}]_i$ that were much smaller (mean peak ~3 μM) than those observed in CA1 neurons (Erecinska and Silver, 1992; Silver and Erecinska, 1992). Increases in neuronal $[Ca^{2+}]_i$ during ischemia correspond to a modest, but significant decrease in extracellular $[Ca^{2+}]$ ($[Ca^{2+}]_e$), suggesting that Ca^{2+} influx from the

extracellular space is primarily responsible for the initial rise in $[Ca^{2+}]_i$ (Nicholson et al., 1977; Hansen, 1985; Silver and Erecinska, 1992).

With restoration of blood flow, energy stores are replenished (Sims, 1992) and neurons are able to repolarize (Silver and Erecinska, 1992). As a result, physiological Ca^{2+} homeostasis is restored in neurons. Specifically, $[Ca^{2+}]_i$ returns to pre-ischemic levels within 20 min and $[Ca^{2+}]_e$ reaches baseline levels with longer periods of reperfusion (Silver and Erecinska, 1990, 1992). The repolarization of neuronal membranes and reinstatement of normal $[Ca^{2+}]_i$ following reperfusion proves that vulnerable neurons are not dead immediately following ischemic brain injury. This highlights the truly delayed nature of post-ischemic neurodegeneration, and suggests that secondary damage is responsible for neuronal death.

A secondary rise in $[Ca^{2+}]_i$ occurs selectively in neurons that undergo delayed cell death after ischemia. Microelectrode measurements from CA1 hippocampal neurons indicate that a second rise in $[Ca^{2+}]_i$ begins as early as 2 h following ischemia-reperfusion (Silver and Erecinska, 1992). More crude measurements of total tissue $[Ca^{2+}]$ or ultrastructural localization of neuronal Ca^{2+} deposits reveal significant accumulation of Ca^{2+} hours to days after ischemia, depending on the injury severity and animal model (Simon et al., 1984; Deshpande et al., 1987; Kumar et al., 1987; Martins et al., 1988). These secondary rises in $[Ca^{2+}]_i$ are specific to selectively vulnerable neurons and do not occur in CA3 pyramidal cells or other neuronal populations that exhibit limited signs of injury following ischemia (Martins et al., 1988; Silver and Erecinska, 1992). Importantly, the secondary rise in $[Ca^{2+}]_i$ and intracellular accumulation of Ca^{2+} following ischemia-reperfusion consistently precede histological evidence of

neurodegeneration. This suggests that delayed, secondary elevation of $[Ca^{2+}]_i$ may signal or initiate neuronal cell death. In contrast to the initial, reversible increase in $[Ca^{2+}]_i$ following ischemia, which is predominately related to Ca^{2+} influx from the extracellular space, the source of the secondary increase in neuronal $[Ca^{2+}]_i$ is unknown.

How might delayed, secondary rises in $[Ca^{2+}]_i$ lead to execution of neuronal death? Sustained elevations in $[Ca^{2+}]_i$ could exert adverse effects by acting directly or indirectly on numerous cell death pathways. For example, Ca^{2+} could trigger delayed post-ischemic neurodegeneration through oxidative stress and mitochondrial dysfunction, or by pathological activation of phosopholipases, endonucleases, and proteases (Kristian and Siesjo, 1998; Neumar, 2000; Szydlowska and Tymianski, 2010). Ca^{2+}-dependent activation of cytoplasmic calpain proteases in particular provides a potentially important feed-forward mechanism for executing cell death. Calpains have been shown to cleave a number of Ca^{2+} regulatory proteins following ischemia, leading to altered substrate function (Bevers and Neumar, 2008; Vosler et al., 2008). Dysfunction of Ca^{2+} regulatory proteins mediated by calpain proteolysis likely contributes to the delayed, secondary rise in $[Ca^{2+}]_i$, and could lead to further activation of calpains and eventual necrotic cell death.

Alterations in $[Ca^{2+}]$ within Intracellular Organelles During Ischemia-Reperfusion

Mitochondria and the ER play critical roles in neuronal Ca^{2+} homeostasis (Berridge et al., 2000; Berridge et al., 2003; Gleichmann and Mattson, 2011; Stutzmann and Mattson, 2011). Not surprisingly, ischemia-reperfusion dramatically alters Ca^{2+} uptake and release from these intracellular organelles. Dysfunction of normal Ca^{2+}

signaling from mitochondria and the ER is likely an important component of the dynamic and pathological changes in $[Ca^{2+}]_i$ following ischemia.

Neuronal mitochondria can serve as a sink for pathological Ca^{2+} overload (Nicholls, 1985). Micromolar $[Ca^{2+}]$ in the cytoplasm during ischemia provides optimal conditions for mitochondrial Ca^{2+} uptake through the mitochondrial uniporter (Colegrove et al., 2000; Collins et al., 2001). Data from ischemic brain tissue reveal a transient rise in mitochondrial $[Ca^{2+}]$ ($[Ca^{2+}]_m$) within 10 to 20 min of reperfusion (Dux et al., 1987; Zaidan and Sims, 1994)). The timing of the increased $[Ca^{2+}]_m$ corresponds to the decrease in $[Ca^{2+}]_i$ immediately following reperfusion, suggesting that mitochondria sequester Ca^{2+} from the cytoplasm after ischemia. $[Ca^{2+}]_m$ also returns to baseline after longer periods of reperfusion (Simon et al., 1984; Dux et al., 1987; Zaidan and Sims, 1994) and normal cellular metabolism is restored to neurons (Arai et al., 1986). Similar to temporal perturbations in $[Ca^{2+}]_i$ described above, delayed secondary increases in $[Ca^{2+}]_m$ have been observed in neurons that go on to die after ischemia (Dux et al., 1987; Zaidan and Sims, 1994). Although the time course of the secondary increase in $[Ca^{2+}]_m$ is variable depending on the model and severity of injury, it reliably precedes histological evidence of neuronal death. Excessive accumulation of Ca^{2+} in the mitochondrial matrix can impair ATP synthesis, increase ROS production, alter mitochondrial membrane permeability, and cause the release of pro-apoptotic factors (Starkov et al., 2004). Many of these pathological consequences of mitochondrial Ca^{2+} overload are involved in the execution of cell death following ischemia-reperfusion (Neumar, 2000; Starkov et al., 2004).

Evidence for the role of disrupted ER Ca^{2+} homeostasis in post-ischemic neuronal death primarily comes from studies examining ER Ca^{2+} uptake and release in ischemic tissue or *in vitro* models. Although not well characterized, there are most likely two distinct phases of ER Ca^{2+} regulation following ischemia—early accumulation and subsequent release (Chen et al., 2008). With restoration of energy stores following early reperfusion, the ER likely sequesters cytoplasmic Ca^{2+} through activation of the sacroplasmic/endoplasmic reticulum Ca^{2+}-ATPase (SERCA) pump, contributing to the return to resting $[Ca^{2+}]_i$. Indeed, data support the idea of increased ER Ca^{2+} filling at early time points after ischemia *in vitro* (Chen et al., 2008; Sirabella et al., 2009). At later time points following ischemia-reperfusion, Ca^{2+} release from the ER may critically contribute to neuronal injury and Ca^{2+}-mediated death. This hypothesis is supported by evidence that: 1) ER Ca^{2+} release significantly contributes to elevated $[Ca^{2+}]_i$ in *in vitro* models of ischemia (Mitani et al., 1993; Pisani et al., 2000), 2) preventing Ca^{2+} release through ER channels is neuroprotective *in vivo* (Wei and Perry, 1996; Rao et al., 2000), and 3) neuronal ER Ca^{2+} stores *in vivo* are relatively depleted at later time points following ischemia-reperfusion (Kohno et al., 1997; Xing et al., 2004).

While disruption of mitochondrial and ER Ca^{2+} homeostasis can both independently contribute to neuronal injury following ischemia, coupling of Ca^{2+} signaling between these organelles suggests that these pathological pathways also overlap. Close proximity of mitochondria to the ER provides a privileged environment for high $[Ca^{2+}]$ microdomains (Csordas et al., 2006; Csordas et al., 2010). The physical and functional connection between mitochondria and the ER may make mitochondria more prone to Ca^{2+} overload (Pinton et al., 2008). This effect may potentially explain the

secondary rise in $[Ca^{2+}]_m$ following ischemia-reperfusion, further emphasizing the role of aberrant ER Ca^{2+} release in post-ischemic cell death.

Neuroprotective Strategies Targeting $[Ca^{2+}]_i$ Following Ischemia

Increased understanding of disrupted neuronal Ca^{2+} homeostasis has inspired development of neuroprotective pharmacologic strategies for intervention following ischemic brain injury (Sahota and Savitz, 2011). The majority of these treatments have targeted plasma membrane Ca^{2+} regulatory proteins in an effort to prevent secondary neuronal Ca^{2+} overload. Unfortunately, despite promising results in animal models, all clinical trials of therapeutic agents have proven ineffective in attenuating post-ischemic neuronal death (Roine et al., 1990; Brain Resuscitation Clinical Trial II Study Group, 1991; Calle et al., 1993; Auriel and Bornstein, 2010; Mongardon et al., 2011; Sahota and Savitz, 2011). Thus, there is an obvious need for improved therapies and molecular targets for intervention following ischemia-reperfusion. Based on the data presented above, we propose that targeting pathological ER Ca^{2+} release may provide an effective strategy for neuroprotection by preventing both ER Ca^{2+} depletion and secondary $[Ca^{2+}]_i$ and $[Ca^{2+}]_m$ overload in post-ischemic neurons.

Role of Calpain in Post-ischemic Neuronal Death

One of the downstream effects of elevated $[Ca^{2+}]_i$ in ischemic brain tissue is pathological activation of proteases (Kristian and Siesjo, 1998; Neumar, 2000; Szydlowska and Tymianski, 2010). Proteolysis is an important component of cell death pathways and substantial evidence exists to support the role of protease activation in

post-ischemic neurodegeneration (Bevers and Neumar, 2008; Nakka et al., 2008). Here, we will explore the role of the Ca^{2+}-dependent calpain family of proteases in mediating neuronal death after ischemia-reperfusion.

Calpain Activation and Function

Calpains—*cal*cium-dependent proteases with pa*pain*-like activity—are cysteine proteases typically thought to be directly and reversibly activated by Ca^{2+}. There are 15 identified members of the calpain family of proteases, a subset of which are expressed in brain (Bevers and Neumar, 2008). Of the calpain isoforms found in the brain, the calpain catalytic subunit isoforms 1 and 2 are the most ubiquitous and best characterized. These cytoplasmic calpains were initially named μ- and m-calpain respectively based on their [Ca^{2+}] requirements for activation determined from *in vitro* assays (Goll et al., 2003). Physiologically, the difference in Ca^{2+} sensitivity of these isoforms is likely served by different subcellular localizations of calpains 1 and 2. Traditionally, calpain 1 is believed to be diffuse throughout the cytoplasm and often associated with cytoskeletal elements (Goll et al., 2003; Bevers and Neumar, 2008), whereas calpain 2 has predominately been localized to membranes and sites of Ca^{2+} entry into the cytoplasm (Hood et al., 2003; Hood et al., 2004; Samanta et al., 2007; Leloup et al., 2010). Calpain activity is regulated by its endogenous inhibitor, calpastatin (Goll et al., 2003). Under normal conditions, the calpain-calpastatin system plays an important role in physiological neuronal processes including signal transduction, neurite growth, and synaptic remodeling (Goll et al., 2003; Bevers and Neumar, 2008).

Calpain proteolysis of substrates is limited and site-specific. There have been substantial efforts to determine or predict primary amino acid sequences preferentially targeted by calpain however, no consensus sequences have been identified (Tompa et al., 2004; Cuerrier et al., 2005). More likely, calpain cleaves substrates via recognition of secondary or tertiary protein structure, making it difficult to identify *de novo* calpain substrates and their precise cleavage sites. Directed calpain proteolysis generally alters rather than eliminates substrate function. Unlike many other proteases, calpain proteolysis does not strictly lead to substrate degradation, and instead can mediate complex physiological and pathological signaling processes.

Role of Calpain in Ischemic Brain Injury

Data collected over the past 2 decades have linked both the initiation and execution of ischemic cell death *in vivo* to the calpain family of proteases. As increased $[Ca^{2+}]_i$ directly activates calpain, temporal evidence of calpain activation in ischemic brain tissue closely mirrors that of the bimodal rises in $[Ca^{2+}]_i$ (Saido et al., 1993; Roberts-Lewis et al., 1994; Neumar et al., 1996; Yamashima et al., 1996; Bartus et al., 1998; Neumar et al., 2001; Zhang et al., 2002; Yamashima et al., 2003). Importantly, pathological calpain activity identified in these studies was localized to selectively vulnerable neuron populations. Pharmacologic inhibition of calpains before (Lee et al., 1991; Rami and Krieglstein, 1993; Yokota et al., 1999) or after global brain ischemia (Li et al., 1998; Frederick et al., 2008) has been effective in attenuating post-ischemic neuronal death. Additionally, genetic approaches to calpain inhibition, either by overexpression of calpastatin (Higuchi et al., 2005) or knockdown of specific calpain

isoforms (Bevers et al., 2010), have been neuroprotective in models of excitotoxic and ischemic brain injury. Together, these data suggest that calpain plays a causal role in mediating neuronal death following ischemia-reperfusion.

Calpain Proteolysis of Ca^{2+} Regulatory Proteins

Due to the numerous and diverse cellular substrates for proteolysis, there are potentially multiple mechanisms by which calpain can initiate or execute neuronal death following ischemia-reperfusion. One particularly compelling model for calpain-mediated cell death in ischemic brain injury is calpain proteolysis of Ca^{2+} regulatory proteins (Bevers and Neumar, 2008). As calpain proteolysis typically alters substrate function, cleavage of Ca^{2+} regulatory proteins provides a unique pathway through which calpain may increase $[Ca^{2+}]_i$, thereby further increasing calpain activity.

A number of different Ca^{2+} regulatory proteins are known substrates for calpain (Table 1.1). In most instances, the functional consequences of proteolysis on substrate function have been investigated. Cleavage of some of these substrates has been observed in ischemic brain tissue, whereas others are only putative targets for calpain-mediated proteolysis following ischemia-reperfusion.

I. Ca^{2+} extrusion mechanisms targeted by calpain

Calpain can cleave several Ca^{2+} pumps and transporters. Evidence from excitotoxic and ischemic injury models provide evidence of calpain cleavage of both the plasma membrane Ca^{2+}-ATPase (PMCA) (Pottorf et al., 2006; Ferragamo et al., 2009) and SERCA (Parsons et al., 1999; French et al., 2006). Proteolysis of PMCA and SERCA lead to a loss of Ca^{2+} pump activity and accumulation of Ca^{2+} in the cytoplasm.

Similarly, calpain proteolysis of NCX eliminates Ca^{2+} transport function (Bano et al., 2005; Samanta et al., 2009), which increases $[Ca^{2+}]_i$ in post-ischemic neurons (Bano et al., 2005). Proteolysis of these substrates may contribute individually or in concert to the delayed secondary rise in $[Ca^{2+}]_i$ following ischemia-reperfusion.

II. Ca^{2+}-permeable ion channels cleaved by calpain

Two ion channels on the plasma membrane are known calpain substrates—L-type Ca^{2+} channel and NMDA receptor. Proteolysis of L-type Ca^{2+} channels increases channel open probability (P_o), likely increasing $[Ca^{2+}]_i$ (De Jongh et al., 1994; Wei et al., 1994; Hell et al., 1996). The NR2 subunit of NMDA receptors is the specific substrate for calpain and has been shown to be cleaved following excitotoxic injury (Guttmann et al., 2002; Simpkins et al., 2003). The functional consequence of NMDA receptor proteolysis is unclear, although the cleaved forms of the channel remain on the plasma membrane and may contribute to excitotoxicity through altered electrophysiological properties or interactions with signaling molecules (Simpkins et al., 2003; Dong et al., 2006).

Additionally, calpain cleaves two ER Ca^{2+} release channels—Ryanodine receptor (RyR) and $InsP_3R1$. Calpain-mediated proteolysis of RyR impairs channel inactivation and increases P_o (Rardon et al., 1990), which may increase $[Ca^{2+}]_i$. Calpain cleavage of $InsP_3R1$ has been observed *in vitro* and *in vivo* (Magnusson et al., 1993; Wojcikiewicz and Oberdorf, 1996; Igwe and Filla, 1997; Diaz and Bourguignon, 2000). However, the functional consequences of calpain proteolysis on electrophysiological properties of $InsP_3R1$ and the potential impact on $[Ca^{2+}]_i$ following ischemia-reperfusion were previously unknown.

Dysfunctional Ca^{2+}-permeable ion channels generated by calpain proteolysis may be central players in disruption of neuronal Ca^{2+} homeostasis following ischemia. Unfortunately, blocking Ca^{2+} entry through voltage-gated Ca^{2+} channels and NMDA receptors has not been a clinically effective strategy for neuroprotection in ischemic brain injury (Mongardon et al., 2011; Sahota and Savitz, 2011). Instead, blocking aberrant ER Ca^{2+} release following ischemia-reperfusion may be an appealing target for future interventional strategies.

Role of $InsP_3R1$ Proteolysis in Ischemic Brain Injury

Prior to the investigations presented in this dissertation, the significance of calpain proteolysis of $InsP_3R1$ was unclear and the role of $InsP_3R$-mediated Ca^{2+} signaling in post-ischemic neuronal death was incompletely understood. We hypothesized that both are potentially important factors in either the initiation or execution of neuronal death following ischemia-reperfusion. In spite of our previously limited understanding of the role of $InsP_3R$ in ischemic brain injury, the molecular structure and physiological functions of $InsP_3R$ have been well studied. Foskett et al. (2007) provides an excellent and extensive review of the $InsP_3R$ Ca^{2+} release channel. The overview presented here provides a brief survey of the literature particularly relevant to this thesis.

Structure and Gating of $InsP_3R$

$InsP_3R$ is a ubiquitous intracellular Ca^{2+} release channel predominately located on the ER membrane. The large $InsP_3R$ protein (2749 amino acids in rat) includes an amino-terminal $InsP_3$ ligand-binding domain, a large, central coupling (modulatory) domain, and 6 transmembrane domains in the carboxyl-terminal region (Figure 1.1)

(Taylor et al., 2004; Bezprozvanny, 2005; Foskett et al., 2007). Within the transmembrane domains, helices 5 and 6 form the basic pore structure of the ion channel and confer selectivity (Taylor et al., 2004; Foskett et al., 2007). $InsP_3Rs$ function as tetrameric channels. The carboxyl-terminal portion of $InsP_3R$ is important for both subunit oligomerization and localization of the channel to the ER membrane (Sayers et al., 1997; Galvan et al., 1999; Parker et al., 2004).

$InsP_3R$ activity is regulated by a number of different ligands, the most important of which are $InsP_3$ and Ca^{2+} (Foskett et al., 2007). Both of these ligands are required for appreciable channel activity, making $InsP_3R$ a molecular coincidence detector. $InsP_3$, a second messenger generated by phospholipase C hydrolysis of phosphatidylinositol 4,5-bisphosphate, connects activation of G_q-coupled receptors on the plasma membrane with $InsP_3R$ channel opening (Streb et al., 1983). $InsP_3$ binding to the ligand-binding domain of $InsP_3R$ is important for both channel gating and modulating $InsP_3R$ sensitivity to its other principal ligand, Ca^{2+} (Foskett et al., 2007). Data suggest that Ca^{2+} binds to $InsP_3R$ at multiple sites with different affinities to regulate $InsP_3$-dependent Ca^{2+} activation, and $InsP_3$-dependent and independent Ca^{2+} inhibition, although the precise binding sites are unclear (Foskett et al., 2010). Ca^{2+} regulation of $InsP_3R$ is biphasic, with non-optimal $[Ca^{2+}]_i$ leading to decreased channel P_o. This modulation by $InsP_3R$'s physiologically permeant ion provides important positive and negative feedback for $InsP_3R$-mediated Ca^{2+} signaling (Foskett et al., 2007; Foskett et al., 2010). Upon binding of optimal concentrations of both ligands, the $InsP_3R$ channel gate opens and Ca^{2+} diffuses down its concentration gradient into the cytoplasm.

The transduction mechanism by which $InsP_3$ and Ca^{2+} binding opens the gate is poorly understood. Initial studies suggested that $InsP_3$ binding induces a conformational change in the channel, which opens the gate (Mignery and Sudhof, 1990). More recent evidence has proposed that an interaction between the ligand-binding domain and carboxyl-terminus of $InsP_3R$ mechanically transmits the signal for gating (Schug and Joseph, 2006; Chan et al., 2010; Yamazaki et al., 2010). Interestingly however, deletion of large portions of the amino-terminus of $InsP_3R$ upstream of the transmembrane domains or through the fourth transmembrane helix generates a channel with constitutive activity (Ramos-Franco et al., 1999; Nakayama et al., 2004). This suggests a different or perhaps more complex model of gating and channel regulation than initially predicted.

Expression and Function of $InsP_3R$ in Neurons

There are 3 distinct isoforms of $InsP_3Rs$, types 1, 2 and 3 (Foskett et al., 2007). Of these, $InsP_3R1$ is the most ubiquitous and abundant isoform expressed in the brain (Furuichi et al., 1993; Sharp et al., 1993). Immunohistochemical labeling of brain tissue reveals heterogeneous expression patterns of $InsP_3R$ across neuronal populations and within cells. Interestingly, the level of $InsP_3R$ expression in neurons positively correlates with vulnerability to ischemic injury. For example, within hippocampus, $InsP_3R$ expression is relatively high in CA1 pyramidal neurons and low in both CA3 pyramidal neurons and granule cells in the dentate gyrus (Sharp et al., 1993). Similarly, $InsP_3R$ expression in cerebellum is predominately localized to Purkinje neurons (Sharp et al., 1993). This expression pattern suggests a possible role for $InsP_3R$-mediated Ca^{2+}

signaling in disruption of Ca^{2+} homeostasis and neuronal injury following ischemia-reperfusion.

As the ER is the major storage organelle for Ca^{2+}, $InsP_3Rs$ are vital to intracellular Ca^{2+} signaling in neurons (Stutzmann and Mattson, 2011). Ca^{2+} release through $InsP_3R$ has diverse temporal and spatial signaling properties. Stimulation of $InsP_3R$ can evoke small, localized elevations in $[Ca^{2+}]_i$ through activation of a only a few channels, or larger waves of increased $[Ca^{2+}]_i$ that propagate through the cell by activating clusters of neighboring $InsP_3Rs$ (Foskett et al., 2007). Differential expression patterns of $InsP_3R$ in somatic, dendritic, and synaptic neuronal compartments leads to even more complex Ca^{2+} signaling patterns that play important roles in neuronal excitability, gene transcription, and synaptic plasticity (Bardo et al., 2006; Stutzmann and Mattson, 2011).

$InsP_3R$-mediated Ca^{2+} Signaling in Neuropathology

In addition to their fundamental importance to neuronal physiology, $InsP_3Rs$ also contribute to pathological Ca^{2+} signaling and neurodegeneration (Verkhratsky and Toescu, 2003; Foskett, 2010). Reports that cells deficient in $InsP_3Rs$ were resistant to apoptosis (Jayaraman and Marks, 1997; Sugawara et al., 1997) initially suggested a role for $InsP_3R$-mediated Ca^{2+} signaling in cell death. Subsequent studies have shown that allosteric modulation of $InsP_3R$ channel function induces aberrant neuronal Ca^{2+} signaling in a variety of neurodegenerative diseases, including Alzheimer's disease (Leissring et al., 1999a; Leissring et al., 1999b; Stutzmann et al., 2004; Cheung et al., 2008; Cheung et al., 2010), Huntington's disease (Tang et al., 2003; Tang et al., 2005;

Higo et al., 2010), spinocerebellar ataxias (Liu et al., 2009), and ischemia (Boehning et al., 2003; Beresewicz et al., 2006).

In models of ischemic brain injury, data suggest additional changes in $InsP_3R$ function that appear unrelated to the characterized allosteric modulation of the channel. Specifically, decreased $InsP_3$ binding (Jorgensen et al., 1991; Nagasawa and Kogure, 1991; Dahl et al., 2000) and decreased $InsP_3$-induced Ca^{2+} release (Nagata et al., 1999) have been observed *in vivo* following ischemia-reperfusion. These changes are not associated with a decrease in $InsP_3R$ protein levels (Dahl et al., 2000). Proteolytic cleavage of the cytosolic amino-terminus of $InsP_3R$ could explain these observations.

Proteolysis of $InsP_3R1$

$InsP_3R1$ is a target for proteolysis by both caspase and calpain cysteine proteases. Cleavage of $InsP_3R1$ by either protease generates a stable ~95 kDa carboxyl-terminal fragment that contains the transmembrane domains and channel pore. While the functional effects of $InsP_3R1$ proteolysis by calpain were previously unexamined, studies of the caspase-cleaved form of the channel provided some initial insights.

Caspase-3 cleaves $InsP_3R1$ at a highly conserved consensus sequence within the coupling domain (Figure 1.1) (Hirota et al., 1999), and $InsP_3R1$ has been identified as a substrate for caspase-3 during apoptosis (Hirota et al., 1999; Diaz and Bourguignon, 2000; Haug et al., 2000; Verbert et al., 2008). Of the 3 $InsP_3R$ isoforms, only the type 1 receptor contains the DEVD sequence for caspase-3 recognition and proteolysis (Hirota et al., 1999). While activation of caspase-3 is traditionally considered an executioner of apoptosis rather than an initiator, there is evidence that caspase-cleavage of $InsP_3R1$ is

required for apoptosis (Assefa et al., 2004) and is an early event in the cell death cascade (Haug et al., 2000). Caspase-3-mediated proteolysis of $InsP_3R1$ in cells results in decreased $InsP_3$ binding (Diaz and Bourguignon, 2000) and diminished $InsP_3$-induced Ca^{2+} release (Hirota et al., 1999; Diaz and Bourguignon, 2000), while preserving structural and functional integrity of the channel domain (Hirota et al., 1999). These studies suggested that caspase-proteolysis of $InsP_3R1$ sensitizes cells to apopotosis by disruption of Ca^{2+} homeostasis.

To directly examine the role of caspase-cleaved $InsP_3R1$ in cell death, previous studies have expressed a truncated, recombinant form of $InsP_3R1$ that corresponds to the carboxyl-terminal channel fragment derived from caspase-3 proteolysis. Expression of caspase-cleaved $InsP_3R1$ in these studies resulted in decreased ER releasable Ca^{2+} (Nakayama et al., 2004; Verbert et al., 2008), increased ER Ca^{2+} leak rate (Verbert et al., 2008), and slowed ER Ca^{2+} uptake (Verbert et al., 2008). These data suggest that caspase-3 proteolysis of $InsP_3R1$ generates a leaky channel that decreases ER Ca^{2+} buffering capacity. Additionally, expression of caspase-cleaved $InsP_3R1$ impaired normal ER Ca^{2+} signaling (Verbert et al., 2008) and increased the rate of apoptosis following injury (Assefa et al., 2004). Together, these data support a role for $InsP_3R1$ proteolysis in disruption of Ca^{2+} homeostasis and cell death.

$InsP_3R1$ is also a known substrate for calpain, which sequentially cleaves the channel into 200, 130, and 95 kDa carboxyl-terminal fragments (Magnusson et al., 1993; Igwe and Filla, 1997). While the stable predominant 95 kDa calpain-derived fragment is reported to be similar in size to the caspase-derived fragment, the cleavage sites are different. To the best of our knowledge, there was no published description of the

functional consequences of calpain cleavage of $InsP_3R1$ prior to our investigation. However, based on studies of the caspase-cleaved channel, we hypothesized that calpain-mediated cleavage of $InsP_3R1$ disrupts normal channel gating, and that this dysregulation increases ER Ca^{2+} release and limits ER Ca^{2+} buffering capacity. We further speculated that $InsP_3R1$ proteolysis by calpain would significantly contribute to delayed $[Ca^{2+}]_i$ and $[Ca^{2+}]_m$ overload and secondary activation of calpain following ischemia-reperfusion.

Rationale

The molecular injury mechanisms that result in neurodegeneration after ischemic brain injury are incompletely understood. However, disruption of Ca^{2+} homeostasis and pathological calpain activation are key components of post-ischemic neuronal death. $InsP_3R1$, as both a Ca^{2+} regulatory protein and proteolytic target of calpain, is critically poised to execute cell death pathways.

At the onset of this investigation, we hypothesized that $InsP_3R1$ proteolysis by calpain irreversibly disrupts cellular Ca^{2+} homeostasis and that Ca^{2+} signaling through the cleaved channel triggers post-ischemic neuronal death (Figure 1.2). Based on earlier studies of $InsP_3R1$ proteolysis, we speculated that calpain cleavage generates a channel with $InsP_3$-independent gating that increases ER Ca^{2+} leak and impairs intracellular Ca^{2+} buffering. These alterations in normal $InsP_3R1$-mediated Ca^{2+} signaling could lead to neuronal Ca^{2+} overload and death by shifting Ca^{2+} from the ER lumen to the cytoplasm and mitochondria. Increases in $[Ca^{2+}]_i$ may initiate a positive feedback loop leading to augmented calpain activity. Alternativey, increased $[Ca^{2+}]_m$ could amplify intrinsic cell death pathways through release of pro-apoptotic factors. Thus, $InsP_3R1$ proteolysis

potentially represents a pivotal transition to irreversible neuronal injury. If calpain proteolysis of $InsP_3R1$ plays a causal role in post-ischemic neuronal death, then blocking the cleaved channel could emerge as a novel therapeutic strategy. The experiments presented in this dissertation serve to elucidate the neuropathologic role of $InsP_3R1$ proteolysis by calpain.

Figure 1.1

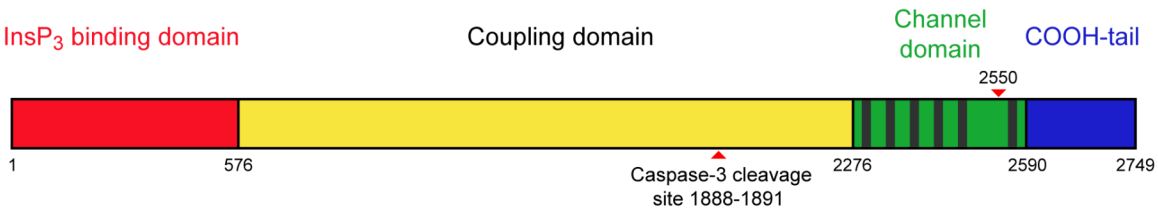

Figure 1.1 Domain structure of $InsP_3R1$

The $InsP_3R1$ protein, depicted as a linear amino acid sequence, contains 3 major domains. The amino-terminal region is the $InsP_3$ ligand-binding domain (*red*). The central coupling domain (*yellow*) contains the DEVD sequence for caspase-3 cleavage (*arrow*). The channel domain (*green*) of $InsP_3R1$ is located near the carboxyl-terminus of the protein and consists of 6 transmembrane domains (*grey*). Mutation of D2550 (to A or N; *arrow*) in the pore forming region eliminates Ca^{2+} permeability of the channel. Residues are numbered according to the rat type 1 SI+, SII+, SIII- sequence (protein accession no. NP_001007236.1; Adapted from Foskett et al., 2007).

Figure 1.2

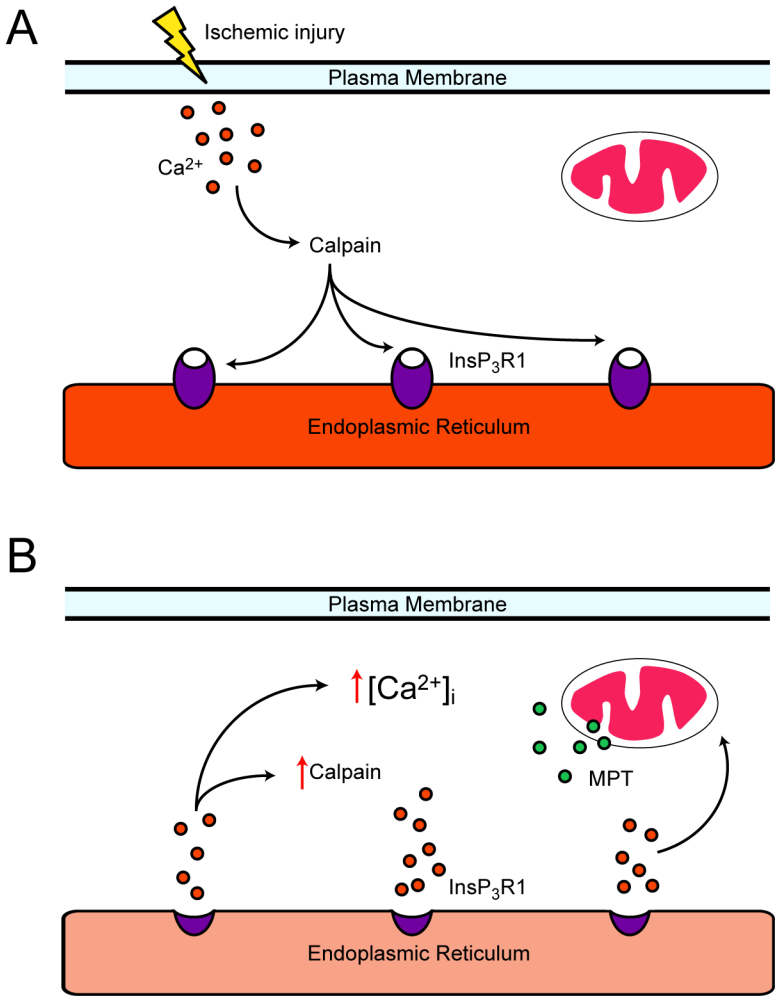

Figure 1.2 Neuropathologic role of $InsP_3R1$ proteolysis

Schematic representation of known and hypothesized molecular cascades initiated by ischemic brain injury. (*A*) Ischemic depolarization of neurons causes Ca^{2+} influx, resulting in an initial increase in $[Ca^{2+}]_i$, and subsequent calpain activation. We hypothesize that this early calpain activity results in proteolysis of $InsP_3R1$. (*B*) We additionally hypothesize that $InsP_3R1$ proteolysis generates a dysregulated channel that leaks Ca^{2+} from the ER, which increases $[Ca^{2+}]_i$. Sustained elevations in $[Ca^{2+}]_i$ can lead to pathological activation of calpain, or mitochondrial Ca^{2+} overload, permeability transition (*MPT*), and release of pro-apoptotic factors (*green*). Together, these events may be responsible for delayed neuronal death following ischemia-reperfusion.

Table 1.1 Calpain proteolysis of Ca^{2+} regulatory proteins

Calpain Substrate	Function in Ca^{2+} Homeostasis	Consequences of Proteolysis	References
PMCA	Cytoplasmic Ca^{2+} removal	Internalization of the pump; Decreased Ca^{2+} extrusion	Pottorf et al., 2006; Ferragamo et al., 2009
SERCA	Cytoplasmic Ca^{2+} removal	Uncoupling of ATP hydrolysis and pump activity; Decreased Ca^{2+} uptake	Parsons et al., 1999; French et al., 2006
NCX	Cytoplasmic Ca^{2+} removal	Decreased Ca^{2+} transport function	Bano et al., 2005; Samanta et al., 2009
L-type Ca^{2+} channel	Plasma membrane Ca^{2+} influx	Enhanced coupling between membrane voltage and gating; Increased P_o	De Jongh et al., 1995; Wei et al, 1994; Hell et al., 1996
NMDA receptor	Plasma membrane Ca^{2+} influx	Unknown	Guttman et al., 2002; Simpkins et al., 2003; Dong et al., 2006
RyR	Intracellular Ca^{2+} release	Diminished channel inactivation; Increased P_o	Rardon et al., 1990
$InsP_3R1$	Intracellular Ca^{2+} release	Unknown	Magnusson et al., 1993; Wojcikiewicz and Oberdorft, 1996; Igwe and Filla, 1997; Diaz and Bourguignon, 2000

Published in the *Journal of Biological Chemistry*

Calpain-Cleaved Type 1 Inositol 1,4,5-Trisphosphate Receptor ($InsP_3R1$) has $InsP_3$-Independent Gating and Disrupts Intracellular Ca^{2+} Homeostasis

Catherine M. Kopil[1]; Horia Vais[2]; King-Ho Cheung[2,4]; Adam P. Siebert[2]; Don-On Daniel Mak[2]; J. Kevin Foskett[2,3]; Robert W. Neumar[1§]

From the Departments of Emergency Medicine[1], Physiology[2] and Cell and Developmental Biology[3], University of Pennsylvania, Philadelphia, PA 19104 and Department of Physiology[4], University of Hong Kong, Pok Fu Lam, Hong Kong

§**Address correspondence to**: Robert W. Neumar, MD, PhD, 3400 Spruce Street, Ground Floor Ravdin Building, Philadelphia, PA 19104. E-mail: neumarr@uphs.upenn.edu; Fax: 215-746-1224

Number of Figures / Supplemental Figures: 8 / 3

Number of Pages: 33

SUMMARY

The type 1 inositol 1,4,5-trisphosphate receptor ($InsP_3R1$) is a ubiquitous intracellular Ca^{2+} release channel that is vital to intracellular Ca^{2+} signaling. $InsP_3R1$ is a proteolytic target of calpain, which cleaves the channel to form a 95 kDa carboxyl-terminal fragment that includes the transmembrane domains, which contain the ion pore. However, the functional consequences of calpain proteolysis on channel behavior and Ca^{2+} homeostasis are unknown. In the present study, we have identified a unique calpain cleavage site in $InsP_3R1$, and utilized a recombinant truncated form of the channel (capn-$InsP_3R1$) corresponding to the stable, carboxyl-terminal fragment to examine the functional consequences of channel proteolysis. Single-channel recordings of capn-$InsP_3R1$ revealed $InsP_3$-independent gating and high open probability (P_o) under optimal cytoplasmic Ca^{2+} concentration ($[Ca^{2+}]_i$) conditions. However, some $[Ca^{2+}]_i$ regulation of the cleaved channel remained, with a lower P_o in sub-optimal and inhibitory $[Ca^{2+}]_i$. Expression of capn-$InsP_3R1$ in N2a cells reduced the Ca^{2+} content of ionomycin-releasable intracellular stores and decreased endoplasmic reticulum Ca^{2+} loading compared with control cells expressing full-length $InsP_3R1$. Using a cleavage-specific antibody, we identified calpain-cleaved $InsP_3R1$ in selectively vulnerable cerebellar Purkinje neurons following *in vivo* cardiac arrest. These findings indicate that calpain proteolysis of $InsP_3R1$ generates a dysregulated channel that disrupts cellular Ca^{2+} homeostasis. Furthermore, our results demonstrate that calpain cleaves $InsP_3R1$ in a clinically relevant injury model, suggesting that Ca^{2+} leak through the proteolyzed channel may act as a feed-forward mechanism to enhance cell death.

INTRODUCTION

Changes in cytoplasmic free Ca^{2+} concentration ($[Ca^{2+}]_i$) act as a ubiquitous signaling system that is essential to proper neuronal function and survival. Conversely, disrupted $[Ca^{2+}]_i$ can serve as a trigger for cell death (Berridge et al., 2000; Orrenius et al., 2003). In particular, compelling evidence suggests that disruption of cellular Ca^{2+} homeostasis, caused in part by dysfunction of Ca^{2+} regulatory proteins, plays a causal role in both acute brain injury and chronic neurodegenerative diseases (Bevers and Neumar, 2008).

The inositol 1,4,5-trisphosphate receptor ($InsP_3R$), a ubiquitous intracellular Ca^{2+} release channel located on the endoplasmic reticulum (ER) membrane, may be an important component of the pathologic cascades leading to disrupted Ca^{2+} homeostasis in many disease states. Cells deficient in $InsP_3Rs$ are resistant to apoptosis (Jayaraman and Marks, 1997; Sugawara et al., 1997) suggesting that $InsP_3R$ mediated Ca^{2+} signaling plays a mechanistic role in cell death. Altered $InsP_3R$ channel function induces aberrant neuronal Ca^{2+} signaling in a variety of neurodegenerative diseases including Alzheimer's disease (Leissring et al., 1999a; Leissring et al., 1999b), Huntington's disease (Tang et al., 2003) and ischemia (Beresewicz et al., 2006). Observations in brain ischemia models also suggest altered $InsP_3R$ function, specifically, decreased $InsP_3$ binding (Nagasawa and Kogure, 1991; Dahl et al., 2000), decreased $InsP_3$-induced Ca^{2+} release (Nagata et al., 1999) and depletion of releasable Ca^{2+} stores (Zaidan and Sims, 1994; Kohno et al., 1997). Proteolytic cleavage of $InsP_3R$ could explain these observations.

The type 1 $InsP_3R$ ($InsP_3R1$), the predominant neuronal isoform, is a substrate for both the caspase and calpain families of cysteine proteases (Foskett et al., 2007). These proteases are indirectly (caspase-3) and directly (calpain) activated by Ca^{2+} and are known to play a central role in apoptotic and necrotic cell death pathways (Wang, 2000). Proteolytic activity of these enzymes is limited and site specific, typically altering rather than eliminating substrate function. In the case of Ca^{2+} regulatory proteins, this may initiate a positive feedback loop that further increases protease activation via increases in $[Ca^{2+}]_i$.

Caspase-3 or calpain cleavage of $InsP_3R1$ generates carboxyl-terminal fragments of approximately 95 kDa (Hirota et al., 1999). Caspase-3 cleaves $InsP_3R1$ at a highly conserved DEVD consensus sequence within the coupling domain (Hirota et al., 1999) (Figure 2.1A). Caspase-mediated proteolysis of the channel has been observed in several models of apoptosis (Hirota et al., 1999; Diaz and Bourguignon, 2000; Haug et al., 2000). Previous studies have demonstrated altered ER Ca^{2+} homeostasis in cell lines expressing a recombinant caspase-derived carboxyl-terminal fragment of $InsP_3R1$, suggesting that cleavage generates an unregulated channel that may leak Ca^{2+} from intracellular stores (Assefa et al., 2004; Nakayama et al., 2004; Verbert et al., 2008). $InsP_3R1$ is also a substrate for calpain, which sequentially cleaves the protein into 200, 130 and 95 kDa carboxyl-terminal fragments (Magnusson et al., 1993; Wojcikiewicz and Oberdorf, 1996; Igwe and Filla, 1997). However the specific calpain cleavage site that generates the stable 95 kDa fragment has not been established, and the functional consequences of proteolysis on channel activity are unknown. We hypothesized that calpain-mediated proteolysis, which removes the amino-terminal ligand binding domain and a large portion

of the regulatory domain, generates a channel with $InsP_3$-independent gating that leaks Ca^{2+} from ER stores.

In the present study, we have identified the unique calpain-cleavage site of $InsP_3R1$ and investigated the electrophysiological and functional properties of the truncated carboxyl-terminal channel. Using a combination of single-channel nuclear patch clamp electrophysiology and single-cell Ca^{2+} imaging, we have determined that the cleaved channel is constitutively active in the absence of $InsP_3$, although its gating retains sensitivity to $[Ca^{2+}]_i$. Constitutive channel activity accounts for an observed reduction in the Ca^{2+} content of the ER lumen in cells expressing recombinant calpain-cleaved $InsP_3R1$. Importantly, we provide evidence of calpain-mediated proteolysis of $InsP_3R1$ in an *in vivo* model of ischemic brain injury. These data highlight the important functional consequences of calpain-mediated channel proteolysis, which may critically disrupt intracellular Ca^{2+} homeostasis, particularly under pathologic conditions where other Ca^{2+} regulatory proteins are also compromised.

EXPERIMENTAL PROCEDURES

Materials—Unless otherwise noted, all chemical reagents were purchased from Sigma-Aldrich.

Antibodies—The anti-$InsP_3R1$ polyclonal antibody targeted against the 20 carboxyl-terminal residues of rat $InsP_3R1$ was generously provided by Dr. Suresh Joseph (Thomas Jefferson University) (Joseph and Samanta, 1993). The antibody to calpain-cleaved spectrin (Ab38) was generously provided by Dr. Robert Siman (University of Pennsylvania). Anti-calreticulin (CRT) polyclonal antibody was purchased from Thermo Scientific Pierce Antibodies (PA3-900). Alexa-488 conjugated secondary antibody used for immunofluorescence was purchased from Invitrogen. The antibody against calpain-cleaved $InsP_3R1$ (Ab2054) was generated against the peptide ASAATRKAC and is described in the Results section.

Cerebellar Microsome Isolation—Male Long-Evans rats were deeply anesthetized with pentobarbital (200 mg/kg) and decapitated. The brain was extracted, and the cerebellum dissected and homogenized in cold MSHE buffer (in mM): 220 mannitol, 70 sucrose, 2 K-HEPES (pH 7.4), 0.5 EGTA with 0.1% fatty-acid free bovine serum albumin (BSA) and protease inhibitor cocktail. The homogenate was centrifuged at 650 x g for 10 min at 4° C to remove nuclei (P1). The supernatant from the preceding fraction (S1) was centrifuged again at 8,000 X g for 10 min at 4° C to separate cytoplasm and microsomes from mitochondria and synaptosomes. The remaining supernatant (S2) was centrifuged at 100,000 X g for 1 h in a micro-ultracentrifuge (ThermoFisher Scientific). The pellet from the final spin (P3) containing microsomes was resuspended

in either MSHE buffer without BSA for western blot or digest buffer for subsequent in vitro digest, snap frozen and stored at -20° C.

$InsP_3R1$ Peptide Generation—The amino acid sequences of rat $InsP_3R1$ from residues 1582 to 1932 or from residues 1932 to 2257 were fused to an amino-terminal glutathione S-transferase (GST) using the linker sequence LEVLFQGP, and cloned into pGEX expression vectors. The fusion protein was grown in BL21 E. coli and purified using Glutathione Sepharose 4B (GE Healthcare). The GST tag was removed from the $InsP_3R1$ 1582-1932aa peptide following purification using PreScission Protease, which recognizes the sequence LEVLFQ/GP and cleaves between the Q and G residues (GE Healthcare).

In Vitro Caspase-3 and Calpain 1 Digests of Microsomes and $InsP_3R1$ Peptide—For in vitro caspase-3 digest of cerebellar microsomes, freshly isolated microsomes were resuspended in lysis buffer (in mM: 50 Tris-HCl (pH 7.4), 5 EDTA, 1 DTT (Fisher) with 1% Triton X-100) and incubated at 4° C for 90 min prior to snap freezing. For subsequent digest, lysed microsomes were diluted to 1 μg/μl in digest buffer (in mM: 100 Tris-HCl (pH 7.4), 2 EDTA, and 20 DTT). Samples were preincubated with 1 μM calpastatin peptide (CAST; EMD Biosciences) to inhibit endogenous calpain activity and then digested with recombinant active human caspase-3 (0.05 units/μl; Millipore) for 4 h at 37° C. Loading buffer was added to the digest to stop the reaction.

For in vitro calpain digest of cerebellar microsomes, freshly isolated microsomes were resuspended in a modified digest buffer (in mM: 25 HEPES (pH 7.4), 250 sucrose, 1 EDTA) and snap frozen. For subsequent digest, microsomes were diluted to 1 μg/μl in complete digest buffer (in mM: 25 HEPES (pH 7.4), 250 sucrose, 1 EDTA, 2 DTT, and 2

$CaCl_2$). Samples were preincubated with 1 mM Z-VAD-FMK (Promega) to inhibit endogenous caspase activity, and then digested with 0.5 μM calpain 1 (μ-calpain) from human erythrocytes (EMD Biosciences) at 4° C for various times. Loading buffer was added to the digest to stop the reaction.

For in vitro calpain digest of the GST-$InsP_3R1$ fusion peptides, purified peptide was diluted in digest buffer (in mM: 25 HEPES (pH 7.5), 250 NaCl, 2 DTT, 1 $CaCl_2$ with 1.2% CHAPS). Samples were digested with 0.1 μM calpain 1 at 4° C for various times. Adding loading buffer to the digest terminated the reaction.

Edman N-terminal Sequencing to Determine Cleavage Site—N-terminal automated Edman sequencing was performed on an Applied Biosystems 494 Protein Sequencer using standard programs and reagents (Wistar Institute, Proteomics Core Facility). Samples were excised from stained PVDF membranes, wetted with MeOH and sonicated in MilliQ water for 5 min. Samples were then removed and placed in MeOH prior to loading into the upper sample cartridge unit. The cartridge was assembled, the sample was dried with argon, inserted into the instrument, and processed with a standard pulsed liquid method for 8 cycles.

Plasmids—The pIRES2-EGFP (Clontech) expression vector for wild type (wt) rat $InsP_3R1$ was previously generated (Li et al., 2007). To construct the expression vector for calpain-cleaved $InsP_3R1$ (capn-$InsP_3R1$; Figure 2.3A), we amplified the 3'-portion of rat $InsP_3R1$ cDNA sequence corresponding to the stable carboxyl-terminal fragment of the channel generated by calpain proteolysis (2.6 kb) using primers 5'—GCGAATTCATGGCATCTGCTGCCACCAG—3' and 5'—GTCTCTAGAAAATGTACTTAAGCGCACAT—3' (underlined regions indicate EcoRI

and XbaI restriction sites). PCR was performed using PfuTurbo DNA polymerase (Stratagene) and subcloned the capn-InsP_3R1 PCR product into the pIRES2-EGFP expression vector using EcoRI and XbaI restriction sites. EGFP was expressed with InsP_3R1 constructs from a single bicistronic mRNA using an internal ribosome entry site in the pIRES2-EGFP expression vector.

Cell Culture, DNA Transfection and Lysate Preparation—Neuro-2A (N2a) cells were cultured in Minimum Essential Medium (Invitrogen) supplemented with 10% fetal bovine serum and maintained at 37° C in a humidified incubator with 5% CO_2. N2a cells were grown on polystyrene multiwell plates (Western blot), polystyrene tissue culture flasks (electrophysiology), or 20 x 50 mm glass coverslips (single-cell Ca^{2+} imaging) and transfected using Lipofectamine 2000 (Invitrogen). For Western blot, cells were harvested by trypsinization and resuspended in homogenization buffer (in mM: 50 Tris, 150 NaCl, 2 EGTA) and sonicated. Lysates were treated with SDS loading buffer, boiled and analyzed on SDS-PAGE gels. Where indicated, capn-InsP_3R1 transfected cells were solubilized and denatured in buffer supplemented with 5 M urea or 1% SDS.

Single-Channel Electrophysiology—Nuclei from N2a cells were isolated 24 h post-transfection as previously described (White et al., 2005; Ionescu et al., 2006; Cheung et al., 2008; Cheung et al., 2010). Briefly, nuclei were mechanically isolated, and plated onto a glass-bottomed dish with standard bath solution (in mM: 140 KCl, 10 Hepes, 0.5 BAPTA and 0.192 $CaCl_2$ (free $[Ca^{2+}] \approx 70$ nM), pH 7.1). The pipette solution contained (in mM): 140 KCl, 0.5 ATP, 10 Hepes pH 7.3, and 0.5 dibromo-BAPTA and 0.3 $CaCl_2$ (free $[Ca^{2+}] \approx 2$ μM), 0.5 BAPTA and 0.192 $CaCl_2$ (free $[Ca^{2+}] \approx 70$ nM), or 0.5 HEDTA and 0.43 $CaCl_2$ (free $[Ca^{2+}] \approx 25$ μM). Where indicated, 10 μM InsP_3 with or without

100 μg/ml heparin were included in the pipette solution. Data were acquired at room temperature using an Axopatch 200A amplifier (Axon Instruments) and analyzed as previously described (Cheung et al., 2010).

Single-Cell Ca^{2+} Imaging—To measure $[Ca^{2+}]_i$, N2a cells were plated onto glass-coverslips (Warner Instruments) and transfected. Six h post-transfection, cells on coverslips were secured in a perfusion chamber, and mounted on the stage of an inverted microscope (Nikon Eclipse TE2000). Cells were loaded with Fura-2-AM (Molecular Probes; 2.5 μM) for 30 min at room temperature in Ca^{2+}-containing extracellular solution (in mM: 137 NaCl, 2 KCl, 2 $CaCl_2$, 10 HEPES, pH 7.3) supplemented with 1% BSA. Fura-2 was alternately illuminated at 340/380 nm, and fluorescence intensity filtered at 510 nm. Data were collected and recorded as described previously (White et al., 2005; Cheung et al., 2008). Cells were perfused with 2 mM Ca^{2+} extracellular solution to establish baseline $[Ca^{2+}]_i$ before ionomycin (Invitrogen; 2 μM) was applied in 0-Ca^{2+} extracellular solution (in mM: 137 NaCl, 2 KCl, 0.5 EDTA, 0.5 EGTA, 10 HEPES, pH 7.3) to measure Ca^{2+} release from intracellular stores. At the end of the experiment, Mn^{2+} was used to quench Fura-2 fluorescence (2 mM Ca^{2+} extracellular solution supplemented with 10 mM $MnCl_2$ and 10 μM ionomycin). The remaining background fluorescence following Mn^{2+} quench was subtracted during analysis.

To measure ER lumenal $[Ca^{2+}]$ ($[Ca^{2+}]_{ER}$), transfected cells (6 h post-transfection) were loaded with the low-affinity Ca^{2+} indicator Mag-Fura-2-AM (Invitrogen; 10 μM) for 30 min at 37° C in HEPES-HBSS buffer (HBSS solution supplemented with (in mM): 10 HEPES, 4.2 $NaHCO_3$, 1.8 $CaCl_2$, and 0.8 $MgCl_2$, pH 7.3) with 1% BSA. After loading, cells were permeabilized with 10 μg/ml digitonin for 2 min in MgATP-free

cytoplasm-like medium (CLM; in mM: 140 KCl, 20 NaCl, 1 EGTA, 0.375 $CaCl_2$ (final concentration ≈ 70 nM), 20 PIPES, pH 7.3). Cells were perfused with CLM for 30 min to wash out digitonin and deplete ER Ca^{2+} stores. ER store loading was activated by addition of 1.5 mM MgATP to the perfusate to stimulate SERCA-mediated Ca^{2+} uptake. Following filling, the passive ER Ca^{2+} leak was evaluated by measuring $[Ca^{2+}]_{ER}$ during exposure to 10 μM cyclopiazonic acid (CPA; Calbiochem) in the absence of MgATP. Mag-Fura-2 excitation and emission were monitored as described above. Rates for ER loading and release were calculated by fitting individual single-cell responses using single exponential functions and determining the mean of those rates.

Changes in $[Ca^{2+}]_i$ and $[Ca^{2+}]_{ER}$ are presented as changes in fluorescence ratio. Dye calibration was achieved by applying experimentally determined constants to the equation: $[Ca^{2+}] = K_d\ \beta(R–R_{min})/(R_{max}–R)$. Macros used for analysis were custom macros written for IGOR Pro (WaveMetrics).

Cardiac Arrest Model—Male Long-Evans rats weighing 300-350 g (Harlan Laboratories Inc.) were subjected to asphyxial cardiac arrest followed by cardiopulmonary resuscitation and post-cardiac arrest temperature regulation as previously described (Katz et al., 1995; Neumar et al., 1995; Che et al., In Press). Rats were anesthetized, orotracheally intubated and mechanically ventilated. Temperature was maintained between 37.0 and 37.5° C. To initiate cardiac arrest, rats were chemically paralyzed using intravenous vecuronium (2 mg/kg) and asphyxia induced by discontinuing mechanical ventilation. Cessation of arterial pulse pressure and reduction of mean arterial pressure to ≤ 20 mmHg was used to confirm circulatory arrest, which usually occurred within 3-4 min. Following the 7 min asphyxia, mechanical ventilation

resumed with 100% O_2, intravenous epinephrine (0.005 mg/kg) and HCO_3 (1.0 mEq/kg) were administered, and external chest compressions were performed (350-400 compressions/min). Following return of spontaneous circulation, rats were maintained on mechanical ventilation for 1 h. An intraperitoneal telemetric temperature probe was surgically implanted in the abdomen (Data Systems International). Rats were then extubated and transferred to a computer controlled temperature regulation chamber, which telemetrically monitored intraperitoneal temperature. Post-cardiac arrest body temperature was maintained between 36.5 and 37.5° C using software-driven relays connected to a heat-lamp, water misters and a cooling fan (Colbourne et al., 1996; Che et al., In Press). This study was approved by the University of Pennsylvania Institutional Animal Care and Use Committee.

Immunohistochemical Staining of Cerebellum—At indicated time points following cardiac arrest (24 or 48 h), rats were anesthetized with pentobarbital (200 mg/kg) and transcardially perfused with cold phosphate buffered saline (PBS, pH 7.4) followed by 4% paraformaldehyde (PFA) in 0.1M phosphate buffer (PB). Brains were extracted, post-fixed in 4% PFA over-night and cryoprotected using serial incubations in 0.1 M PB containing 10%, 20% and 30% sucrose. Serial sagittal sections through the cerebellum (40 μm) were cut on a freezing sliding microtome and stored in cryoprotectant (0.1 M PB with 30% sucrose and 30% glycerol) at -20°C for future use. Immunohistochemistry to identify calpain-cleaved $InsP_3R1$ (Ab2054) required heat-induced epitope retrieval (HIER). Cerebellar tissue sections were removed from cryoprotectant, rinsed in dH_2O, and incubated in citrate buffer (10 mM sodium citrate with 0.05% Tween-20, pH 6.0) at 95°C for 20 min. Following HIER, tissue was

removed from heat and rinsed in PBS (pH 7.2). Standard immunohistochemical staining procedures followed.

Floating cerebellar brain sections were rinsed in PBS (pH 7.2) and blocked using PBS with 4% normal goat serum and 0.5% Triton X-100. Sections were incubated in primary antibody (Ab38 or Ab2054) diluted in block solution overnight at 4° C. Sections were rinsed with PBS and incubated with Alexa 488 fluorescent secondary antibody. Finally, sections were rinsed with PBS, counterstained with Hoescht (5 μg/ml in PBS) to label nuclei, mounted on slides and coverslipped under Fluormount-G (Electron Microscopy Sciences).

For Fluoro-Jade labeling, PFA-fixed sections were mounted onto gelatin-coated slides and dried. Tissue was treated with 100% ethanol, 70% ethanol and dH_2O rinses. Hydrated tissue was incubated with 0.06% potassium permanganate for 10 min, rinsed with dH_2O, and stained with 0.0004% Fluoro-Jade B (Millipore) in 0.1% acetic acid for 20 min. Stained tissue was rinsed with dH_2O, dried at 37°C, dehydrated with xylene and coversliped using Permount (Fisher Scientific).

Immunofluorescence was studied at 100X using an epifluorescence microscope (Leica DM4500B).

Analyses and Statistics—Data are presented as the mean ± SEM, and statistical significance of differences between the means was assessed using either unpaired t-tests or analysis of variance (ANOVA) for repeated-measures using Barlett's test for equal variances and a Bonferroni correction. Differences between means were accepted as statistically significant at the 95% level ($p < 0.05$).

RESULTS

Identifying the calpain-cleavage site of $InsP_3R1$

$InsP_3R1$ is a known substrate of calpain, which sequentially cleaves the protein into 200, 130, and 95 kDa carboxyl-terminal fragments, with the 95 kDa fragment being the stable, predominant cleavage product (Figure 2.1B) (Magnusson et al., 1993; Wojcikiewicz and Oberdorf, 1996; Igwe and Filla, 1997). While the 95 kDa calpain-derived fragment is similar in size to the caspase-derived fragment, the cleavage sites are different. To determine the calpain cleavage site of $InsP_3R1$, we first examined the relative sizes of the caspase- and calpain-cleaved carboxyl-terminal fragments of $InsP_3R1$ using *in vitro* digests of rat cerebellar tissue, which is enriched in $InsP_3R1$. We performed *in vitro* digests of cerebellar microsomes with either recombinant, constitutively active caspase-3 or exogenous calpain 1. A Western blot of the digest products using a carboxyl-terminal $InsP_3R1$ antibody demonstrated loss of the full-length protein and generation of stable carboxyl-terminal fragments of approximately 95 kDa (Figure 2.1C). Shown here for the first time, calpain cleavage of $InsP_3R1$ generates a slightly smaller fragment than the fragment generated by caspase cleavage.

Caspase cleavage of $InsP_3R1$ is known to occur at the carboxyl-terminal end of the ^{1888}DEVD consensus sequence (Figure 2.1A) (Hirota et al., 1999). Based on the relative sizes of the caspase and calpain $InsP_3R1$ cleavage products, we deduced that the calpain cleavage site responsible for generating the 95 kDa stable fragment was less than 30 residues downstream of the caspase-3 cleavage site. To identify the site we utilized a GST-fusion peptide containing residues 1583 to residue 1932 of rat $InsP_3R1$, which

includes the caspase-3 cleavage site (Supplemental Figure 2.1A). As a control, we used a GST-fusion peptide containing an adjacent sequence within $InsP_3R1$ (residues 1932 to 2257) that does not include the caspase-3 cleavage site. We digested both GST-fusion peptides with exogenous calpain 1, separated reaction products using SDS-PAGE, and transferred them to PVDF membranes for protein staining. Protein staining of digest products identified a single proteolytic fragment derived from the 1582-1932aa peptide, but not the 1932-2257aa peptide, confirming that the calpain-cleavage site is between residues 1582 and 1932 (Supplemental Figure 2.1B). Addition of the calpain inhibitor calpastatin blocked generation of the proteolytic fragment produced by calpain digest of $InsP_3R1$ peptide 1582-1932aa (Figure 2.1D). Eight rounds of Edman degradation and N-terminal sequencing of the proteolytic fragment from the calpain-digested GST-fusion peptide returned 4 potential sequences, only one of which (^{1918}ASAATRKA) was downstream of the caspase-DEVD site (Figure 2.1E). Based on the location of this sequence in $InsP_3R1$, the predominant calpain cleavage product is expected to have a molecular mass of 94.84 kDa. This fragment is 3.02 kDa smaller than the caspase-cleaved fragment, which is consistent with Western blot comparisons of calpain and caspase *in vitro* digests of microsomal $InsP_3R1$ (Figure 2.1C). These data demonstrate that calpain cleaves rat $InsP_3R1$ between residues 1917 and 1918 to generate the 95 kDa carboxyl-terminal fragment. The sequences surrounding the cleavage site are highly conserved in $InsP_3R1$ across species, although it is not present in type 2 or type 3 receptors.

Calpain-cleaved $InsP_3R1$ antibody

To facilitate investigations of calpain-cleaved $InsP_3R1$, we generated an antibody specific to the calpain-derived carboxyl-terminal fragment of the channel using a neoepitope specific approach (Roberts-Lewis et al., 1994). The peptide ASAATRKAC, corresponding to the new amino-terminus of $InsP_3R1$ following calpain-cleavage, was synthesized and covalently linked to a keyhole limpet hemocyanin to elicit an immune response (Figure 2.2A; Covance ImmunoTechnologies). A New Zealand White rabbit (2054) was immunized by subcutaneous injections of the peptide, and serum ELISA demonstrated a 1:843,000 titer at the time of test-bleed 1.

We tested specificity of Ab2054 for the 95 kDa calpain-derived $InsP_3R1$ fragment by Western blot of rat cerebellar microsomes following *in vitro* digestion. Using a carboxyl-terminal $InsP_3R1$ antibody, we detected full-length, caspase-digested and calpain-digested $InsP_3R1$ (Figure 2.2B). Using Ab2054 on the same blot, we detected no signal in undigested microsomes or microsomes digested with caspase-3, but a single band at ~95 kDa was observed in microsomes digested with calpain 1, indicating the antibody reacts exclusively with the stable 95 kDa calpain-cleaved form of $InsP_3R1$ (Figure 2.2C). These data validate Ab2054 as specific antibody for calpain-cleaved $InsP_3R1$.

Expression of recombinant $InsP_3R1$ constructs

To examine the consequences of calpain cleavage of $InsP_3R1$ on channel function, we generated a truncated cDNA of the protein (△1-1917) corresponding to the stable carboxyl-terminal fragment derived from calpain cleavage (capn-$InsP_3R1$). We used full-

length wild type (wt) rat $InsP_3R1$ as a control (Figure 2.3A).

For all functional experiments, we studied wt- and capn-$InsP_3R1$ expressed transiently in N2a mouse neuroblastoma cells. We chose N2a cells as they are neural in tissue origin and have high transfection efficiency. To examine the time course of expression of recombinant rat $InsP_3R1$ in N2a cells, we transiently transfected cells with either wt-$InsP_3R1$ or capn-$InsP_3R1$ and harvested cells at 6, 16, 24, or 48 h later. Western blotting of whole-cell lysates using the carboxyl-terminal $InsP_3R1$ antibody demonstrated expression of both wt- and capn-$InsP_3R1$ by 6 h post-transfection. For capn-$InsP_3R1$, expression was maximal at 24 and decreased by 48 h post-transfection, whereas expression of the wt channel continued to increase up to 48 h, suggesting toxicity or cellular regulation of gene expression associated with capn-$InsP_3R1$ (Figure 2.3B). In lysates from wt-$InsP_3R1$ cells, we occasionally observed lower molecular weight fragments, which are possibly proteolytic degradation products. In lysates from cells expressing capn-$InsP_3R1$, we observed high molecular weight smears, which are likely aggregates of capn-$InsP_3R1$. Similar high molecular weight smears have been observed when expressing the caspase-3 cleaved form of $InsP_3R1$ (Nakayama et al., 2004). These smears were eliminated by harvesting capn-$InsP_3R1$ transfected cells in lysis buffer containing either 5 M urea or 1% SDS (Supplemental Figure 2.2).

$InsP_3$-independent gating of capn-$InsP_3R1$

To determine whether capn-$InsP_3R1$ still functioned as an ion channel, we examined single channel activity in native ER membranes. We utilized patch clamp electrophysiology of the outer membrane of isolated N2a cell nuclei to study the channel

activities of recombinant $InsP_3R1$ constructs (Foskett et al., 2007). To maximize the likelihood of recording recombinant channels, we performed patch clamp experiments at 24 h post-transfection, when expression of capn-$InsP_3R1$ was maximal. We monitored channel activity with the pipette solution (cytoplasmic side) containing 2 μM Ca^{2+} and 0.5 mM ATP. In untransfected cells, we observed endogenous $InsP_3R$ with single channel conductance of 395 ± 12 pS with saturating 10 μM $InsP_3$ in the pipette solution (Supplemental Figure 2.3A-B). In nuclei from cells transfected with recombinant rat wt-$InsP_3R1$, we observed channel activities that had a smaller single channel conductance (231 ± 10 pS; Supplemental Figure 2.3C). Despite their smaller single channel conductance, we identified these channels as $InsP_3R$ based on their dependence on $InsP_3$ for activation (n=10; Figure 2.4A) and their sensitivity to competitive inhibition by heparin (100 μg/ml in pipette solution; n=5; Figures 2.4A, 2.4C-D). With 10 μM $InsP_3$ in the pipette solution, the recombinant wt channels had an open probability (P_o) of 0.69 ± 0.08 (n=8; Figures 2.4A, 2.4C-D). In cells transfected with capn-$InsP_3R1$, we observed channel activities with a single channel conductance (230 ± 10 pS) similar to the recombinant wt-$InsP_3R1$ (Supplemental Figure 2.3D). Strikingly, we observed these channels even in the absence of $InsP_3$ in the pipette solution. Exposed to pipette solution containing no $InsP_3$, 2 μM Ca^{2+} and 0.5 mM ATP, the spontaneously active capn-$InsP_3R1$ channels had high P_o in either the absence (P_o=0.82 ± 0.04, n=9) or presence (P_o=0.74 ± 0.09, n=5) of heparin (Figures 2.4B-D). These results indicate that a truncated $InsP_3R1$ corresponding to the carboxyl-terminal calpain cleavage fragment forms a functional ion channel with $InsP_3$-independent gating.

Ca^{2+} regulation of capn-$InsP_3R1$ gating

Channel activity of $InsP_3R1$ is both activated and inhibited by Ca^{2+}, resulting in a biphasic, bell-shaped P_o dependence on $[Ca^{2+}]_i$ (Foskett et al., 2007). While $InsP_3$ regulation of the truncated channel was absent, we asked whether any Ca^{2+} regulation of capn-$InsP_3R1$ remained. Accordingly, we next examined channel activity at low $[Ca^{2+}]$ (70 nM), typical of resting cytoplasmic levels. With 10 μM $InsP_3$ and 70 nM free Ca^{2+} in the pipette solution, P_o of wt-$InsP_3R1$ was 0.016 ± 0.004 (n=8; Figures 2.5A, C), significantly lower than the observed P_o in 2 μM Ca^{2+} (P_o~0.7; p<0.001). With no $InsP_3$ and 70 nM free Ca^{2+} included in the pipette solution, P_o of capn-$InsP_3R1$ was 0.26 ± 0.06 (n=5; Figures 2.5B-C), also significantly lower than the observed P_o in 2 μM Ca^{2+} (P_o~0.8; p<0.001), but significantly higher than that of wt-$InsP_3R1$ at low Ca^{2+} (p<0.001). These data suggest that capn-$InsP_3R1$ may constitute an ER Ca^{2+} leak permeability in resting cells. To determine whether high $[Ca^{2+}]$ still inhibits capn-$InsP_3R1$, we examined channel activity at 25 μM Ca^{2+}, which corresponds to pathologic neuronal cytoplasmic levels immediately following ischemia (Erecinska and Silver, 1992; Silver and Erecinska, 1992). With 10 μM $InsP_3$ and 25 μM free Ca^{2+} in the pipette solution, P_o of wt-$InsP_3R1$ was 0.22 ± 0.06 (n=8; Figures 2.5A, C). In the absence of $InsP_3$, with heparin (100 μg/ml) and 25 μM free Ca^{2+} in the pipette solution, P_o of capn-$InsP_3R1$ was 0.39 ± 0.08 (n=8; Figures 2.5B-C). P_o of wt- and capn-$InsP_3R1$ channels in 25 μM Ca^{2+} were significantly lower than the corresponding P_o of each channel in 2 μM Ca^{2+} (p<0.001). P_o of capn-$InsP_3R1$ at 25 μM Ca^{2+} was not, however, significantly different from P_o of wt-$InsP_3R1$ at that $[Ca^{2+}]$. These data demonstrate that Ca^{2+} regulation of channel activity is preserved in capn-$InsP_3R1$.

Decreased intracellular Ca^{2+} stores in cells expressing capn-$InsP_3R1$

To investigate the functional consequence of $InsP_3R1$ proteolysis on cellular Ca^{2+} homeostasis, we first used single-cell Ca^{2+} imaging to examine $[Ca^{2+}]_i$ and estimate total Ca^{2+} content of intracellular stores. We identified individual transfected cells by EGFP expression driven by the pIRES2-EGFP expression vector. To avoid potential complications from compensatory changes in gene expression, we performed Ca^{2+} imaging at an early time point (6 h) following transfection. $[Ca^{2+}]_i$ was monitored with Fura-2 in transiently transfected N2a cells expressing wt-$InsP_3R1$, capn-$InsP_3R1$ or a control plasmid (EGFP). We utilized the Ca^{2+} ionophore ionomycin (2 μM) to liberate Ca^{2+} from intracellular stores in the absence of extracellular Ca^{2+} and measured the resulting increase in $[Ca^{2+}]_i$ (Figure 2.6A). We used ionomycin instead of a sarcoplasmic/endoplasmic reticulum Ca^{2+}-ATPase (SERCA) inhibitor because it produces a much faster leak and consequent rise in $[Ca^{2+}]_i$, providing a better estimate of the Ca^{2+} content of intracellular stores. Expression of capn-$InsP_3R1$ did not effect resting $[Ca^{2+}]_i$ in N2a cells (Figure 2.6B). However, expression of capn-$InsP_3R1$ significantly decreased the ionomycin-induced peak $[Ca^{2+}]_i$ (252 ± 15 nM) compared with control cells (540 ± 30 nM) or cells over-expressing wt-$InsP_3R1$ (520 ± 60 nM; $p<0.001$; Figure 2.6C). These data indicate that capn-$InsP_3R1$ causes partial depletion of intracellular Ca^{2+} stores consistent with the hypothesis that calpain-cleaved $InsP_3R1$ is a Ca^{2+} leak channel.

Decreased ER Ca^{2+} loading in cells expressing capn-$InsP_3R1$

To directly examine ER Ca^{2+} leak caused by truncated $InsP_3R1$, we monitored

$[Ca^{2+}]_{ER}$ in N2a cells using Mag-Fura-2 at 6 h post-transfection. We permeabilized the plasma membranes of Mag-Fura-2 loaded EGFP expressing cells by a brief exposure to digitonin under microscopic observation. After depleting ER stores by washing with ATP-free CLM for 30 min, we initiated Ca^{2+} filling of ER stores by perfusing permeabilized cells with saturating 1.5 mM MgATP to stimulate the SERCA pump. After a steady-state $[Ca^{2+}]_{ER}$ was reached, we observed the ER Ca^{2+} leak by inhibiting the pump with CPA (10 μM) and removing ATP (Figure 2.7A). Expression of capn-$InsP_3R1$ significantly decreased the steady-state loading level of the ER to 26.8 ± 1.1 μM compared with 36.3 ± 0.9 μM in controls and 33.4 ± 1.0 μM in cells expressing wt-$InsP_3R1$ ($p<0.001$; Figure 2.7B).

To compare the kinetics of ER Ca^{2+} loading and passive leak in cells expressing various $InsP_3R1$ constructs, we determined the average rate of ER loading and release by fitting each respective portion of single-cell responses with a single exponential equation. Expression of capn-$InsP_3R1$ reduced the rate of ER Ca^{2+} loading compared with cells expressing wt-$InsP_3R1$, although the rate was similar to that observed in EGFP-expressing cells (Figure 2.7C), suggesting that SERCA activity was sufficient to overcome Ca^{2+} leak through the truncated channel. Expression of capn-$InsP_3R1$ and, to a lesser extent, wt-$InsP_3R1$ significantly increased the ER Ca^{2+} leak rate compared with control ($p<0.001$; Figure 2.7D). Taken together, these data demonstrate that calpain-cleaved $InsP_3R1$ alters ER Ca^{2+} homeostasis.

Calpain-mediated proteolysis of $InsP_3R1$ following in vivo ischemia

To determine whether calpain proteolysis of $InsP_3R1$ occurs *in vivo* in a clinically

relevant injury model, we examined rat cerebellum following 7 min of asphyxial cardiac arrest. We chose this model because cerebellar Purkinje neurons express high levels of $InsP_3R1$ and are selectively vulnerable to transient global ischemia caused by cardiac arrest (Neumar, 2000). We first performed Western blot analysis of rat cerebellar microsomes from naïve animals or from animals resuscitated from cardiac arrest. Using the carboxyl-terminal $InsP_3R1$ antibody, which reacts with both unproteolyzed and cleaved $InsP_3R1$, we observed evidence of $InsP_3R1$ proteolysis and the appearance of a faint ~95 kDa fragment at both 1 and 24 h after return of spontaneous circulation (Figure 2.8A). Using Ab2054, which specifically recognizes the stable 95 kDa carboxyl-terminal fragment generated by calpain proteolysis, we identified calpain-cleaved $InsP_3R1$ in both post-cardiac arrest samples (Figure 2.8B).

To determine which cell populations within the cerebellum contained calpain-cleaved $InsP_3R1$, we performed immunohistochemical analysis of rat cerebellum 24 and 48 h following cardiac arrest using naïve animals as a control (Figure 2.8C). Immunolabeling with Ab38, which reacts with calpain-cleaved spectrin, demonstrated robust calpain activity within sub-populations of Purkinje neurons at 24 h post-cardiac arrest, which decayed but was still evident at 48 h post-cardiac arrest. Using Ab2054, we detected calpain-cleaved $InsP_3R1$ in sub-populations of Purkinje neurons in a distribution similar to that of calpain-cleaved spectrin (Figure 2.8C). The intensity of Ab2054 staining was comparable at 24 and 48 h after cardiac arrest, suggesting that the calpain-derived $InsP_3R1$ fragment is more stable than the spectrin fragment.

Finally, to evaluate the relationship between calpain cleavage of $InsP_3R1$ and cell death, we used Fluoro-Jade B to identify degenerating neurons in the cerebellum (Figure

2.8C). At both time points examined following cardiac arrest, we observed selective Fluoro-Jade labeling of sub-populations of Purkinje neurons. The intensity of Fluoro-Jade staining was greater at 48 h compared with 24 h post-cardiac arrest, and was accompanied by a shrunken somatic morphology consistent with neurodegeneration. The morphological changes and increased Fluoro-Jade intensity in Purkinje cells at 48 h post-injury suggests that both enhanced calpain activity and cleavage of $InsP_3R1$ precede neurodegeneration. We did not observe any Ab38, Ab2054 or Fluoro-Jade labeling in naïve tissue.

Together, these data demonstrate that calpain cleaves $InsP_3R1$ *in vivo* in a clinically relevant model of brain ischemia, and that calpain-mediated proteolysis of $InsP_3R1$ is an early molecular event in the injury cascade.

DISCUSSION

The present study is the first functional investigation of calpain-cleaved $InsP_3R1$. Based on our results from single-channel electrophysiology and Ca^{2+} imaging experiments, we conclude that capn-$InsP_3R1$ forms a dysregulated channel with $InsP_3$-independent gating, which functions as a leak channel in the ER. Moreover, evidence of calpain-mediated $InsP_3R1$ proteolysis in the brain following cardiac arrest demonstrates that $InsP_3R1$ proteolysis is a clinically relevant cellular pathway that is active in a neurodegenerative disease.

Calpain proteolyzes $InsP_3R1$ at a unique cleavage site

Previous reports (Magnusson et al., 1993; Wojcikiewicz and Oberdorf, 1996; Igwe and Filla, 1997) and data presented here (Figure 2.1) establish that $InsP_3R1$ is a proteolytic target of calpain, which cleaves the channel at multiple sites to form 200, 130, and 95 kDa carboxyl-terminal fragments. Calpains, unlike caspases, do not use consensus sequences for target recognition and proteolysis. Our data show that calpain cleaves $InsP_3R1$ between residues 1917 and 1918 to generate the stable 95 kDa channel fragment (Figure 2.1D-E). The $InsP_3R1$ calpain cleavage site and surrounding residues are highly conserved in mouse and human homologs, and are unique to the type 1 isoform of the channel. Our cleavage specific antibody (Ab2054; Figure 2.2) targeting the new amino-terminus of $InsP_3R1$ following calpain proteolysis provides a useful tool for studying the truncated form of the channel in multiple species, including human (data not shown).

To begin characterizing the functional consequences of calpain proteolysis of $InsP_3R1$, we utilized a recombinant channel construct corresponding to the 95 kDa carboxyl-terminal fragment of $InsP_3R1$ produced by calpain cleavage (Figure 2.3). We expected the recombinant truncated $InsP_3R1$ to tetramerize in the ER, as previous studies demonstrated that the transmembrane domains and carboxyl-terminal tail of the channel are sufficient for ER localization and oligomerization (Sayers et al., 1997; Galvan et al., 1999). We had attempted to study capn-$InsP_3R1$ on a null-background using the $InsP_3R$-deficient DT40 cell line. The extremely low transfection efficiency of these cells requires working in stable lines. However, we were unable to generate stable $InsP_3R$-deficient DT40 lines expressing capn-$InsP_3R1$ despite our lab and others being able to generate stable lines expressing the similarly sized caspase-3 cleaved form of the channel (Assefa et al., 2004; Verbert et al., 2008).[1] The apparent toxicity associated with expression of capn-$InsP_3R1$ in the DT40 cell system suggests that the truncated channel may cause cell death or attenuate proliferation. Instead of using stable lines, we studied capn-$InsP_3R1$ in transiently transfected N2a cells at early time points following transfection to minimize the impact of potentially confounding compensatory changes as seen in stable lines over-expressing wt-$InsP_3R1$ (Fischer et al., 1994; Mackrill et al., 1996; Davis et al., 1999). Furthermore, studying capn-$InsP_3R1$ in transiently transfected cells expressed under the CMV promoter strongly increases the probability that the recombinant truncated subunits form homotetramers. Thus, heteroligomerization of truncated subunits with endogenous, full-length $InsP_3R$ was unlikely in the studies presented here. However, understanding

[1] C.M. Kopil, H. Vais, K.-H.Cheung, A.P. Siebert, D.-O.D. Mak, J.K. Foskett, and R. W. Neumar, unpublished observation.

the possible existence and implications of heteroligomerization of truncated and full-length $InsP_3R$ requires additional studies.

Our approach to studying the functional consequence of calpain proteolysis of $InsP_3R1$ using capn-$InsP_3R1$ does have limitations. Foremost, it is unknown if the amino-terminus of $InsP_3R1$ completely dissociates from the channel domain following proteolysis. Limited digestion of cerebellar microsomes with trypsin results in channel fragments that remain associated via noncovalent or indirect interactions (Joseph et al., 1995; Yoshikawa et al., 1999). The trypsinized channel also remains functional, demonstrated by $InsP_3$-induced Ca^{2+} release from microsomes (Yoshikawa et al., 1999). Thus, expression of capn-$InsP_3R1$ may not accurately reflect the conformation that exists following proteolysis *in vivo*. Caspase-3 proteolysis of $InsP_3R1$ however, results in loss of $InsP_3$-mediated Ca^{2+} release from microsomes in a manner that corresponds to the percentage of digestion (Hirota et al., 1999). The same is likely true for calpain-cleaved $InsP_3R1$. By studying capn-$InsP_3R1$, we are likely examining a model of an $InsP_3R1$ channel in which all four subunits have been completely proteolyzed by calpain. Understanding the behavior of $InsP_3R1$ channels with both intact and calpain-cleaved subunits warrants future investigation.

Calpain-cleaved $InsP_3R1$ has $InsP_3$-independent, Ca^{2+}-dependent channel gating

To explore how calpain cleavage affects $InsP_3R1$ channel function, we examined the single channel properties of recombinant capn-$InsP_3R1$ using nuclear patch clamp electrophysiology. Recordings from N2a nuclei expressing recombinant $InsP_3R1$ revealed channels with smaller single channel conductances than that of endogenous

$InsP_3R$. This difference is potentially mediated by interactions with endogenous proteins, which may modulate recombinant rat $InsP_3R1$ activity differently than endogenous mouse $InsP_3R$. The low conductance of recombinant $InsP_3R1$ was cell type specific, as we did not observe such reduction in conductances when the channels were expressed in HEK293 cells.[2] Nevertheless, it provided a means to distinguish recombinant and endogenous $InsP_3R$ channels in N2a cells. In examining capn-$InsP_3R1$ specifically, we observed activity of single channels in patches in the absence of $InsP_3$, indicating that calpain cleavage does not eliminate channel function but instead leads to constitutive $InsP_3$-independent gating (Figure 2.4B). Previous studies of the caspase-3 cleaved form of $InsP_3R1$ similarly suggested that the proteolyzed channel retained activity (Nakayama et al., 2004; Verbert et al., 2008).

In addition to $InsP_3$, Ca^{2+} is the most important ligand for $InsP_3R1$ (Foskett et al., 2007). Even in saturating concentrations of $InsP_3$, $[Ca^{2+}]_i$ greater than 100 nM is required for the $InsP_3R1$ channel to be appreciably activated (Foskett et al., 2007). Unlike the $InsP_3$-binding site in $InsP_3R1$, which is known and missing in the carboxyl-terminal fragment generated by calpain proteolysis, the location of functionally important Ca^{2+} binding sites within the primary sequence of $InsP_3R1$ are largely unknown (Foskett et al., 2007). Therefore, while we expected that capn-$InsP_3R1$ activity would be $InsP_3$-independent if it formed a functional channel, we made no *a priori* assumptions about Ca^{2+} regulation of capn-$InsP_3R1$ activity. To experimentally determine if the Ca^{2+} requirement for channel activation was retained in capn-$InsP_3R1$, we also studied

[2] C.M. Kopil, H. Vais, K.-H.Cheung, A.P. Siebert, D.-O.D. Mak, J.K. Foskett, and R. W. Neumar, unpublished observation.

recombinant channel gating at non-optimal [Ca^{2+}] (70 nM and 25 μM). As expected, the P_o of wt-$InsP_3R1$ was significantly decreased at 70 nM and 25 μM Ca^{2+} compared with channel P_o at optimal 2 μM Ca^{2+} (Figure 2.5). Notably, the constitutively active capn-$InsP_3R1$ channel demonstrated a similar behavior (Figure 2.5). This result suggests that the carboxyl-terminal part of $InsP_3R1$ beyond residue 1917 contains functionally relevant Ca^{2+} binding sites involved in channel activation and inhibition. The P_o of capn-$InsP_3R1$ at 70 nM Ca^{2+} was, however, significantly greater than that of wt-$InsP_3R1$ at this [Ca^{2+}]. This difference may reflect loss of the high affinity, $InsP_3$-regulated Ca^{2+} binding site in the truncated channel (Foskett et al., 2007). However, because of the complexity of Ca^{2+} regulation of $InsP_3R$ channel activity, involving multiple functional Ca^{2+} binding sites (Foskett et al., 2010), future studies are required to determine what elements of Ca^{2+} regulation are modified in the truncated channel. These investigations may provide critical clues needed to identify additional Ca^{2+} binding sites within the primary $InsP_3R$ sequence.

Expression of capn-$InsP_3R1$ decreases Ca^{2+} content of intracellular Ca^{2+} stores

How does $InsP_3$-independent activity of capn-$InsP_3R1$ affect cellular Ca^{2+} regulation? Using changes in $[Ca^{2+}]_i$ to indirectly measure the Ca^{2+} content of intracellular stores, we observed that expression of capn-$InsP_3R1$ significantly reduced ionomycin releasable Ca^{2+} compared with wt-$InsP_3R1$ and EGFP controls, although it did not completely deplete intracellular stores (Figure 2.6A and C). The kinetics of the ionomycin response in capn-$InsP_3R1$ expressing cells was also slower than in EGFP wt-$InsP_3R1$ controls, which suggests a smaller Ca^{2+} driving force, consistent with a smaller

intracellular Ca^{2+} store. On the other hand, expression of capn-$InsP_3R1$ was not associated with an increased basal $[Ca^{2+}]_i$, suggesting that Ca^{2+} transport mechanisms were able to compensate for enhanced ER Ca^{+} leak through the cleaved channel, at least at the early times after transfection studied (Figure 2.6B). In ER Ca^{2+} imaging experiments, expression of capn-$InsP_3R1$ significantly reduced the steady-state Ca^{2+} loading capacity of the ER compared with wt-$InsP_3R1$ and EGFP controls (Figure 2.7A and B). The steady-state $[Ca^{2+}]_{ER}$ represents the equilibrium between the passive Ca^{+} leak and Ca^{2+} uptake by SERCA. Under steady-state filling conditions, the enhanced Ca^{2+} leak induced by expression of capn-$InsP_3R1$ exceeds the SERCA mediated Ca^{2+} uptake rate, resulting in lower $[Ca^{2+}]_{ER}$. The small effect of capn-$InsP_3R1$ expression on the ER filling rate may reflect the negligible driving force for Ca^{2+} leak under these conditions (Figure 2.7C). Of note, the ER leak rate in capn-$InsP_3R1$ was considerably higher than that observed in control or wt-$InsP_3R1$ expressing cells. (Figure 2.7D). Taken together, our results suggest that capn-$InsP_3R1$ acts as a Ca^{2+} leak channel that perturbs normal ER Ca^{2+} homeostasis.

The results from nuclear patch clamp electrophysiology and Ca^{2+} imaging experiments together elucidate the physiologic relevance of calpain-mediated $InsP_3R1$ proteolysis. Evidence that $InsP_3$-independent gating of capn-$InsP_3R1$ remains Ca^{2+} dependent may explain why expression of capn-$InsP_3R1$ induces only a moderate, albeit significant decrease in intracellular and ER Ca^{2+} stores, at least at the early time point examined following transfection (6 h). The electrophysiology data suggest that resting $[Ca^{2+}]_i$ is insufficient to fully activate the truncated channel, thus reducing the Ca^{2+} leak. It is interesting to speculate that this result may also account for conflicting findings

regarding the effects of caspase-3 cleavage of $InsP_3R1$ on Ca^{2+} homeostasis. Previous studies have reported that expression of caspase-cleaved $InsP_3R1$, which is only 26 residues longer than the calpain-cleaved form, either depletes (Nakayama et al., 2004) or does not deplete (Verbert et al., 2008) Ca^{2+} stores in the resting state. While it was agreed that caspase-3-cleaved $InsP_3R1$ represents a leak channel, the size and impact of that leak remains disputed. It is possible that different $[Ca^{2+}]_i$ in the two studies resulted in channels with different P_o, which would likely lead to distinct effects on cellular Ca^{2+} homeostasis. Electrophysiological recordings of caspase-cleaved $InsP_3R1$, similar to those performed here for capn-$InsP_3R1$, may clarify the functional consequences of caspase-mediated channel proteolysis.

$InsP_3R1$ is cleaved by calpain following ischemic brain injury

Under pathologic conditions, particularly those associated with elevated $[Ca^{2+}]_i$ and impaired ATP-dependent Ca^{2+} removal mechanisms, as in ischemia, calpain cleavage of $InsP_3R1$ may be an important mechanistic component of cell death. Brain ischemia and reperfusion dramatically disrupt neuronal Ca^{2+} homeostasis, and there is compelling evidence for a causal role of both Ca^{2+} overload and consequent pathologic calpain activation in ischemic neurodegeneration (Neumar, 2000; Bevers and Neumar, 2008). As both a Ca^{2+} regulatory protein and calpain substrate, $InsP_3R1$ is at a critical intersection between protease activation and disruption of cellular Ca^{2+} homeostasis during the molecular injury cascade. Here, we demonstrate that $InsP_3R1$ proteolysis occurs *in vivo* in an animal model of ischemic brain injury (Figure 2.8). In this cardiac arrest model, calpain cleavage of $InsP_3R1$ occurred in cerebellar Purkinje neurons, which are

selectively vulnerable to post-ischemic neurodegeneration (Neumar, 2000). Moreover, identification of calpain-cleaved $InsP_3R1$ in cerebellar microsomes as early as 1 h after cardiac arrest and reperfusion demonstrates that channel proteolysis is an early event in the cell death cascade rather than merely reflecting broad cellular degradation. The persistence and stability of calpain-cleaved $InsP_3R1$ at the latest time point examined after cardiac arrest (48 h) also suggests that the leaky, proteolyzed channel may act as a feed-forward mechanism for Ca^{2+} overload and increased calpain activation that eventually lead to neuronal death. In addition to $InsP_3R1$, a number of Ca^{2+} regulatory proteins are also calpain substrates, including the NMDA receptor, plasma membrane Ca^{2+}-ATPase, Na^+/Ca^{2+} exchanger, L-type Ca^{2+} channel, SERCA and ryanodine receptor (Bevers and Neumar, 2008). Thus, calpain cleavage of $InsP_3R1$ may be an important component of a broader pathway of calpain-mediated disruption of neuronal Ca^{2+} homeostasis in neurodegenerative diseases associated with Ca^{2+} dysregulation.

Conclusions

In summary, our results indicate that calpain proteolysis of $InsP_3R1$ creates an ER Ca^{2+} release channel that is $InsP_3$-independent and constitutively active. Expression of the truncated channel reduces the content of intracellular Ca^{2+} stores, which may have detrimental effects on Ca^{2+} signaling and buffering under pathologic conditions. Evidence of calpain cleavage of $InsP_3R1$ in neurons following cardiac arrest provides a potential mechanism to account for decreased $InsP_3$ binding (Nagasawa and Kogure, 1991; Dahl et al., 2000), depletion of ER Ca^{2+} stores (Kohno et al., 1997) and disruption of Ca^{2+} homeostasis reported in previous studies of *in vivo* brain ischemia. Together,

these results provide important insights into a molecular pathway that may act as a feed-forward mechanism to enhance cell death. Futhermore, the results presented here identify a novel target for therapeutic intervention following brain ischemia or in other neurodegenerative disorders associated with Ca^{2+} dysregulation and protease activation.

ACKNOWLEDGEMENTS

We thank Dr. Suresh Joseph (Thomas Jefferson University) and Dr. Robert Simon (University of Pennsylvania) for supplying antibodies. We thank Jun Yang for the GST-$InsP_3R1$ peptides in pGEX expression vectors and for his excellent technical expertise in cloning. We also thank Nicole Gorman and the Wistar Institute for help with N-terminal sequencing. This work was supported by National Institutes of Health grants NS039481 (RWN), NS069951 (RWN), NS071828 (CMK), MH059937 (JKF) and GM065830 (D-ODM and JKF), and American Heart Association Grant 0815440D (CMK).

FIGURES AND LEGENDS

Figure 2.1

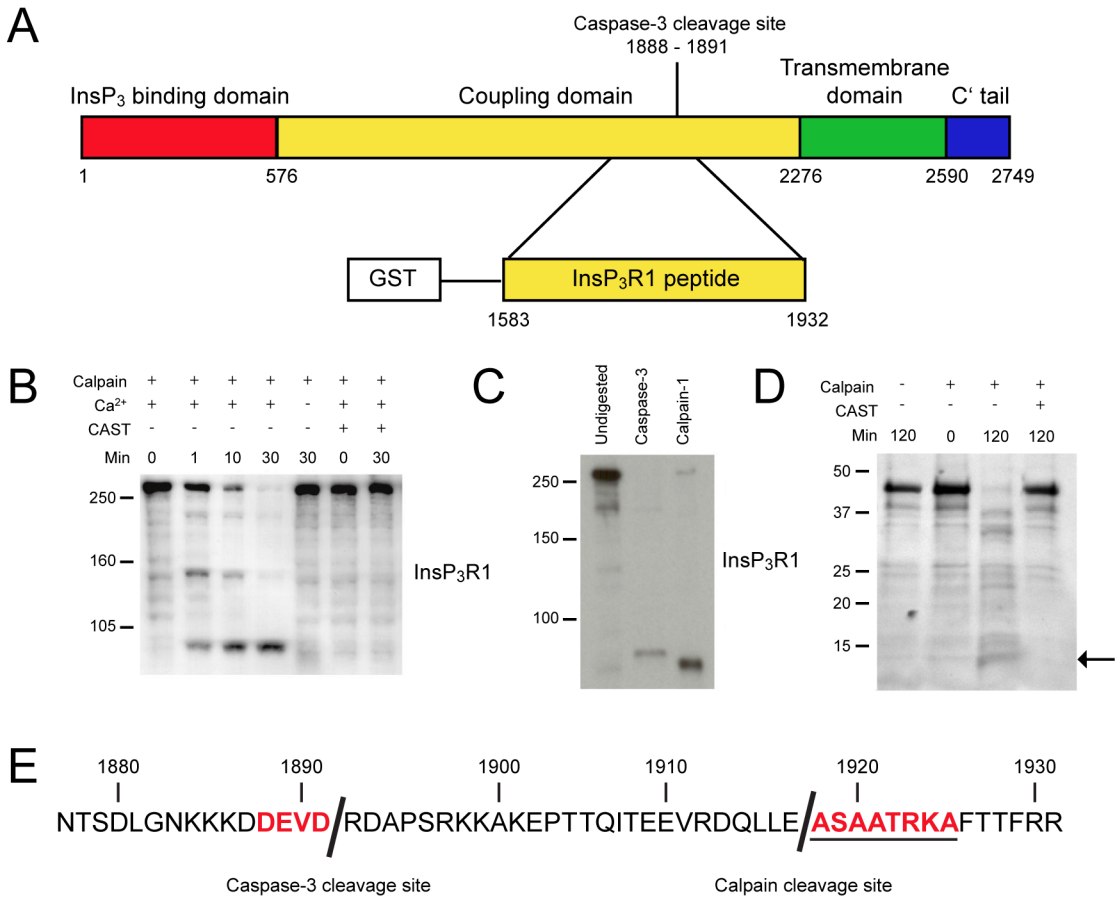

Figure 2.1 Calpain cleavage site in $InsP_3R1$

(*A*) Domain structure of $InsP_3R1$ protein (*top*), and GST-$InsP_3R1$ fusion peptide containing residues 1583 to 1932 (*bottom*). Residues numbered according to rat type 1 SI+, SII+, SIII- sequence (protein accession NP_001007236.1). (*B*) Western blot of rat cerebellar microsomes following *in vitro* digestion with calpain-1 using antibody against the carboxyl-terminal 20 amino acids of rat $InsP_3R1$ (1:5,000). Digestion with calpain-1 results in cleavage of $InsP_3R1$ into 200, 130 and 95 kDa carboxyl-terminal fragments. With longer digestion, the 95 kDa fragment becomes predominant. Proteolysis does not occur in the absence of Ca^{2+} and is blocked by the addition of the calpain inhibitor calpastatin (*CAST*), demonstrating the calpain dependence. (*C*) Western blot of microsomes following *in vitro* digest with caspase-3 (4 h) and calpain-1 (1 h) using carboxyl-terminal $InsP_3R1$ antibody, demonstrating difference in size of the resulting stable carboxyl-terminal $InsP_3R1$ fragments. (*D*) Amido black protein stain of PVDF membrane demonstrating calpain-mediated degradation of the GST-$InsP_3R1$ fusion peptide. *Arrow* indicates unique calpain-degradation product, which was not present in samples without exogenous calpain or samples treated with CAST. The ~12 kDa band (*arrow*) was submitted for N-terminal sequencing. (*E*) Amino acid sequence of $InsP_3R1$ at caspase-3 and calpain-cleavage sites. DEVD consensus sequence for caspase-3 proteolysis highlighted in *red*. The new N-terminus of $InsP_3R1$ generated by calpain proteolysis and the sequence identified by Edman N-terminal sequencing is *underlined* and highlighted in *red*.

Figure 2.2

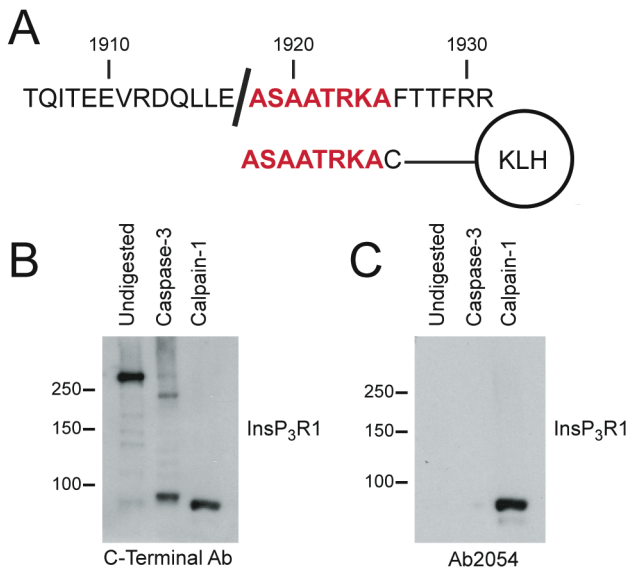

Figure 2.2 Antibody targeted against calpain-cleaved $InsP_3R1$

(*A*) Calpain cleavage site of rat $InsP_3R1$ and corresponding synthetic peptide used to generate polyclonal antibody Ab2054. (*B*) Western blot of rat cerebellar microsomes following *in vitro* digestion with caspase-3 or calpain 1 using carboxyl-terminal $InsP_3R1$ antibody that reacts with unproteolyzed, caspase-cleaved and calpain-cleaved $InsP_3R1$. (*C*) Western blot in B, stripped and reprobed using Ab2054 (1:10,000). Ab2054 reacts specifically with the 95 kDa carboxyl-terminal fragment of calpain-cleaved $InsP_3R1$.

Figure 2.3

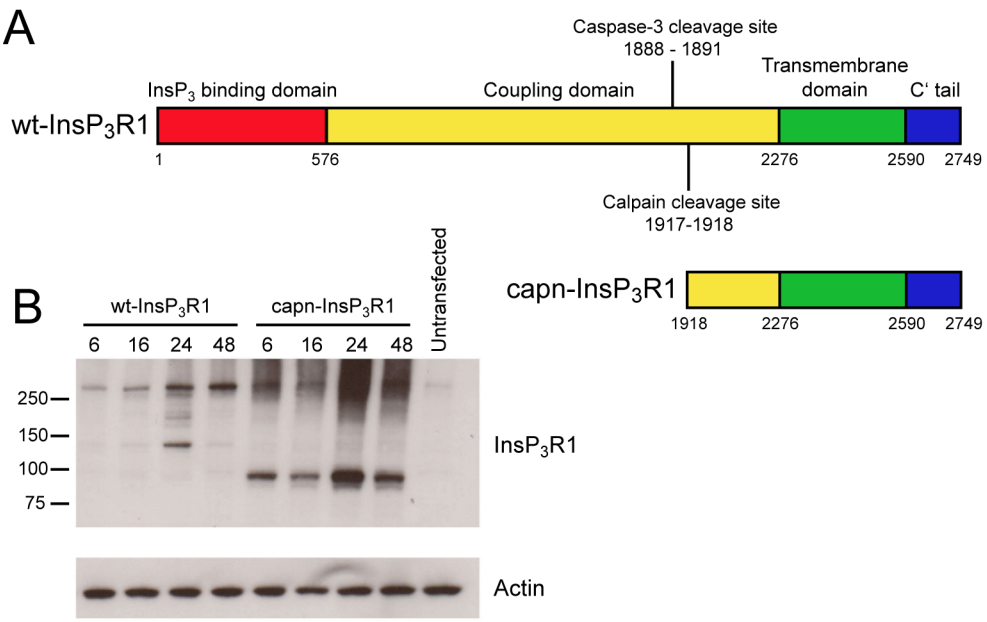

Figure 2.3 Schematic representation and expression of recombinant capn-$InsP_3R1$

(*A*) Domain structure of the full-length (wt) and calpain-cleaved $InsP_3R1$ recombinant proteins. (*B*) Western blot analysis of whole cell lysates from untransfected N2a cells or N2a cells expressing wt- or capn-$InsP_3R1$ at 6, 16, 24 and 48 h post-transfection. Carboxyl-terminal $InsP_3R1$ antibody was used to detect endogenous and recombinant $InsP_3R1$. Antibody against actin (1:3,000) used as loading control.

Figure 2.4

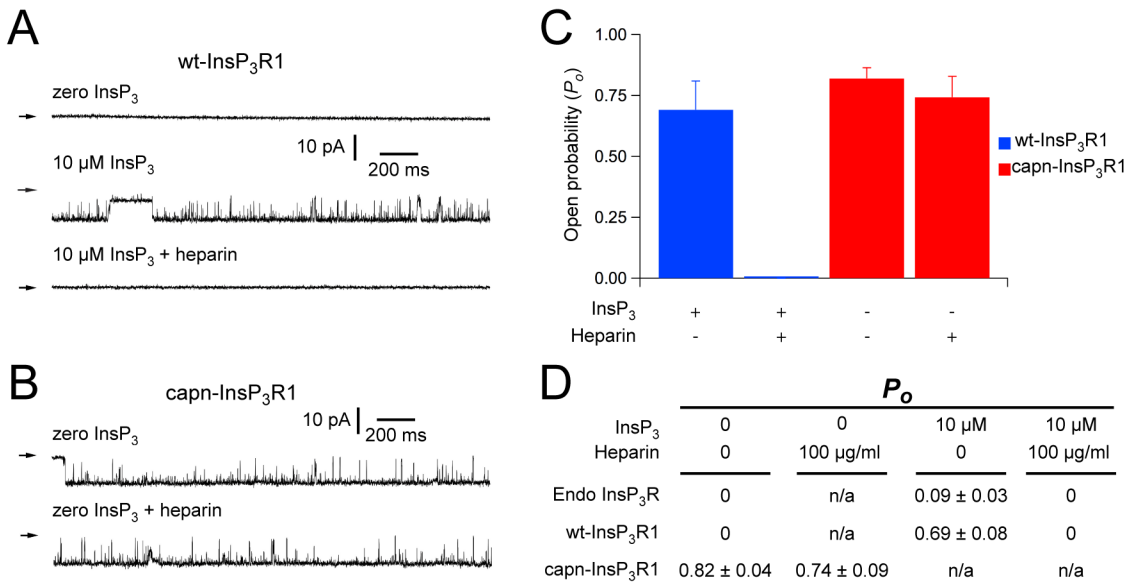

Figure 2.4 Capn-InsP$_3$R1 channel activity in the absence of InsP$_3$

(*A*) Representative current traces recorded in outer membrane of nuclei isolated from N2a cells transfected with wt-InsP$_3$R1 in the absence (*top panel*) or presence (*middle/bottom panels*) of saturating InsP$_3$ in the pipette solution. Pipette solution contained 2 μM Ca^{2+}. *Arrow* indicates closed channel current level. Channel activity of wt-InsP$_3$R1 required InsP$_3$ and was inhibited by heparin. (*B*) Representative current recordings in isolated nuclei from N2a cells expressing capn-InsP$_3$R1 in absence of InsP$_3$. Heparin did not inhibit channel activity of capn-InsP$_3$R1, confirming that InsP$_3$-independent gating was not caused by local InsP$_3$ in the patch pipette. (*C*) Summary of effects of InsP$_3$ and heparin on P_o of recombinant InsP$_3$R1. (*D*) Summary of P_o from endogenous InsP$_3$R (*Endo InsP$_3$R*) and recombinant wt- and capn-InsP$_3$R1. There is no statistically significant difference between mean P_o values of recombinant wt- and capn-InsP$_3$R1 by one-way ANOVA.

Figure 2.5

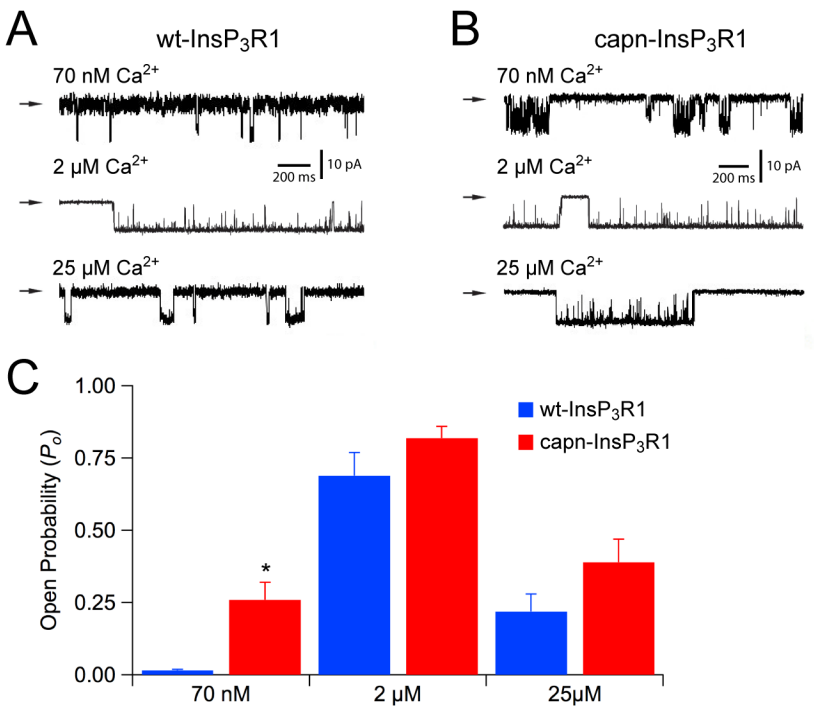

Figure 2.5 Ca^{2+} regulation of capn-$InsP_3R1$

(*A*) Representative current traces recorded in outer membrane of nuclei isolated from N2a cells transfected with wt-$InsP_3R1$ with 10 μM $InsP_3$ and 70 nM (*top*), 2 μM (*middle*), or 25 μM (*bottom*) Ca^{2+} included in the pipette solution. (*B*) Representative current traces recorded in outer membrane of nuclei isolated from N2a cells transfected with capn-$InsP_3R1$ in the absence of $InsP_3$ with 70 nM (*top*), 2 μM (*middle*), or 25 μM (*bottom*) Ca^{2+}. (*C*) Summary of effects of [Ca^{2+}] on P_o of wt- and capn-$InsP_3R1$ (P_o data at 2 μM Ca^{2+} are the same as shown in Figure 2.4). P_o of both wt- and capn-$InsP_3R1$ at 70 nM and 25 μM Ca^{2+} were decreased compared to the P_o of either channel at 2 μM Ca^{2+} (unpaired *t*-tests, $p<0.001$). At 70 nM Ca^{2+}, P_o of capn-$InsP_3R1$ was higher than that of wt-$InsP_3R1$ at 70 nM Ca^{2+} (unpaired *t*-test with unequal variance; *, $p<0.001$).

Figure 2.6

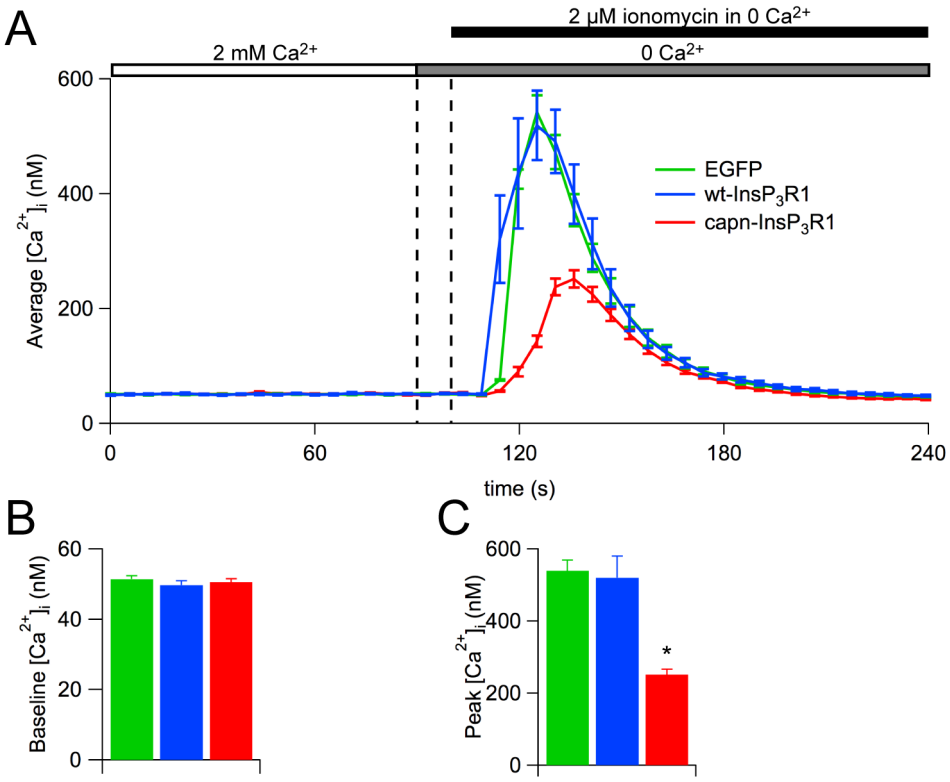

Figure 2.6 Expression of capn-InsP$_3$R1 decreases Ca^{2+} content of intracellular stores

(*A*) Averaged single-cell $[Ca^{2+}]_i$ responses to 2 μM ionomycin in Fura-2 loaded N2a cells transfected with empty vector (*green*), wt-InsP$_3$R1 (*blue*) or capn-InsP$_3$R1 (*red*). (*B*) Summary of resting $[Ca^{2+}]_i$. (*C*) Summary of peak $[Ca^{2+}]_i$ responses elicited by 2 μM ionomycin, demonstrating a decrease in releasable Ca^{2+} in capn-InsP$_3$R1 expressing cells (unpaired *t*-tests with unequal variance; *, $p<0.001$).

Figure 2.7

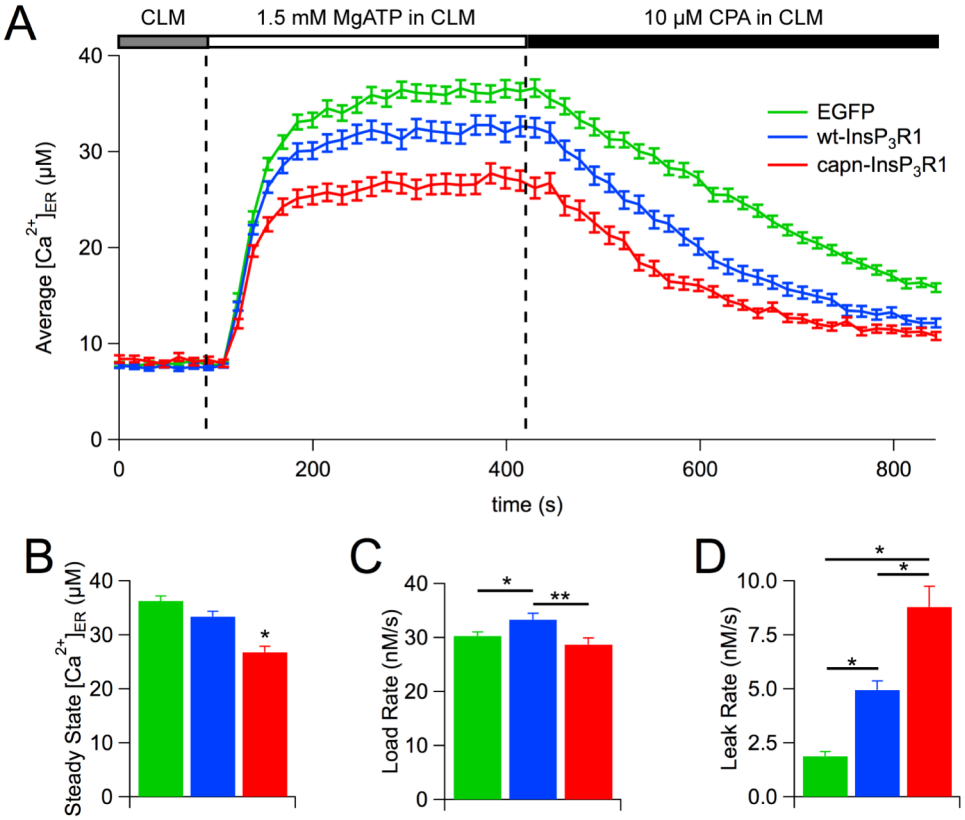

Figure 2.7 Capn-InsP$_3$R1 decreases ER Ca^{2+} loading

(*A*) Averaged single-cell responses demonstrating ER Ca^{2+} loading and release in response to 1.5 mM MgATP and 10 µM CPA/ 0 ATP, respectively. Averaged traces are from permeabilized Mag-Fura-2 loaded N2a cells transfected with empty vector (*green*), wt-InsP$_3$R1 (*blue*) or capn-InsP$_3$R1 (*red*). (*B*) Summary of steady state $[Ca^{2+}]_{ER}$, showing decreased ER loading in cells expressing capn-InsP$_3$R1 (one-way ANOVA; *, $p<0.001$). (*C*) Summary of averaged single-cell ER loading rates in response to MgATP stimulation of SERCA in transfected cells (unpaired *t*-tests; *, $p<0.05$, **, $p<0.01$). (*D*) Summary of averaged single-cell ER leak rates in response to CPA inhibition of SERCA in transfected cells. Expression of capn-InsP$_3$R1 and to a lesser extent wt- InsP$_3$R1 increase leak rate compared to control (unpaired *t*-tests with unequal variance; *, $p<0.001$).

Figure 2.8

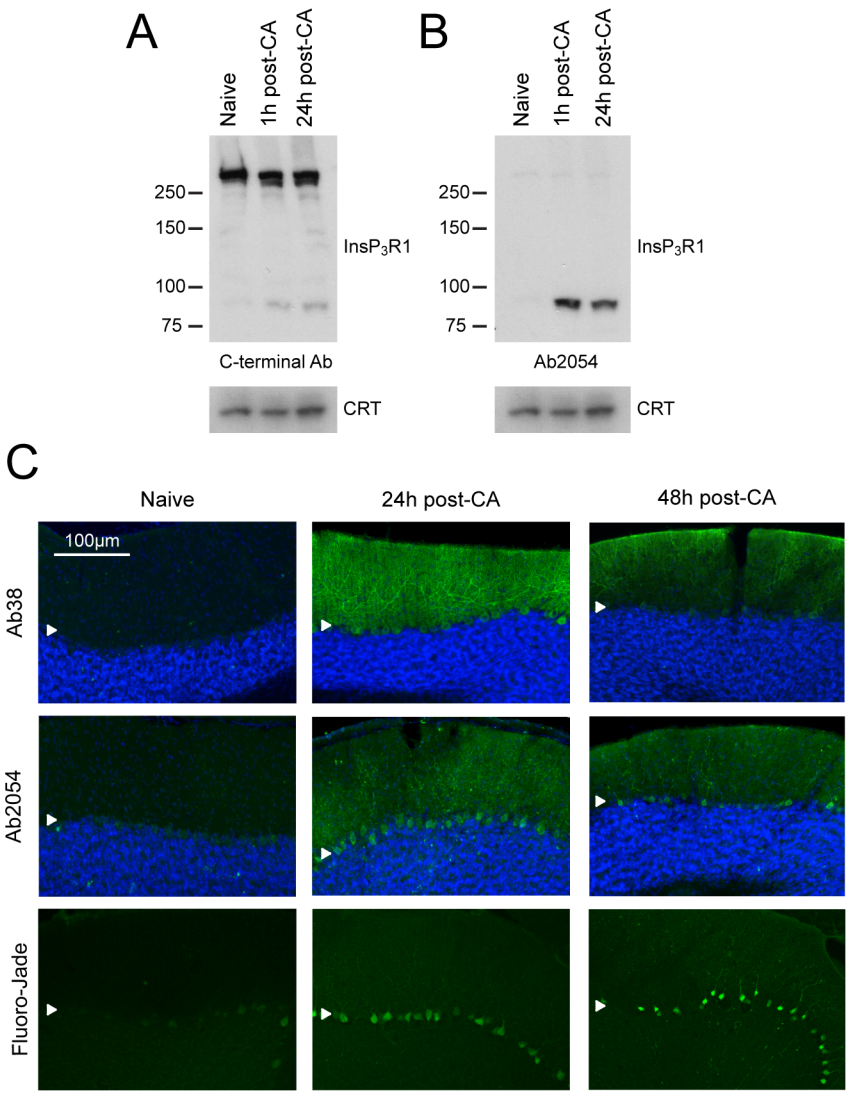

Figure 2.8 Calpain-cleavage of $InsP_3R1$ *in vivo* following cardiac arrest

Western blot of rat cerebellar microsomes 1 and 24 h after resuscitation from cardiac arrest. (*A*) A carboxyl-terminal $InsP_3R1$ antibody used to detect full-length and cleaved $InsP_3R1$ shows the appearance of a faint band at 95 kDa with cardiac arrest. An antibody against calreticulin (*CRT*; 1:1,000) was used as a loading control. (*B*) Western blot in A stripped and reprobed with Ab2054, demonstrating calpain-cleaved $InsP_3R1$ in post-cardiac arrest samples. (*C*) Immunofluorescence staining of naïve rat cerebellum and rat cerebellum 24 and 48 h after resuscitation from cardiac arrest. *Arrows* indicate Purkinje cell layer. Ab38 (1:10,000; *top panel*) was used as a marker of calpain-activity with a Hoechst counterstain. Following heat-induced epitope retrieval, Ab2054 (1:10,000; *middle panel*) labels calpain-cleaved $InsP_3R1$ with a Hoechst counterstain. Fluoro-Jade B was used to label degenerating neurons (*bottom panel*). Here, we detect calpain-activity, calpain-cleaved $InsP_3R1$ and neurodegeneration in Purkinje cells from post-cardiac arrest brains.

SUPPLEMENTAL DATA

Supplemental Figure 2.1

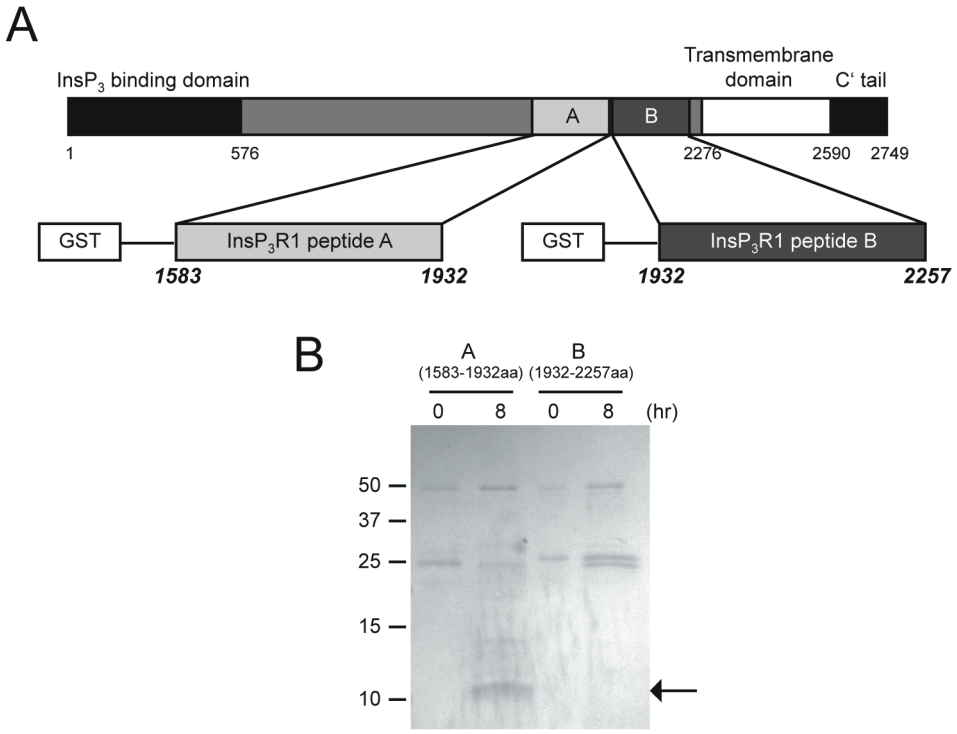

Supplemental Figure 2.1 Site-specific calpain proteolysis of $InsP_3R1$

(*A*) Schematic of the linear $InsP_3R1$ protein with regions corresponding to two different GST-$InsP_3R1$ fusion peptides indicated as A and B (*top*). GST-$InsP_3R1$ fusion peptides containing residues 1583 to 1932 (peptide A) or residues 1932 to 2257 (peptide B) are also depicted (*bottom*). (*B*) Amido black protein stain of PVDF membrane demonstrating calpain mediated degradation of GST-$InsP_3R1$ fusion peptide A following 8 h incubation with exogenous calpain 1. *Arrow* indicates the unique calpain-degradation product, which was not present in either undigested peptide or calpain-digested fusion peptide B.

Supplemental Figure 2.2

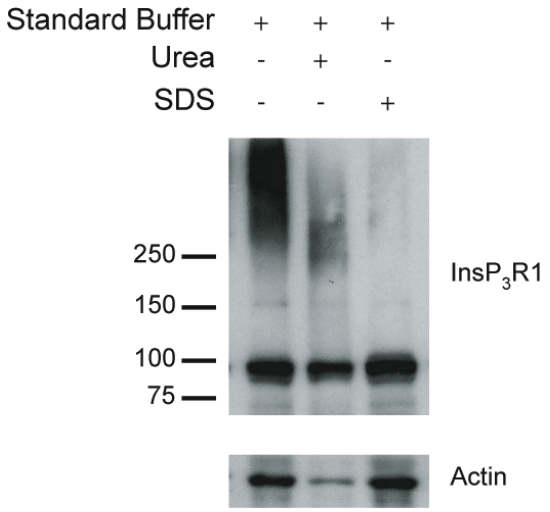

Supplemental Figure 2.2 High molecular weight smears of capn-InsP$_3$R1 can be solubilized and denatured

Western blot analysis of whole cell lysates from N2a cells expressing capn-InsP$_3$R1 at 24 h post-transfection. Cells were harvested in standard homogenization buffer (*lane 1*) or buffer supplemented with 5 M urea (*lane 2*) or 1% SDS (*lane 3*). Lysis buffer containing urea or SDS resolved the high molecular weight smear associated with expression of capn-InsP$_3$R1. Carboxyl-terminal InsP$_3$R1 antibody was used to detect endogenous and recombinant InsP$_3$R1. Antibody against actin was used as loading control.

Supplemental Figure 2.3

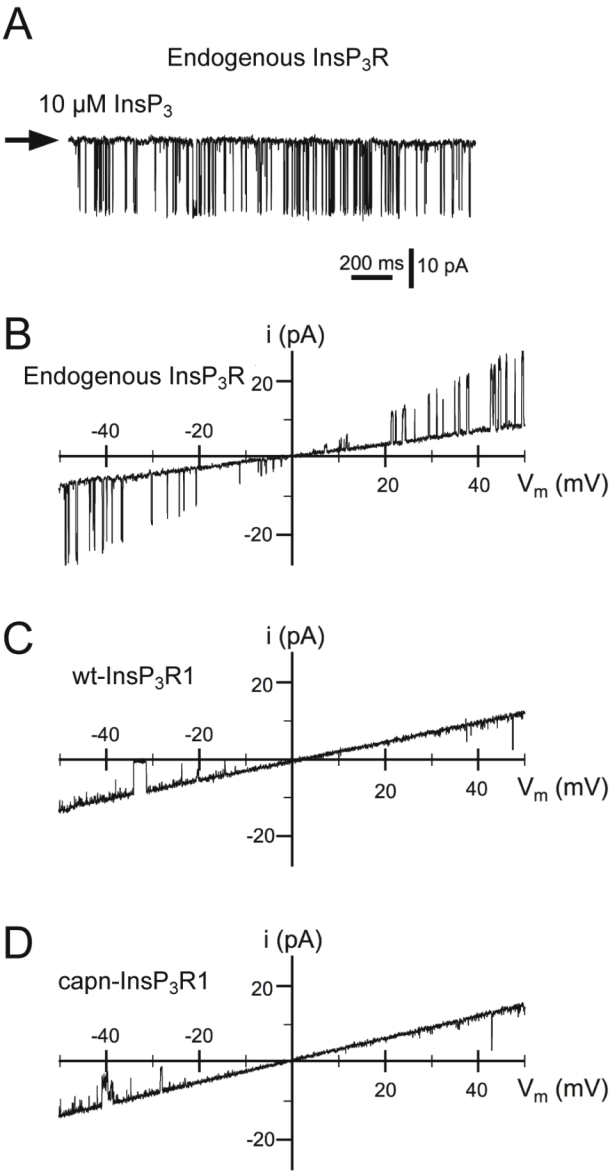

Supplemental Figure 2.3 Recombinant rat $InsP_3R1$ channels have smaller conductances than endogenous $InsP_3R$ in N2a cells

(*A*) Representative current traces recorded in outer membrane of nuclei isolated from untransfected N2a cells with 2 μM Ca^{2+} and 10 μM $InsP_3$ included in the pipette solution. Channel activity of endogenous $InsP_3R$ required $InsP_3$. (*B*) I-V relation from voltage-ramp protocol for endogenous $InsP_3R$ in untransfected N2a cells. (*C*) I-V relation for recombinant wt-$InsP_3R1$ with 2 μM Ca^{2+} in presence of $InsP_3$. (*D*) I-V relation for capn-$InsP_3R1$ from voltage-ramp protocol with 2 μM Ca^{2+} in absence of $InsP_3$. Capn-$InsP_3R1$ displays linear I-V relation, characteristic of $InsP_3R1$.

Portions to be submitted for peer-reviewed publication

Calpain-cleaved Type 1 Inositol 1,4,5-Trisphosphate Receptor Impairs Neuronal ER Ca^{2+} Buffering and Causes Neurodegeneration in Primary Cortical Neurons and Hippocampal Neurons *In Vivo*

Catherine M. Kopil[1]; Adam P. Siebert[2]; J. Kevin Foskett[2,4]; Robert W. Neumar[1,§]

From the Departments of Emergency Medicine[1], Physiology[2], and Cell and Developmental Biology[4], University of Pennsylvania, Philadelphia, PA 19104

[§]**Corresponding Author:**

Robert W. Neumar, MD, PhD

Phone: (215) 898-4960

Fax: (215) 573-5140

Email: neumarr@uphs.upenn.edu

Number of Figures / Supplemental Figures: 6 / 4

Number of Pages: 29

SUMMARY

Disruption of neuronal Ca^{2+} homeostasis plays a well-established role in cell death in a number of neurodegenerative disorders. Recent evidence suggests that proteolysis of the type 1 inositol 1,4,5-trisphosphate receptor ($InsP_3R1$), a Ca^{2+} release channel on the endoplasmic reticulum (ER), generates a dysregulated channel, which may contribute to aberrant Ca^{2+} signaling and neurodegeneration in disease states. However, the specific effects of $InsP_3R1$ proteolysis on neuronal Ca^{2+} homeostasis are unknown, as are the functional contributions of this pathway to neuronal death. This study evaluates the consequences of calpain-mediated $InsP_3R1$ proteolysis on neuronal Ca^{2+} signaling and survival using adeno-associated viruses to express a recombinant cleaved form of the channel (capn-$InsP_3R1$) both *in vitro* and *in vivo*. Here, we demonstrate that expression of capn-$InsP_3R1$ in rat primary cortical neurons reduced cellular viability. This effect was associated with increased resting cytoplasmic Ca^{2+} concentration ($[Ca^{2+}]_i$), increased $[Ca^{2+}]_i$ response to glutamate, and enhanced sensitivity to excitotoxic stimuli. *In vivo*, expression of capn-$InsP_3R1$ in rat brain triggered selective degeneration of CA2 pyramidal neurons in the hippocampus. Together, our results demonstrate that $InsP_3R1$ proteolysis disrupts neuronal Ca^{2+} homeostasis, and potentially acts as a feed-forward pathway to initiate or execute neuronal death.

INTRODUCTION

Spatial and temporal regulation of cytoplasmic free Ca^{2+} concentration ($[Ca^{2+}]_i$) plays a vital role in neuronal signaling, and dysregulation of $[Ca^{2+}]_i$ can trigger neuronal cell death (Berridge et al., 2000; Berridge et al., 2003; Orrenius et al., 2003; Mattson, 2007). Under physiological conditions, changes in neuronal $[Ca^{2+}]_i$ are tightly controlled by transmembrane Ca^{2+} pumps, Ca^{2+}-binding proteins, and intracellular organelles. The endoplasmic reticulum (ER), the primary Ca^{2+} storage organelle in neurons, is capable of both Ca^{2+} sequestration and release. Proper ER Ca^{2+} regulatory function is essential to neuronal $[Ca^{2+}]_i$ buffering, signaling, and survival (Mattson et al., 2000; Bardo et al., 2006; Stutzmann and Mattson, 2011).

A ubiquitous mechanism for Ca^{2+} signaling in neurons is Ca^{2+} release from the ER lumen through the inositol 1,4,5-trisphosphate receptor ($InsP_3R$) (Foskett et al., 2007). Of the 3 identified $InsP_3R$ genes, type 1 $InsP_3R$ ($InsP_3R1$) is the most abundant isoform expressed in the brain (Furuichi et al., 1993; Sharp et al., 1993). Physiological $InsP_3R1$-mediated Ca^{2+} signaling in neurons is important for gene expression, synaptic plasticity, membrane excitability, and learning and memory (Furuichi and Mikoshiba, 1995; Bardo et al., 2006; Foskett et al., 2007). $InsP_3R1$ dysfunction has been implicated in a number of neurodegenerative disease states as a mechanism for impaired ER Ca^{2+} buffering, disruption of neuronal Ca^{2+} homeostasis, and neuronal death (Verkhratsky and Toescu, 2003; Foskett, 2010). In most of these cases, $InsP_3R1$ dysfunction has been associated with allosteric modulation of the channel (Foskett et al., 2007). However, increasing evidence suggests that proteolytic modification of $InsP_3R1$ can also

dramatically disrupt channel physiology (Assefa et al., 2004; Nakayama et al., 2004; Verbert et al., 2008; Kopil et al., 2011), and may potentially contribute to neurodegeneration.

$InsP_3R1$ is a target for caspase-3 and calpain-mediated proteolysis, which generate similarly sized ~95 kDa carboxyl-terminal fragments (Magnusson et al., 1993; Wojcikiewicz and Oberdorf, 1996; Hirota et al., 1999; Haug et al., 2000; Kopil et al., 2011). Both caspase and calpain-mediated proteolysis of $InsP_3R1$ remove the amino-terminal ligand-binding domain and a large portion of the coupling domain, leaving the pore-forming transmembrane domains intact. Studies examining the functional properties of the caspase-derived carboxyl-terminal $InsP_3R1$ fragment demonstrated increased ER Ca^{2+} leak, and corresponding decreased ER $[Ca^{2+}]$ ($[Ca^{2+}]_{ER}$) and buffering capacity in cell lines expressing the recombinant channel (Assefa et al., 2004; Nakayama et al., 2004; Verbert et al., 2008). These effects were mediated by $InsP_3$-independent Ca^{2+} release through caspase-cleaved $InsP_3R1$, and expression of the truncated channel increased cellular sensitivity to apoptotic stimuli (Assefa et al., 2004). Our laboratory recently identified the calpain-cleavage site for $InsP_3R1$ and determined that the calpain-derived carboxyl-terminal channel fragment displayed $InsP_3$-independent gating and constitutive channel activity (Kopil et al., 2011). When expressed in cell lines, calpain-cleaved $InsP_3R1$ decreased $[Ca^{2+}]_{ER}$ via increased ER Ca^{2+} leak (Kopil et al., 2011). Although no study to date has investigated the effects of caspase- or calpain-cleaved $InsP_3R1$ on neuronal Ca^{2+} homeostasis, these observations suggest that proteolysis of $InsP_3R1$ may profoundly transform spatial and temporal regulation of neuronal $[Ca^{2+}]_i$

and potentially signal cell death. Consistent with this hypothesis, we previously identified calpain-cleaved $InsP_3R1$ in selectively vulnerable cerebellar Purkinje cells at both early and late times following ischemic brain injury (Kopil et al., 2011).

To define the role of $InsP_3R1$ proteolysis in disruption of neuronal Ca^{2+} homeostasis and neurodegeneration, we examined responses of primary neurons and neurons *in vivo* to expression of calpain-cleaved $InsP_3R1$. Expression of the cleaved channel reduces viability of primary cortical neurons, and increases their sensitivity to excitotoxic injury. Using single-cell Ca^{2+} imaging, we have determined that calpain-cleaved $InsP_3R1$ increases resting neuronal $[Ca^{2+}]_i$ and leads to greater rises in $[Ca^{2+}]_i$ in response to physiological stimuli. Interestingly, we found that expression of calpain-cleaved $InsP_3R1$ also causes degeneration of a select subpopulation of hippocampal neurons *in vivo*. Together, these data suggest a specific role for proteolyzed $InsP_3R1$-mediated Ca^{2+} signaling in the molecular injury cascade in neurons, which has important therapeutic implications for neurodegenerative disorders associated with Ca^{2+} dysregulation.

RESULTS

Expression of recombinant $InsP_3R1$ constructs in primary cortical neurons

Previously, we showed that expression of a recombinant form of rat $InsP_3R1$ corresponding to the stable carboxyl-terminal fragment generated by calpain proteolysis (capn-$InsP_3R1$; Δ1-1917; Figure 3.1A) altered $[Ca^{2+}]_i$ homeostasis in immortalized cell lines. In the current study we examined the functional consequences of capn-$InsP_3R1$ expression in neurons, which are a more metabolically demanding and electrically active cell type. To achieve high transduction efficiency of primary cortical cultures, we utilized adeno-associated virus (AAV) 2/1 mediated gene delivery of capn-$InsP_3R1$, which transduces over 90% of cells in primary mixed cortical cultures (Royo et al., 2008; Bevers et al., 2009). As a control for $InsP_3$-independent Ca^{2+} release through the truncated channel, we generated AAV 2/1 vector expressing capn-$InsP_3R1$ with a D2550A point mutation in the putative pore-forming region of the channel (capn-$InsP_3R1$ D2550A; Figure 3.1A). This point mutation eliminates Ca^{2+} permeability of wild type (wt) $InsP_3R1$ (Boehning and Joseph, 2000; Boehning et al., 2001; Cardenas et al., 2010). Because of the genome size of AAV, viral packaging capacity of transgenes is limited (Dong et al., 1996), and we were unable to generate control AAV vectors expressing the 8.5 kb full-length $InsP_3R1$ with or without the D2550A mutation. We used AAV 2/1 expressing lacZ to control for effects of viral transduction.

To examine expression of $InsP_3R1$ constructs in neurons, we stably transduced cortical cultures with AAV 2/1 expressing capn-$InsP_3R1$, capn-$InsP_3R1$ D2550A, or lacZ

at 7 d *in vitro* (DIV) and harvested cells 1 week later (14 DIV). Western blotting of whole-cell lysates using a carboxyl-terminal $InsP_3R1$ antibody demonstrated expression of endogenous 260 kDa wt-$InsP_3R1$ in all samples (Figure 3.1B). In lysates from cultures transduced with capn-$InsP_3R1$ and capn-$InsP_3R1$ D2550A, we also detected the 95 kDa form of the channels confirming expression of our recombinant $InsP_3R1$ constructs.

Expression of capn-$InsP_3R1$ reduces viability of primary cortical neurons

To determine the effects of capn-$InsP_3R1$ on viability of primary cortical neurons, we transduced 7 DIV cultures with capn-$InsP_3R1$, capn-$InsP_3R1$ D2550A, or lacZ control vectors. One week post-transduction (14 DIV), we immunostained the cultures for microtubule associated protein 2 (MAP2; Figure 3.2A, left) and quantified the number of surviving neurons (Figure 3.2B). Expression of capn-$InsP_3R1$ resulted in significant decrease in the percentage of viable neurons compared with expression of capn-$InsP_3R1$ D2550A or lacZ (capn-$InsP_3R1$=65.3 ± 5.5%, capn-$InsP_3R1$ D2550A=112.7 ± 5.8%, lacZ=100.0 ± 3.8%; $p<0.001$). To confirm the capn-$InsP_3R1$ toxicity phenotype, we incubated transduced cultures with calcein-AM and propidium iodide (PI) to identify living and dead cells respectively (Figure 3.2A, right). A significant decrease in the percentage of surviving cells was again observed in cultures transduced with capn-$InsP_3R1$ compared with controls (capn-$InsP_3R1$=76.7 ± 4.5%, capn-$InsP_3R1$ D2550A=112.5 ± 6.5%, lacZ=100.0 ± 4.0%; $p<0.001$; Figure 3.2C). Interestingly, the percentage of viable cells in capn-$InsP_3R1$-transduced cultures determined by calcein-AM and PI staining was significantly higher than the percent of viable cells in the same cultures quantified by counts of MAP2 labeled cells ($p<0.05$). This likely reflects the

mixed constituents of the cortical cultures, which contain ~10% glia [3] that are identified using calcein-AM but not MAP2, suggesting that glial viability is not altered by capn-$InsP_3R1$. Together, these results suggest that expression of capn-$InsP_3R1$ specifically reduces neuronal viability.

We hypothesized that expression of capn-$InsP_3R1$ reduced neuronal viability by disrupting intracellular Ca^{2+} homeostasis. The recombinant cleaved channel, which has $InsP_3$-independent gating and increases ER Ca^{2+} leak (Kopil et al., 2011), could potentially trigger neurodegeneration through either ER Ca^{2+} depletion and induction of ER stress, or by increased $[Ca^{2+}]_i$ and feed-forward activation of proteases. To examine the mechanism responsible for capn-$InsP_3R1$ reductions in neuronal viability, we performed Western blotting of whole-cell lysates from transduced cultures. Using an antibody against the stress-inducible ER chaperone protein BiP (Supplemental Figure 3.1A), we did not detect differences in activation of the ER stress pathway in capn-$InsP_3R1$-transduced cultures compared with controls (Supplemental Figure 3.1B). Nor did we detect differences in calpain or caspase-3 protease activation using an antibody against a shared substrate, α-spectrin (Supplemental Figures 3.1C and D). Absence of Western blot evidence of increased ER stress or protease activation with expression of capn-$InsP_3R1$ does not conclusively imply that neither pathologic cascade plays a causal role in capn-$InsP_3R1$ induced neuronal death. However, if either pathway is responsible for executing cell death in capn-$InsP_3R1$-transduced cultures, Western blotting of neuronal lysates is not sensitive enough to detect it at the times examined here.

[3] C.M. Kopil, A.P. Siebert, J.K. Foskett and R.W. Neumar, unpublished observation.

Capn-InsP$_3$R1 does not deplete intracellular Ca^{2+} stores

Previous data from our laboratory indicated that capn-InsP$_3$R1 functions as a Ca^{2+} leak channel in the ER (Kopil et al., 2011). To examine whether this leak was sufficient to deplete intracellular Ca^{2+} stores in neurons, we utilized single-cell Ca^{2+} imaging to measure InsP$_3$-induced changes in [Ca^{2+}]$_i$. We monitored somatic [Ca^{2+}]$_i$ using Fura-2 in primary cortical cultures transduced with capn-InsP$_3$R1, capn-InsP$_3$R1 D2550A or lacZ (Figure 3.3A). To stimulate Ca^{2+} release from InsP$_3$-sensitive stores, we applied saturating concentrations of the Group I metabotropic glutamate receptor agonist (S)-3,5-dihydroxyphenylglycine (DHPG; 10 μM). Expression of capn-InsP$_3$R1 significantly increased resting [Ca^{2+}]$_i$ in neurons (90 ± 3.3 nM) compared with capn-InsP$_3$R1 D2550A (70 ± 1.8 nM) and lacZ controls (70 ± 1.6 nM; p<0.001; Figure 3.3B), supporting previous evidence that capn-InsP$_3$R1 leaks Ca^{2+} from the ER. Application of DHPG elicited responses, defined as >10% increase from baseline, in a majority of neurons from all transduced cultures (Figure 3.3C). Despite the apparent basal Ca^{2+} leak through the cleaved channel, expression of capn-InsP$_3$R1 did not affect the DHPG-induced peak [Ca^{2+}]$_i$ in neurons (Figure 3.3D) or the maximum change in [Ca^{2+}]$_i$ from baseline to peak (Figure 3.3E). These data demonstrate that expression of the cleaved channel, while sufficient to increase resting [Ca^{2+}]$_i$, does not deplete [Ca^{2+}]$_{ER}$.

Decreased ER Ca^{2+} buffering in neurons expressing capn-InsP$_3$R1

To examine the effect of calpain-cleaved InsP$_3$R1 on neuronal Ca^{2+} homeostasis more broadly, we measured changes in [Ca^{2+}]$_i$ in response to acute glutamate (10 μM) application (Figure 3.4A), which activates both ionotropic and metabotropic glutamate

receptors (Michaelis, 1998). Consistent with results from Ca^{2+} imaging experiments above, resting $[Ca^{2+}]_i$ was significantly increased in neurons expressing capn-$InsP_3R1$ compared with capn-$InsP_3R1$ D2550A and lacZ expressing cells ($p<0.001$; Figure 3.4B). Additionally, expression of capn-$InsP_3R1$ significantly increased the glutamate-induced peak $[Ca^{2+}]_i$ (1,520 ± 43 nM) compared with capn-$InsP_3R1$ D2550A (1,030 ± 36 nM) and lacZ controls (940 ± 25 nM; $p<0.001$; Figure 3.4C). Stimulation of an alternate pathway for Ca^{2+} influx also resulted in a significantly increased peak $[Ca^{2+}]_i$ in cultures transduced with capn-$InsP_3R1$ (50 mM KCl; Supplemental Figure 3.2). This result suggests that the increased glutamate-induced $[Ca^{2+}]_i$ in capn-$InsP_3R1$-transduced neurons is not dependent on increased glutamate receptor expression. Instead, the increased $[Ca^{2+}]_i$ rise is likely due to an impaired ability to buffer Ca^{2+} influx from the extracellular space. Together, these data indicate that capn-$InsP_3R1$ disrupts normal intracellular Ca^{2+} homeostasis.

Capn-$InsP_3R1$ increases sensitivity to glutamate-induced neurotoxicity

To determine whether the observed capn-$InsP_3R1$-induced impairment of ER Ca^{2+} buffering increased neuronal susceptibility to excitotoxic injury, we exposed transduced 14 DIV primary cortical cultures to 1 μM glutamate or HEPES buffered saline (HBS) vehicle. We selected this dose from initial studies performed in untransduced cultures, where treatment with 1 μM glutamate resulted in negligible injury (Supplemental Figure 3.3). After incubation in glutamate for 24 h, the cultures were immunostained for MAP2 to quantify the number of surviving neurons (Figure 3.5A). To account for baseline

differences in viability between capn-InsP$_3$R1- and control-transduced cultures, the percentage of MAP2-positive neurons in glutamate-injured cultures was normalized to vehicle-treated cultures transduced with the same vector. Exposure to 1 μM glutamate resulted in significant loss of neurons in all cultures compared with vehicle treated controls (p<0.05). Interestingly, cultures transduced with capn-InsP$_3$R1 were particularly susceptible (survival: capn-InsP$_3$R1=36.9 ± 10.6%, capn-InsP$_3$R1 D2550A=77.2 ± 10.1%, lacZ=79.5 ± 9.2%; p<0.001). This result indicates that capn-InsP$_3$R1 increases neuronal susceptibility to excitotoxic injury.

To further examine the enhanced vulnerability to glutamate-mediated injury in capn-InsP$_3$R1-transduced cultures, we treated primary cortical neurons with a wide range of glutamate doses (0.01 to 50 μM). As we did not observe differences between neuronal survival in lacZ- and capn-InsP$_3$R1 D2550A-transduced cultures at baseline or following glutamate injury, we chose a single control (lacZ) for these experiments. Transduced primary cortical neurons were incubated with glutamate or HBS vehicle and the number of surviving neurons was quantified 24 h later by MAP2 staining (Figure 3.5B). Glutamate concentrations ≥ 0.3 μM induced significant loss of neurons in cultures transduced with capn-InsP$_3$R1 (p<0.01), whereas lacZ-transduced cultures were only sensitive at concentrations ≥ 1 μM. To facilitate comparison across doses, we fit data using a Hill equation to produce normalized dose-response curve. Capn-InsP$_3$R1 expression resulted in a leftward shift of the glutamate dose-response curve compared with lacZ control. These results suggest that the proteolyzed channel increases neuronal sensitivity to glutamate-mediated injury and decreases the threshold for excitotoxicity.

Capn-InsP$_3$R1 triggers neurodegeneration of hippocampal pyramidal neurons in vivo

Since primary neuron cultures do not fully recapitulate the metabolism and connectivity of mature neurons *in vivo*, we have begun to translate studies of capn-InsP$_3$R1 to an *in vivo* model. To examine whether calpain-cleaved InsP$_3$R1 can cause neurodegeneration in mature neurons *in vivo* without prior activation of calpain proteolytic injury cascades, we performed stereotaxic intracerebral injections of AAV 2/1 vector expressing capn-InsP$_3$R1 and a fluorescent marker protein (mCherry; Figure 3.6A) into rat striatum, cortex and hippocampus (n=4; Figures 3.6B and C; Supplemental Figure 3.4). We selected these brain regions as they contain neuron subpopulations that are selectively vulnerable to ischemic brain injury (Neumar, 2000), a model where we previously identified calpain-cleaved InsP$_3$R1 *in vivo* (Kopil et al., 2011). The results of these experiments are preliminary, and additional control injections of capn-InsP$_3$R1 D2550A and mCherry controls are pending.

To determine whether expression of capn-InsP$_3$R1 induced neurodegeneration *in vivo*, we used Fluoro-Jade B to identify degenerating neurons. We performed Fluoro-Jade staining on tissue from naïve (n=1) and mCherry injected (n=1) animals as controls. At 3 weeks post-injection, we did not observe Fluoro-Jade labeling of capn-InsP$_3$R1 transduced neurons in the striatum, cortex or the majority of the hippocampus. However, expression of capn-InsP$_3$R1 caused selective degeneration of hippocampal CA2 sector pyramidal neurons (Figures 3.6D and E). In 3 out of 4 animals injected with AAV 2/1 expressing capn-InsP$_3$R1 and mCherry, we observed transduction of this population of neurons as identified by mCherry fluorescence. In 2 of those 3 animals, CA2 pyramidal

neurons labeled with Fluoro-Jade. To confirm these results, we performed immunolabeling of adjacent tissue sections with an antibody targeting neuronal nuclei (NeuN). Interestingly, in animals where we identified Fluoro-Jade positive cells, we observed a concurrent loss of NeuN labeling in CA2 pyramidal neurons (Figures 3.6 F and G). We did not observe any Fluoro-Jade labeling or alterations in NeuN immunostaining in controls. These preliminary data provide the first *in vivo* evidence that expression of calpain-cleaved $InsP_3R1$ is sufficient to induce neurodegeneration independent of prior $[Ca^{2+}]_i$ dysregulation or calpain activity.

DISCUSSION

While several studies have examined the effects of $InsP_3R1$ proteolysis on cellular Ca^{2+} homeostasis (Assefa et al., 2004; Nakayama et al., 2004; Verbert et al., 2008; Kopil et al., 2011), the current study presents the first functional investigation of calpain-cleaved $InsP_3R1$ in neurons. We have demonstrated that capn-$InsP_3R1$ disrupts $[Ca^{2+}]_i$ homeostasis and decreases neuronal viability *in vitro*. Impaired ER Ca^{2+} buffering caused by the leaky channel also likely accounts for the increased sensitivity to excitotoxic injury observed in primary cortical neurons expressing capn-$InsP_3R1$. Results from our *in vivo* experiments further demonstrate that capn-$InsP_3R1$-mediated Ca^{2+} signaling is sufficient to trigger neurodegeneration in specific neuronal populations. Together, these results suggest that $InsP_3R1$ proteolysis is a novel possible feed-forward pathway for executing neuronal cell death.

Capn-$InsP_3R1$ is sufficient to signal neuronal death in culture

Previous studies examining caspase- or calpain-cleaved $InsP_3R1$ in cell lines did not report effects of the dysregulated channel on baseline cell viability (Assefa et al., 2004; Nakayama et al., 2004; Verbert et al., 2008; Kopil et al., 2011). This is likely due to the relatively low open probability of the cleaved channel at resting $[Ca^{2+}]_i$ (Kopil et al., 2011). Unlike cell lines however, primary neurons in culture form complex networks with spontaneous activity and neurotransmission, leading to transient increases in $[Ca^{2+}]_i$ (Murphy et al., 1992; Maeda et al., 1995). Thus, we hypothesized that expression of capn-$InsP_3R1$ in neurons would be sufficient to signal cell death through disruption of

neuronal Ca^{2+} homeostasis. To examine the effect of capn-$InsP_3R1$ on neuronal viability, we employed AAV mediated gene delivery to achieve high transduction efficiency in primary cortical cultures. We determined that expression of capn-$InsP_3R1$ indeed significantly decreased neuronal viability at baseline (Figure 3.2). However, capn-$InsP_3R1$ expression did not lead to complete cell loss, as the majority (~65%) of capn-$InsP_3R1$-transduced neurons were viable, at least at the time studied. This likely explains why we were unable to determine the mechanism(s) for capn-$InsP_3R1$ induced cell death using Western blotting (Supplemental Figure 3.1). The moderate effect of capn-$InsP_3R1$ on baseline neuron viability may suggest gene expression heterogeneity within the population of neurons in primary cortical cultures. Identifying gene expression differences and understanding their potential interactions with capn-$InsP_3R1$ that modulate neuronal death requires additional investigation.

Functional properties of heteroligomeric $InsP_3R1$

Studying capn-$InsP_3R1$ in neurons using AAV mediated gene delivery has some limitations. Foremost, the limited packaging capacity of AAV prohibits viral vector expression of full-length $InsP_3R1$ as a control (Dong et al., 1996; Donnelly et al., 2001). As an alternative control, we expressed capn-$InsP_3R1$ with a point mutation in the putative pore selectivity filter between transmembrane domains 5 and 6. In wt-$InsP_3R1$, replacing the aspartate at residue 2550 with alanine (D2550A) results in a channel that is still able to bind $InsP_3$ and gates normally, but lacks Ca^{2+} permeability and does not have Ca^{2+} release activity (Boehning and Joseph, 2000; Boehning et al., 2001; Cardenas et al.,

2010). The capn-$InsP_3R1$ D2550A mutant channel is expected to have reduced Ca^{2+} conductance similar to the mutant full-length channel, but with $InsP_3$ independent gating, similar to capn-$InsP_3R1$. Thus, the structure and function of capn-$InsP_3R1$ D2550A serves as a specific control for the effects of $InsP_3$-independent Ca^{2+} release through capn-$InsP_3R1$.

Studying the Ca^{2+} permeable and impermeable capn-$InsP_3R1$ in neurons may be complicated by heteroligomerization of the recombinant truncated channels with endogenous $InsP_3R$. At 14 DIV, we observed expression of each 95 kDa $InsP_3R1$ constructs at an approximately 1:1 ratio with endogenous 260 kDa $InsP_3R1$ (Figure 3.1B; densitometry analysis not shown). Additional studies are required to fully elucidate the stochiometry and functional properties of the different heteroligomeric channels. The single-cell Ca^{2+} imaging results may provide some initial insights into the functional properties of heteroligomeric channels. Specifically, we did not observe a reduction in the percentage of cells with $InsP_3$-induced Ca^{2+} release in capn-$InsP_3R1$ D2550A-transduced cultures (Figure 3.3C). Nor did we observe a reduction in Ca^{2+} released from $InsP_3$ sensitive stores (Figures 3.3D and E). Assuming that recombinant $InsP_3R1$ subunits oligomerized with endogenous $InsP_3R$ in transduced neurons, we conclude that expression of the D2550A mutant under the conditions of our experiments did not exert a dominant-negative effect on Ca^{2+} permeability. This is consistent with theoretical models of a similar mutation in the ryanodine receptor, where mutating a negatively charged residue in the selectivity filter of an individual subunit resulted in only a partial decrease in Ca^{2+} conductance (Gao et al., 2000; Wang et al., 2005). By analogy, we speculate that

calpain cleavage of a single $InsP_3R1$ subunit in the tetrameric $InsP_3R$ is unlikely to induce an all-or-nothing effect and may be insufficient to completely eliminate the $InsP_3$-requirement for channel gating. By studying the effects of stable capn-$InsP_3R1$ expression in neurons with endogenous $InsP_3R$, we are perhaps more closely modeling a physiologically relevant process of limited proteolysis of the channel.

Neuronal Ca^{2+} homeostasis is disrupted by capn-$InsP_3R1$

How does $InsP_3$-independent Ca^{2+} release through capn-$InsP_3R1$ affect neuronal Ca^{2+} homeostasis? Using single-cell Ca^{2+} imaging, we observed normal $InsP_3$-induced Ca^{2+} release in capn-$InsP_3R1$ transduced cortical neurons through activation of G_q coupled mGluR1 and mGluR5 receptors (Figures 3.3B and D-E) (Conn and Pin, 1997; Fagni et al., 2000). This result is consistent with previous reports showing that expression of caspase- or calpain-cleaved $InsP_3R1$ does not deplete $[Ca^{2+}]_{ER}$, even though it increases the rate of ER Ca^{2+} leak (Assefa et al., 2004; Verbert et al., 2008; Kopil et al., 2011). This increased ER Ca^{2+} leak in neurons expressing capn-$InsP_3R1$ was manifested as elevated resting $[Ca^{2+}]_i$ (Figures 3.3B and 3.4B, Supplemental Figure 3.2B). While the resting $[Ca^{2+}]_i$ was variable across experiments performed on cortical cultures from different embryos and platings, the ~20 nM increase in $[Ca^{2+}]_i$ in capn-$InsP_3R1$-transduced neurons versus controls remained consistent. This elevated resting $[Ca^{2+}]_i$ suggests that capn-$InsP_3R1$ generates an ER Ca^{2+} leak that can not be fully compensated for by other Ca^{2+} transport mechanisms. This is in contrast to our previous data from Neuro-2A cells, where we did not detect any effect of capn-$InsP_3R1$ on resting $[Ca^{2+}]_i$

(Kopil et al., 2011). The elevated basal $[Ca^{2+}]_i$ observed here could be a cell-type specific effect, or a consequence of chronic capn-$InsP_3R1$ expression, as our previous study examined changes in $[Ca^{2+}]_i$ at 6 h post-transfection. In either case, chronic elevations in resting $[Ca^{2+}]_i$ may explain the decreased neuronal viability in primary cortical cultures expressing capn-$InsP_3R1$.

The apparent increased ER Ca^{2+} leak through capn-$InsP_3R1$ resulted in more pronounced changes in neuronal $[Ca^{2+}]_i$ in response to Ca^{2+} influx. Expression of capn-$InsP_3R1$ significantly increased the peak $[Ca^{2+}]_i$ response to glutamate (Figure 3.4C). This likely reflects a decreased capacity of normal ER Ca^{2+} buffering in neurons expressing capn-$InsP_3R1$. The kinetics of the glutamate Ca^{2+} responses were also altered in capn-$InsP_3R1$-transduced cultures. $[Ca^{2+}]_i$ in lacZ- and capn-$InsP_3R1$ D2550A-transduced neurons rapidly reached a plateau after the initial rise, whereas $[Ca^{2+}]_i$ in capn-$InsP_3R1$-transduced neurons continued to rise until glutamate was removed from the bath (Figure 3.4A). Interestingly, average peak $[Ca^{2+}]_i$ in capn-$InsP_3R1$ expressing neurons approached 2 μM, which is optimal $[Ca^{2+}]_i$ for wt-$InsP_3R1$ and capn-$InsP_3R1$ activation (Foskett et al., 2007; Kopil et al., 2011). We expect that increased channel open probability of capn-$InsP_3R1$ at this higher $[Ca^{2+}]_i$ compromises ER Ca^{2+} buffering, and provides a potential mechanism for increased sensitivity to glutamate injury (Figure 3.5) through irreversible disruption of neuronal Ca^{2+} homeostasis.

It is important to note that we measured somatic $[Ca^{2+}]_i$ in these experiments. As neuronal dendritic and synaptic structure is complex, with heterogeneous distributions of ER and $InsP_3R$ (Bardo et al., 2006; Stutzmann and Mattson, 2011), capn-$InsP_3R1$ may

exert varying influences in these cellular compartments. Understanding the spatial complexity and functional consequences of capn-$InsP_3R1$-mediated Ca^{2+} signaling in dendrites and synapses warrants future investigation.

Role of calpain-cleavage of $InsP_3R1$ in neurodegeneration

Sustained pathological rises in $[Ca^{2+}]_i$ are a key component of both apoptotic and necrotic cell death (Berridge et al., 2000; Orrenius et al., 2003; Mattson, 2007). Therefore, we hypothesized that the dramatic glutamate-induced rise in $[Ca^{2+}]_i$ in capn-$InsP_3R1$ expressing primary cortical neurons would increase their sensitivity to excitotoxic injury. We tested this by exposing transduced cultures to glutamate rather than NMDA, as expression of pathogenic NMDA receptor subunits is developmentally regulated in primary neurons (O'Donnell et al., 2006) and glutamate produced a more consistent, dose-dependent injury in untransduced 14 DIV cultures.[4] As predicted, expression of capn-$InsP_3R1$ significantly decreased the percentage of surviving neurons over a range of glutamate concentrations (Figure 3.5). Enhanced glutamate-induced cell death is likely precipitated by Ca^{2+}-induced Ca^{2+} release through capn-$InsP_3R1$ in addition to decreased basal ER Ca^{2+} buffering in these cells. Together, these impairments of neuronal Ca^{2+} homeostasis increase sensitivity to excitatory stimuli, leading to $[Ca^{2+}]_i$ overload. The downstream effects of this $[Ca^{2+}]_i$ overload may signal cell death through either necrotic or apoptotic pathways. Sustained elevations of $[Ca^{2+}]_i$ could directly lead to pathologic activation of calpains and calpain-mediated cell death (Goll et al., 2003;

[4] C.M. Kopil, A.P. Siebert, J.K. Foskett and R.W. Neumar, unpublished observation.

Vosler et al., 2008). Alternatively, $[Ca^{2+}]_i$ overload could enhance mitochondrial Ca^{2+} uptake triggering mitochondrial permeability transition and caspase-mediated apoptosis (Orrenius et al., 2003; Taylor et al., 2008). Future mechanistic studies are required to clarify the precise pathologic pathway(s) activated by capn-$InsP_3R1$-mediated Ca^{2+} signaling. However, current available data suggest that calpain proteolysis of $InsP_3R1$ in neurons acts to activate and accelerate cell death pathways after injury through $[Ca^{2+}]_i$ overload.

To fully elucidate the role of capn-$InsP_3R1$-mediated Ca^{2+} signaling in neurodegeneration, we have begun translating experiments from primary cortical cultures to mature neurons in the brain. Although we transduced neurons in the striatum, cortex and hippocampus, capn-$InsP_3R1$ expression only caused obvious neurodegeneration in a subpopulation of hippocampal neurons (Figures 3.6D-G; Supplemental Figure 3.4) at the time examined. This preliminary result provides the first *in vivo* evidence that capn-$InsP_3R1$ expression is sufficient for signaling neuronal death without upstream disruption of Ca^{2+} homeostasis or prior calpain activation. The apparent selective vulnerability of hippocampal CA2 pyramidal neurons raises a number of interesting questions, particularly because of the dearth of information about these cells compared with CA1 and CA3 pyramidal cells. Molecular profiling has emerged as a useful tool for distinguishing between CA subregions and may be the most definitive way to identify CA2 pyramidal neurons (Zhao et al., 2001; Lein et al., 2004; Lein et al., 2007). The molecular characteristics that confer susceptibility to capn-$InsP_3R1$-mediated

neurodegeneration in CA2 neurons are a subject for future investigations, and priority should be devoted to studying genes related to Ca^{2+} signaling in these cells.

Conclusions

In summary, our results indicate that expression of calpain-cleaved $InsP_3R1$ impairs neuronal ER Ca^{2+} buffering, leading to increased sensitivity to excitotoxic stimuli and neurodegeneration *in vitro* and *in vivo*. As an early part of the molecular injury pathway (Kopil et al., 2011), calpain proteolysis of $InsP_3R1$ could contribute a feed-forward pathway to accelerate neuronal death through $[Ca^{2+}]_i$ overload. Thus, inhibiting Ca^{2+} release through calpain-cleaved $InsP_3R1$ is a potentially important therapeutic strategy for intervention in disorders associated with calpain activity and disruption of Ca^{2+} homeostasis.

MATERIALS AND METHODS

Materials—Unless otherwise noted, all chemicals were purchased from Sigma-Aldrich (USA).

Antibodies—Rabbit polyclonal antibody targeted against the 20 carboxyl-terminal residues of rat $InsP_3R1$ was generated using previously described methods (Joseph and Samanta, 1993; Kopil et al., 2011) (Covance ImmunoTechnologies). Rabbit polyclonal antibody to MAP2 was a gift from Dr. Virginia Lee (University of Pennsylvania). Mouse monoclonal antibody to BiP/GRP78 was purchased from BD Biosciences. Mouse monoclonal antibody to α-spectrin (Ab1622) was purchased from Chemicon International. Mouse monoclonal antibody to NeuN (MAB377) was purchased from Millipore. Alexa Fluor 488- and Alexa Fluor 568-conjugated secondary antibodies used for immunofluorescence were purchased from Invitrogen. Horseradish peroxidase-linked secondary antibodies used for immunoblotting were purchased from Perkin Elmer.

Rat Primary Mixed Cortical Cultures—Rat primary cortical neurons were cultured using standard technique described previously (Cummings et al., 1996). Briefly, cortices from E19 Sprague-Dawley rat embryos were trypsinized in Dulbecco's minimum essential medium (DMEM; Whittaker Bioproducts) at 4ºC for 20 min. Cells were triturated in media consisting of DMEM supplemented with 10% bovine calf serum (Hyclone), 10% Ham's F12 with glutamine (Whittaker Bioproducts), and 50 U/ml penicillin-streptomycin. Dissociated cortical cultures were plated on poly-L-lysine coated 35-mm dishes (400,000 cells/mL; Western blot), 12-mm glass coverslips in 24-well plates (200,000 cells/mL; immunofluorescence), or 20 X 50-mm glass coverslips in

4-well plates (800,000 cells/mL; single-cell Ca^{2+} imaging). Dissociated cells were grown in serum-free Neurobasal medium (Gibco) supplemented by B27 (Gibco) and cultured at 37ºC in a humidified 5% CO_2 incubator. Mitotic inhibitors and antibiotics were not used.

Constructs and Site Directed Mutagenesis—The transgene for rat calpain-cleaved $InsP_3R1$ (capn-$InsP_3R1$; Figure 3.1A) was previously generated (Kopil et al., 2011). To construct the inactivating D2550A pore mutation (capn-$InsP_3R1$ D2550A), site-directed mutagenesis was performed with QuikChange (Stratagene) using primers (5'–GGCGGAGTAGGA**GCT**GTGCTCAGGAAG–3' and 5'–CTTCCTGAGCAC**AGC**TCCTACTCCGCC–3' (codon change is shown in boldface type and underlined)) and capn-$InsP_3R1$ as a template. The mutation was confirmed by DNA sequencing. For transduction of primary neurons, both capn-$InsP_3R1$ and capn-$InsP_3R1$ D2550A were subcloned into a plasmid containing the AAV inverted terminal repeats (ITRs) and polyA sequence for viral vector generation. For transduction of neurons *in vivo*, we utilized an AAV plasmid containing a cis-acting hydrolase element (CHYSEL) to create vectors with bicistronic expression of transgenes and a marker protein (mCherry) from a single transcript. The CHYSEL sequence contains a canonical DVIEXNPG(2A)P(2B) motif, which results in cleavage between the 2A glycine and 2B proline (Donnelly et al., 2001; de Felipe et al., 2003; Szymczak et al., 2004).

Viral Vector Generation—Recombinant AAV vectors were generated by the University of Pennsylvania Vector core as previously described (Fisher et al., 1997). Briefly, AAV vectors were prepared by triple transfection of HEK293 cells and purified by cesium chloride gradient sedimentation. AAV 2/1 vectors were designed to express

capn-InsP_3R1, capn-InsP_3R1 D2550A or lacZ control. All transgenes were expressed under the control of the cytomegalovirus promoter (CMV).

AAV 2/1 Vector Transduction of Primary Neurons—Rat primary cortical cultures were transduced at 7 DIV by adding AAV 2/1 vector in a vehicle of phosphate-buffered saline (PBS) with 10% glycerol directly to the culture media. Cultures were transduced with 7.5 x 10^{10} genome copies (GC) per mL. All cell viability, biochemical, and functional assays were performed 1 week later (14 DIV).

Cell Viability Assays—Transduced cultures were fixed with 4% paraformaldehyde (PFA), immunolabeled for the neuronal marker MAP2 with a goat anti-rabbit secondary antibody (Alexa Fluor 568), and counterstained with 4,6-diamidino-2-phenylindole (DAPI) nuclear label (Vector Laboratories). Five random 100X images were taken from each 12-mm coverslip. The number of surviving MAP2-labeled neurons per coverslip was estimated by blinded counting of all captured fields. For each transduction condition, 8 to 12 coverslips were counted from 2 or more independent experiments. To control for variability in culture health between experiments, the percentage of viable cells was determined by normalizing to the average cell count from lacZ transduced cultures for each independent experiment. The average of the normalized experiments is shown. Reported SE and error bars reflect propagated error through normalization.

Cell viability was independently measured by staining cultures with calcein-AM and PI (Invitrogen). Live cultures were incubated with 3 μM calcein-AM and 5 μM PI in Dulbecco's PBS (DPBS; Gibco) for 30 min at 37ºC and 5% CO_2. Cultures were rinsed with DPBS and immediately imaged. Five random 100X images were taken from each

12-mm coverslip. The number of surviving, calcein-AM-positive, PI-negative cells per coverslip was estimated by blinded counting of all captured fields. For each transduction condition, 6 to 14 coverslips were counted from 2 or more independent experiments. The number of viable cells in each transduction condition was normalized to lacZ controls as described above.

Western Blotting of Primary Neuron Cultures—Media was removed from transduced cultures and replaces with 4ºC DPBS. Cells were harvested by scraping and resuspended in homogenization buffer (50 mM Tris, 150 mM NaCl, 2 mM EGTA) with a protease inhibitor cocktail and sonicated. Lysates were treated with SDS loading buffer, boiled and analyzed on SDS-PAGE gels. Western blots were visualized using enhanced chemiluminescence supplies purchased from Perkin Elmer. Protein and polypeptide densities were quantified by computer densitometry (ImageJ) and normalized to lacZ controls.

Single-Cell Ca^{2+} Imaging—Cortical cultures were plated onto glass-coverslips (Warner Instruments) and transduced with AAV 2/1 at 7 DIV. One week following transduction, cells on coverslips were secured in a perfusion chamber, and mounted on the stage of an inverted microscope (Nikon Eclipse TE2000). Cells were loaded with Fura-2-AM (Molecular Probes; 2.5 μM) for 45 min at 37ºC and 5% CO_2 in Ca^{2+}-containing extracellular solution (in mM: 120 NaCl, 4 KCl, 20 HEPES, 15 Glucose, 2 $CaCl_2$, 1 $MgCl_2$, pH 7.3). Fura-2 was alternately illuminated at 340/380 nm, and fluorescence intensity filtered at 510 nm. Data were collected and recorded as described previously (White et al., 2005; Cheung et al., 2008). Cells were perfused with 2 mM

Ca^{2+} extracellular solution to establish baseline $[Ca^{2+}]_i$ before glutamate (10 μM), KCL (50 mM), or DHPG (10 μM) was applied in the extracellular solution. At the end of the experiment, Mn^{2+} was used to quench Fura-2 fluorescence (Ca^{2+}-containing extracellular solution supplemented with 10 mM $MnCl_2$ and 10 μM ionomycin). The remaining background fluorescence following Mn^{2+} quench was subtracted during analysis. Glial cells were identified by enhanced Fura-2 loading and morphological characteristics, and were excluded from analysis. Experiments using glutamate, KCL and DHPG were performed on different weeks, in cultures from different platings. Within each experiment using either glutamate, KCl or DHPG however, the studied lacZ, capn-$InsP_3R1$ D2550A and capn-$InsP_3R1$ transduced cultures were derived from the same plating.

Changes in $[Ca^{2+}]_i$ are presented as changes in fluorescence ratio. Dye calibration was achieved by applying experimentally determined constants to the equation: $[Ca^{2+}] = K_d\ \beta(R–R_{min})/(R_{max}–R)$. Macros used for analysis were custom macros written for IGOR Pro (WaveMetrics).

Glutamate Injury Characterization—HBS (in mM: 145 NaCl, 3 KCl, 10 HEPES, 8 Glucose, 2 $CaCl_2$, 1 $MgCl_2$, pH 7.4) with or without L-glutamic acid was added to the media of transduced cortical cultures at 14 DIV. Twenty-four hours after HBS or glutamate application, cultures were fixed with 4% PFA, immunolabeled for MAP2, and counter-stained with DAPI. Five random 100X images were taken from each 12-mm coverslip. The number of surviving MAP2-labeled neurons per coverslip was estimated by blinded counting of all captured fields. For each transduction condition, 6 to 8

coverslips were counted from 2 or more independent experiments. To control for variability in culture health between experiments and differences in baseline toxicity, the percent of viable cells at each glutamate dose was determined by normalizing within transduction conditions to the average cell count from HBS treated cultures. Data were normalized within independent experiments and the average of the normalized experiments is shown. Reported SE and error bars reflect propagated error through normalization. Dose response curves were calculated by fitting plotted mean data points using the Hill equation and holding the base and max values at 0 and 100 respectively. Reported error for LD_{50} values represent error of the fit.

Viral Vector Injection—Intracranial injection of AAV 2/1 vectors was performed as described previously (Bevers et al., 2010). Briefly, male rats weighing 375-425 g were anesthetized by inhalation of 4% isoflurane in 70% O_2 and 30% N_2O and a surgical plan of 2% isoflurane. A longitudinal surgical incision in the scalp was made and the skull exposed by blunt dissection. Bilateral burr holes were centered 2.6 mm lateral to the midline and 1.6 mm caudal to Bregma (for striatum and overlying cortex) and 2.0 mm lateral to the midline and 3.8 mm caudal to Bregma (for hippocampus and overlying cortex). Sterotaxically-guided injections were made at depths of 4.4 mm (striatum), 3.0 mm (hippocampus), and either 1.0 or 1.8 mm (cortex) below the dural surface. At each site, 2 µl of AAV 2/1 vector solution (1×10^{10} GC total) was infused at a rate of 0.5 µl/min. After injection, the needle was held in place for 5 min and then removed slowly over 2 min. The scalp was sutured closed and rats recovered.

Immunohistochemical Staining of Rat Forebrain—At 3 weeks post-intracranial vector injection, rats were anesthetized with pentobarbital (200 mg/kg) and transcardially perfused with cold PBS (pH 7.4) followed by 4% PFA in 0.1M phosphate buffer (PB). Brains were extracted, post-fixed in 4% PFA for 4 h and cryoprotected using serial incubations in 0.1 M PB containing 10%, 20% and 30% sucrose. Serial coronal sections through the forebrain (40 μm) were cut on a freezing sliding microtome. Sections were immunolabeled with primary antibody targeting the neuron-specific marker protein NeuN and a goat anti-mouse secondary antibody (Alexa Fluor 488). Sections were counterstained with Hoechst (5 μg/mL) and mounted with Fluoromount medium (Electron Microscopy Sciences).

For Fluoro-Jade labeling, PFA-fixed sections were processed as described previously (Kopil et al., 2011). As Fluoro-Jade labeling decreased mCherry fluorescence, tissue was mounted, temporarily coversliped with water and imaged for expression of mCherry. Coverslips were then removed, and hydrated tissue was incubated with 0.06% potassium permanganate for 10 min, rinsed with dH_2O, and stained with 0.0004% Fluoro-Jade B (Millipore) in 0.1% acetic acid for 20 min. Stained tissue was rinsed with dH_2O, dried at 37°C, dehydrated with xylene and coversliped using Permount (Fisher Scientific).

Data analysis and statistics— Data are presented as the mean ± SE, and statistical significance of differences between the means was assessed using either unpaired t-tests or analysis of variance for repeated-measures using Barlett's test for equal variances and

a Bonferroni correction. Differences between means were accepted as statistically significant at the 95% level ($p < 0.05$).

ACKNOWLEDGEMENTS

We thank Margaret Maronski for the preparation of cortical cultures. We thank Dr. Virginia Lee for supplying antibodies. We thank Dr. Shu-Jen Chen, Dr. Arbansjit Sandhu, and the University of Pennsylvania Vector Core for excellent technical expertise in cloning and viral vector generation. We also thank Dr. Don-On Daniel Mak for IGOR macros and helpful discussions, and Dr. Horia Vais for thoughtful comments on the manuscript. This work was supported by National Institutes of Health grants NS039481 (RWN), NS069951 (RWN), NS071828 (CMK), MH059937 (JKF), and GM065830 (JKF).

FIGURES AND LEGENDS

Figure 3.1

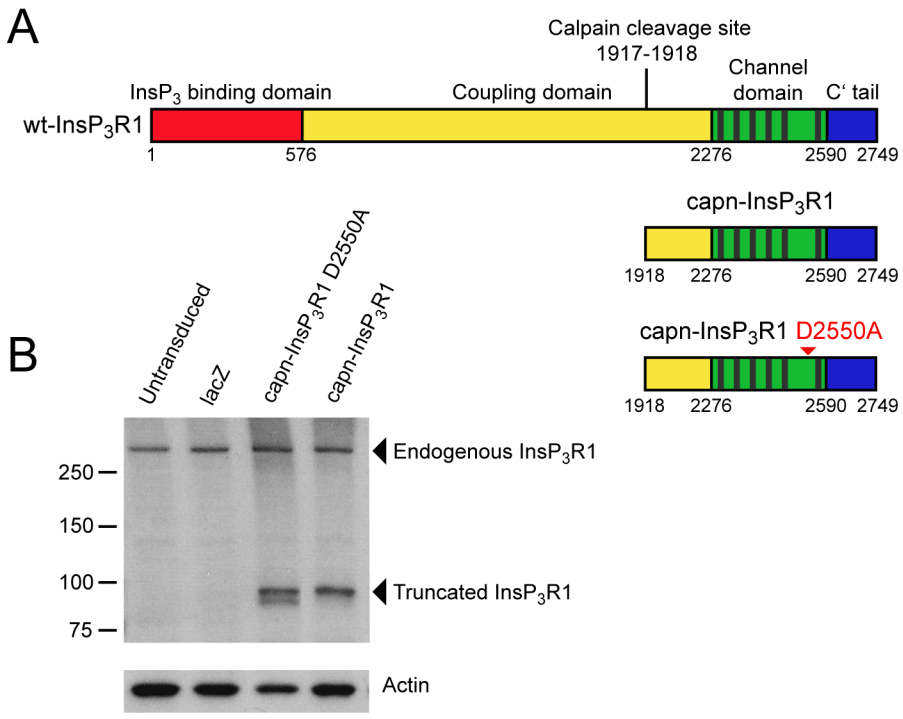

Figure 3.1 Schematic representation and expression of recombinant $InsP_3R1$ constructs in primary neurons

(*A*) Protein domain structure of wt-$InsP_3R1$ (*top*), calpain-cleaved $InsP_3R1$ (*middle*), and calpain-cleaved $InsP_3R1$ with the D2550A point mutation (*bottom; red arrowhead*). Residues numbered according to rat type 1 SI+, SII+, SIII- sequence (protein accession NP_001007236.1). (*B*) Western blot analysis of whole cell lysates from untransduced rat primary cortical cultures and primary cortical cultures transduced with AAV 2/1 expressing lacZ, capn-$InsP_3R1$ D2550A, or capn-$InsP_3R1$ at 1 week post-transduction (14 DIV). Carboxyl-terminal $InsP_3R1$ antibody was used to detect endogenous and recombinant truncated rat $InsP_3R1$. Antibody against actin was used as a loading control.

Figure 3.2

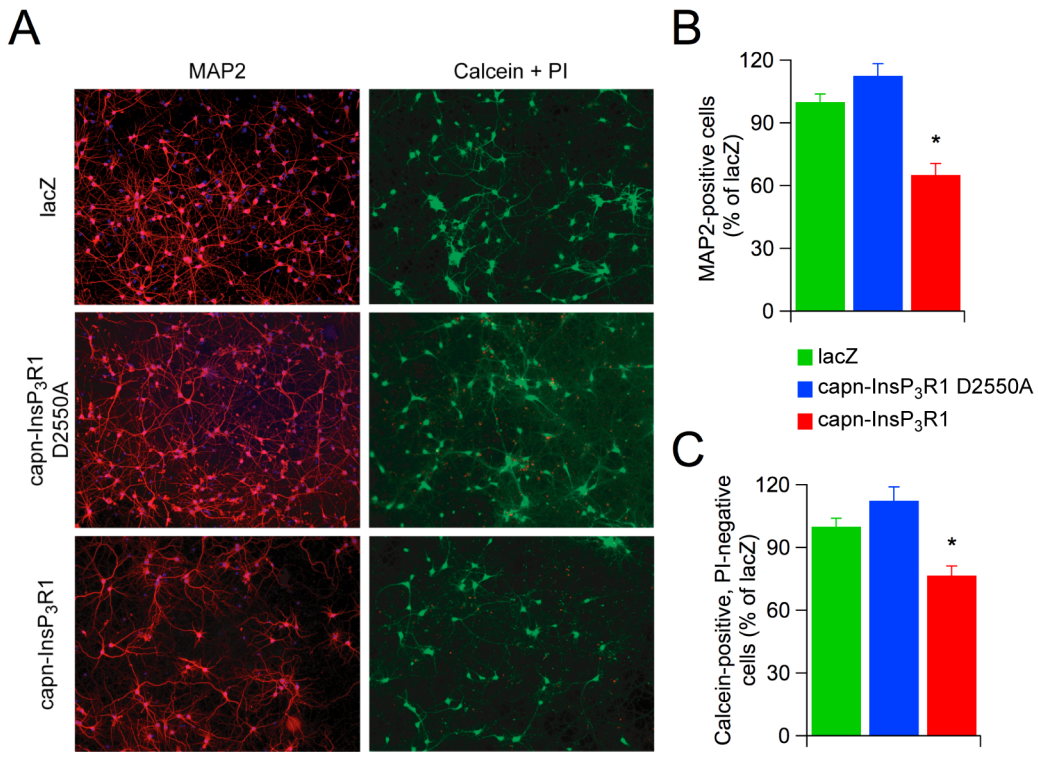

Figure 3.2 Primary cortical neuron viability is reduced by expression of capn-InsP$_3$R1

Rat primary cortical cultures were transduced with AAV 2/1 expressing lacZ, capn-InsP$_3$R1 D2550A, or capn-InsP$_3$R1 (7 DIV). (*A*) One week following transduction (14 DIV), cultures were stained for MAP2 (*red*) and nuclei (*blue*; *left panel*), or incubated with calcein-AM (*green*) and PI (*red*; *right panel*). Representative 100X epifluorescence images captured for counting are shown. **(***B*) Percent neuronal survival as determined by counts of MAP2 reactive cells (one-way analysis of variance; *, $p<0.001$). (*C*) Percent cell survival as determined by counts of calcein-AM positive, PI-negative cells (unpaired *t* tests with unequal variance; *, $p<0.001$). Expression of capn-InsP$_3$R1 resulted in a significant decrease in the percentage of viable neurons compared with lacZ and capn-InsP$_3$R1 D2550A as determined by both assays.

Figure 3.3

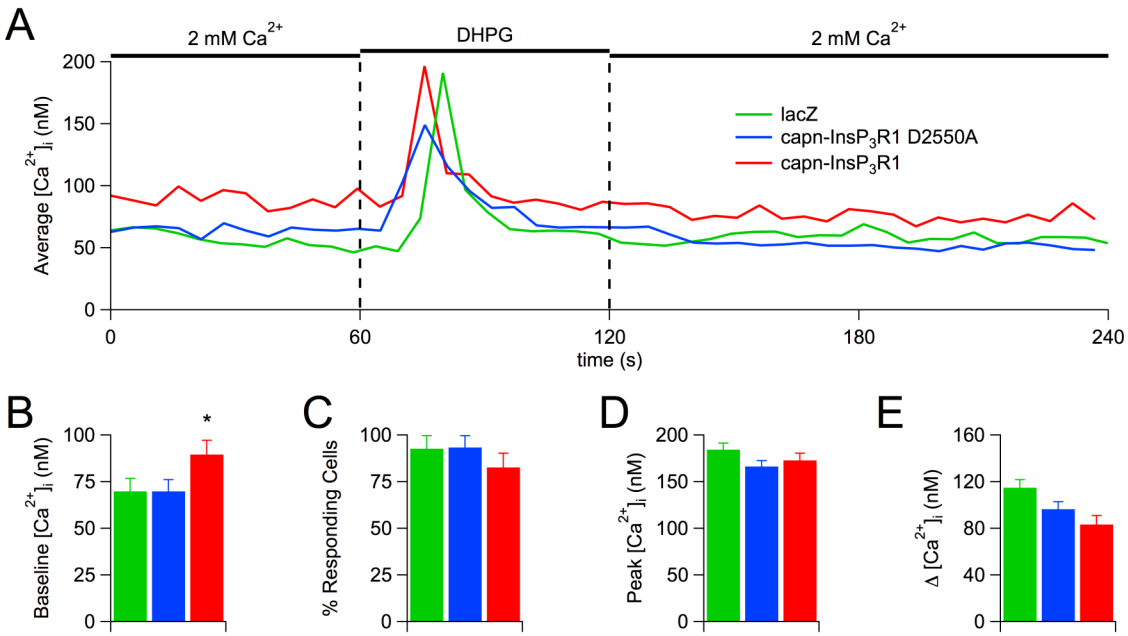

Figure 3.3 Capn-InsP$_3$R1 does not deplete InsP$_3$-sensitive stores

(*A*) Representative single cell $[Ca^{2+}]_i$ responses to DHPG in Fura-2 loaded primary cortical neurons (14 DIV) transduced with lacZ (*green*), capn-InsP$_3$R1 D2550A (*blue*) or capn-InsP$_3$R1 (*red*). (*B*) Summary of average resting $[Ca^{2+}]_i$ in neurons from cultures used for DHPG Ca^{2+} imaging experiments. Neurons expressing capn-InsP$_3$R1 demonstrate increased resting $[Ca^{2+}]_i$ (unpaired *t*-tests with unequal variance; *, $p<0.001$). (*C*) Percentage of neurons in transduced cortical cultures that exhibited >10% increase in $[Ca^{2+}]_i$ in response to DHPG. (*D*) Summary of average peak $[Ca^{2+}]_i$ responses elicited by DHPG. (*E*) Summary of average change in $[Ca^{2+}]_i$ from resting to peak $[Ca^{2+}]_i$. Despite significant differences in resting $[Ca^{2+}]_i$ in these experiments, no statistical differences were observed in average change in $[Ca^{2+}]_i$.

Figure 3.4

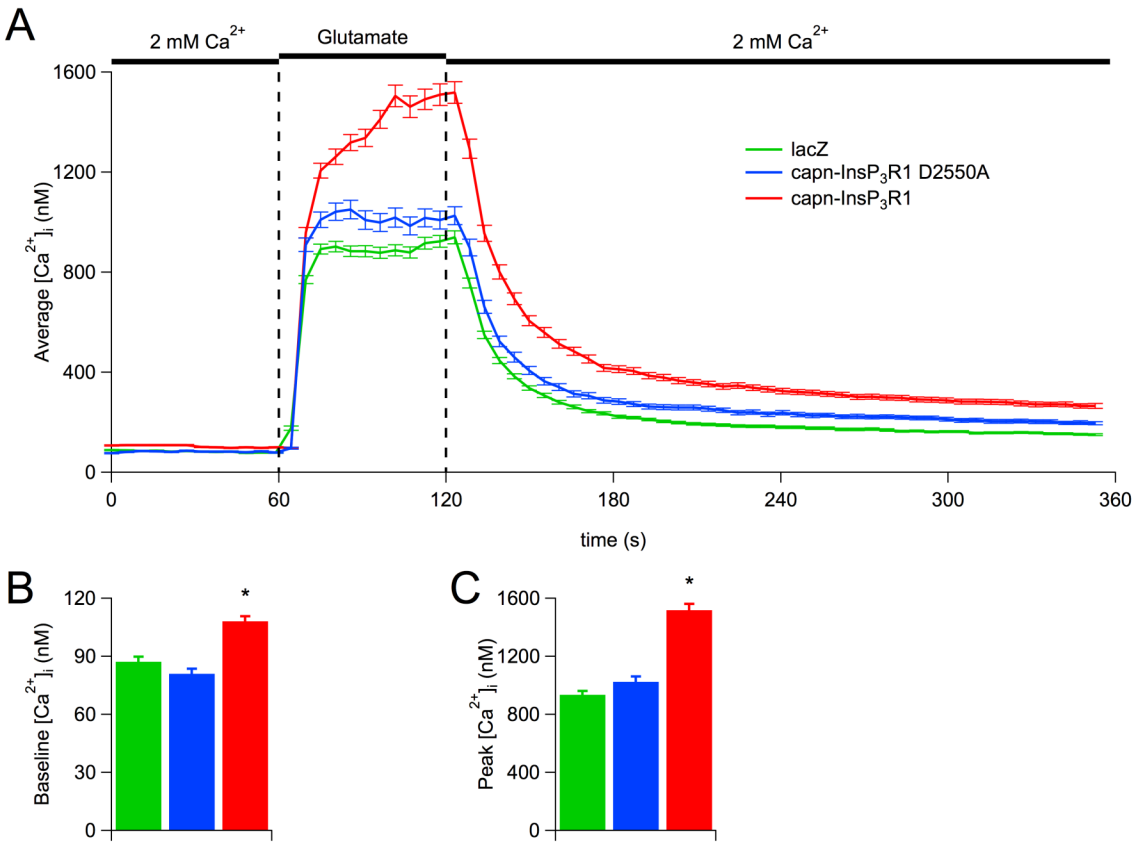

Figure 3.4 Neurons expressing capn-InsP$_3$R1 have increased glutamate-induced rises in $[Ca^{2+}]_i$

(*A*) Averaged single-cell $[Ca^{2+}]_i$ responses to glutamate in Fura-2 loaded primary cortical neurons (14 DIV) transduced with lacZ (*green*), capn-InsP$_3$R1 D2550A (*blue*) or capn-InsP$_3$R1 (*red*). (*B*) Summary of average resting $[Ca^{2+}]_i$ in neurons from cultures used for glutamate Ca^{2+} imaging experiments. Expression of capn-InsP$_3$R1 significantly increased resting $[Ca^{2+}]_i$ in neurons (108.2 ± 2.6 nM) compared with capn-InsP$_3$R1 D2550A (81.0 ± 2.5 nM) and lacZ controls (87.3 ± 2.6 nM; unpaired *t*-tests with unequal variance; *, $p<0.001$). (*C*) Summary of average peak $[Ca^{2+}]_i$ responses elicited by glutamate shows an increased maximum $[Ca^{2+}]_i$ achieved in capn-InsP$_3$R1 expressing neurons (unpaired *t*-tests with unequal variance; *, $p<0.001$).

Figure 3.5

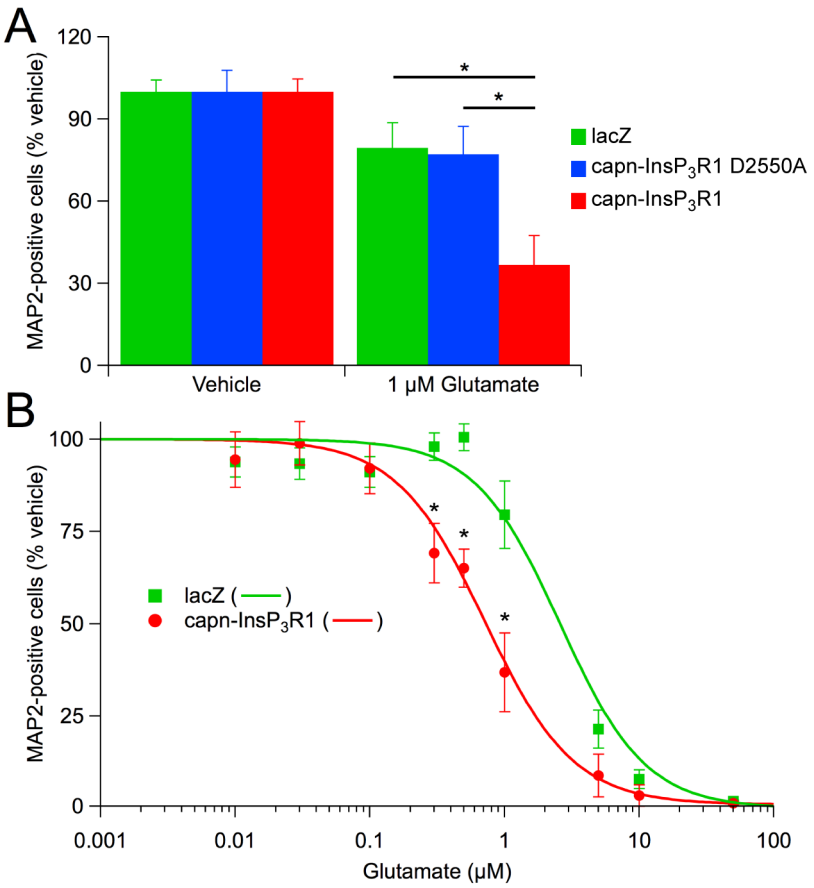

Figure 3.5 Expression of capn-InsP$_3$R1 increases neuronal susceptibility to glutamate-mediated injury

(*A*) Transduced primary cortical cultures (14 DIV) were exposed to 1 μM glutamate or HBS vehicle. Twenty-four hours later, cultures were stained for MAP2 and percent neuronal survival quantified relative to vehicle treated cultures. Expression of capn-InsP$_3$R1 resulted in a significant decrease in percentage of MAP2-positive cells following glutamate injury compared with lacZ and capn-InsP$_3$R1 D2550A (one-way analysis of variance; *, $p<0.01$). **(***B*) Glutamate dose-response curves for lacZ and capn-InsP$_3$R1 transduced cultures (data at 1 μM glutamate are the same as shown in Figure 3.5A). Expression of capn-InsP$_3$R1 significantly decreased the percentage of MAP2-positive cells following treatment with 0.3, 0.5, and 1 μM glutamate compared with lacZ (unpaired *t* tests; *, $p<0.01$) and resulted in a shift in the glutamate-dose response curve. LD$_{50}$ for glutamate in neurons expressing capn-InsP$_3$R1 (0.75 ± 0.19 μM) is reduced compared with neurons expressing lacZ (2.61 ± 0.78 μM).

Figure 3.6

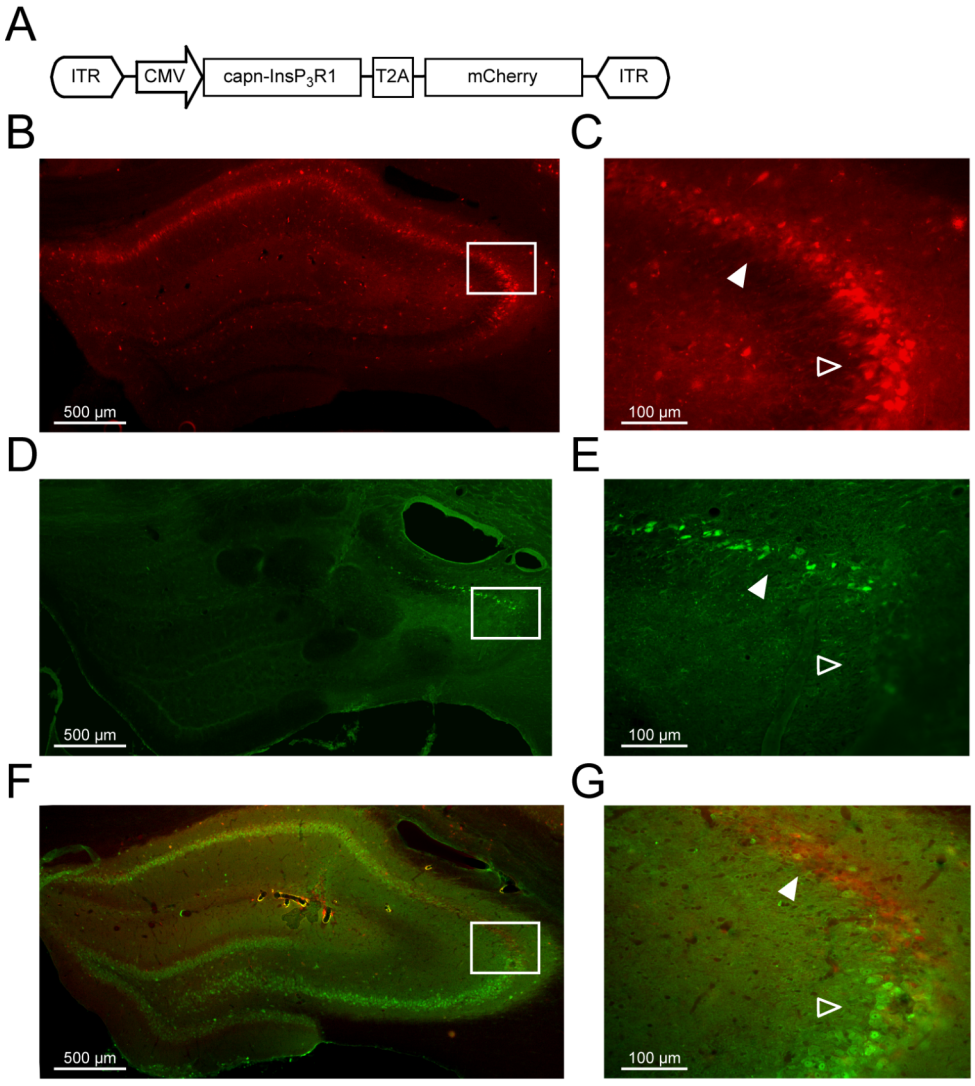

Figure 3.6 Expression of capn-InsP$_3$R1 causes neurodegeneration in subpopulations of hippocampal neurons *in vivo*.

(*A*) Vector design for transduction of neurons *in vivo*. Plasmid contains AAV-specific ITRs for vector generation and a CHYSEL sequence (*T2A*) for bicistronic expression of capn-InsP$_3$R1 and mCherry. (*B*) mCherry expression in rat hippocampus 3 weeks after injection of AAV 2/1 vector shown in *A*. Hippocampal neurons in CA1, CA2, and CA3 were transduced in this animal. (*C*) Higher magnification of region highlighted in *B* (*white box*). *Closed arrow* indicates CA2 region, *open arrow* indicates CA3 region. (*D*) Fluoro-Jade labeling of adjacent tissue section. Degenerating neurons were identified in the CA2 region. (*E*) Region highlighted in *D* at higher magnification shows shrunken somatic morphology of Fluoro-Jade positive cells consistent with neurodegeneration. (*F*) Immunostaining of adjacent tissue section using NeuN (*green*) to label neurons. mCherry (*red*) expression identifies transduced cells. Fluoro-Jade positive region shown in *D* does not label with NeuN. (*G*) Region highlighted in *F* at higher magnification shows loss of NeuN labeling and presence of red debris. Expression of capn-InsP$_3$R1 *in vivo* leads to selective neurodegeneration of CA2 hippocampal neurons in the pyramidal layer.

SUPPLEMENTAL DATA

Supplemental Figure 3.1

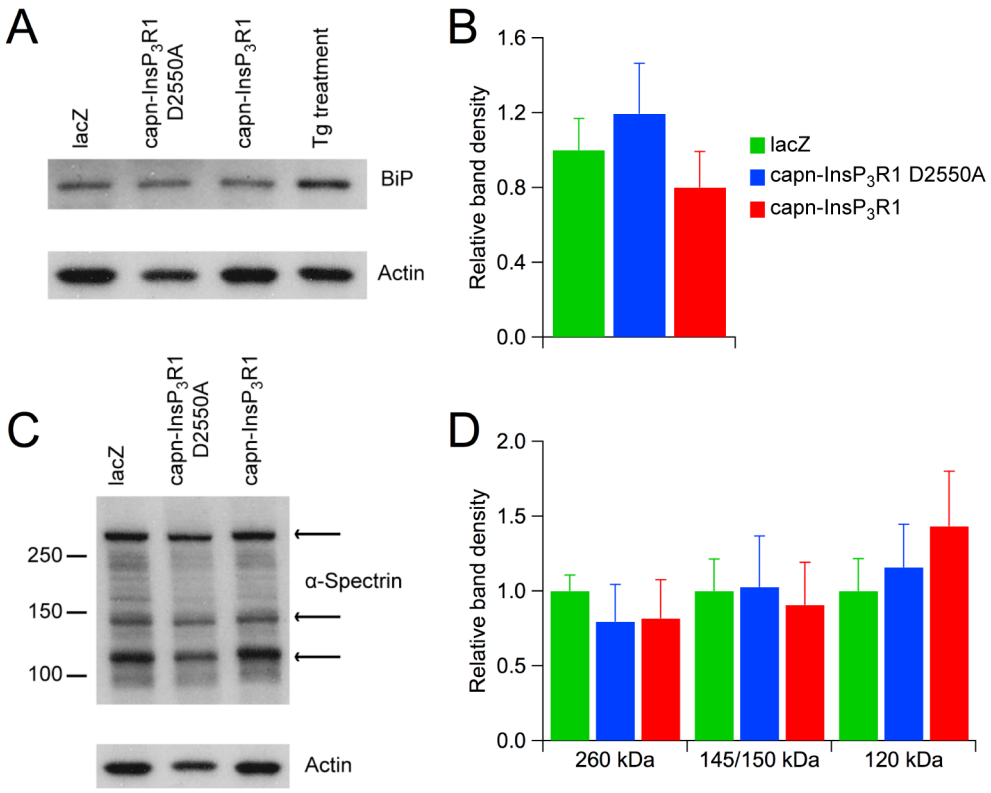

Supplemental Figure 3.1 Activation of ER stress markers and proteases in transduced primary cortical neurons

Western blot analysis of whole cell lysates from primary cortical cultures transduced with AAV 2/1 expressing lacZ, capn-InsP$_3$R1 D2550A, or capn-InsP$_3$R1 at 1 week post-transduction (14 DIV). (*A*) Antibody against BiP was used to detect activation of ER stress response. Untransduced cultures were treated with thapsigargin (*Tg*; 1 µM) as a positive control for ER stress and increased BiP. Antibody against actin was used as a loading control. (*B*) BiP band densities were quantified and normalized to actin. Changes in protein expression are expressed relative to lacZ controls. (*C*) Antibody against α-spectrin was used to detect calpain- and caspase-mediated proteolysis. Calpain-mediated cleavage of α-spectrin (260 kDa) generates 150 and 145 kDa polypeptides while caspase-mediated cleavage generates 150 and 120 kDa polypeptides. (*D*) Full-length (260 kDa) and proteolyzed (145/150 kDa and 120 kDa) α-spectrin band densities were quantified and normalized to actin. Changes in intact α-spectrin and α-spectrin fragment densities are expressed relative to lacZ controls. There are no statistically significant differences between BiP or α-spectrin band densities in lacZ-, capn-InsP$_3$R1 D2550- and capn-InsP$_3$R1-transduced cultures.

Supplemental Figure 3.2

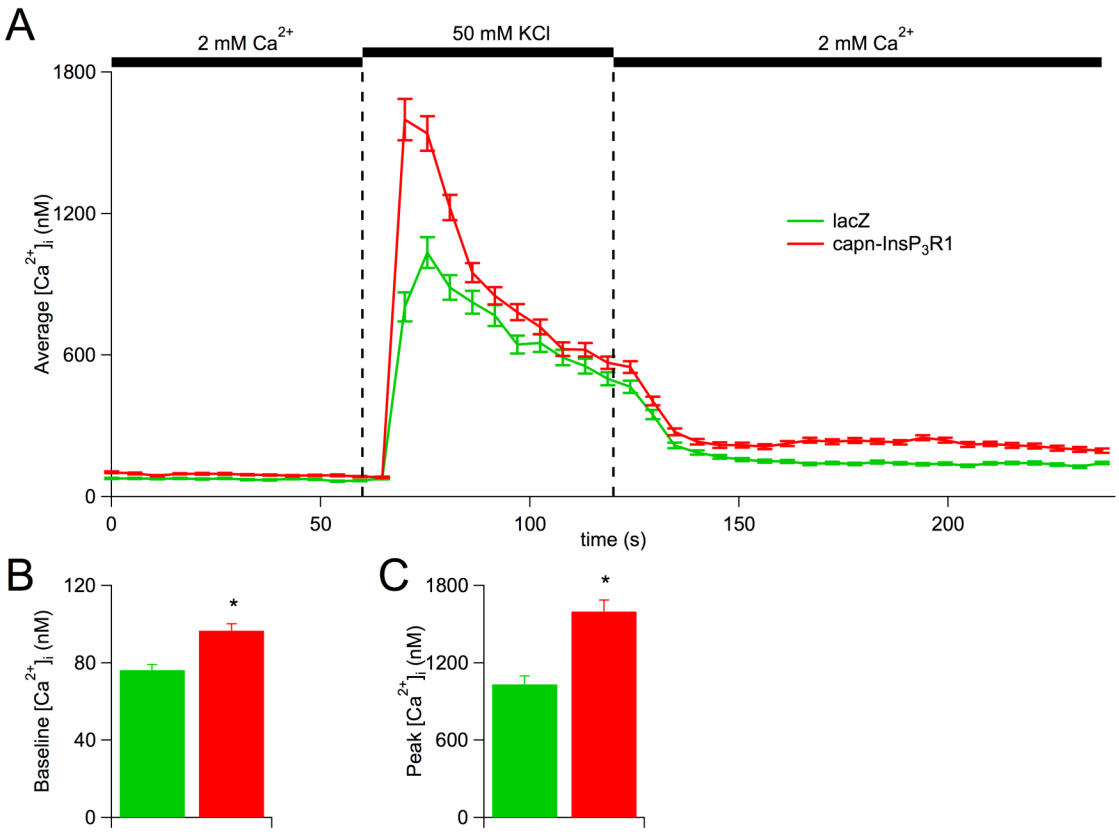

Supplemental Figure 3.2 Neurons expressing capn-InsP$_3$R1 have increased rises in $[Ca^{2+}]_i$ in response to depolarization

(*A*) Averaged single-cell $[Ca^{2+}]_i$ responses to depolarization with 50 mM KCl in Fura-2 loaded primary cortical neurons (14 DIV) transduced with lacZ (*green*) or capn-InsP$_3$R1 (*red*). (*B*) Summary of average resting $[Ca^{2+}]_i$ in neurons from cultures used for KCl Ca^{2+} imaging experiments. Consistent with data presented in Figures 3.4B and 3.5B, cultures expressing capn-InsP$_3$R1 demonstrate increased baseline $[Ca^{2+}]_i$ (capn-InsP$_3$R1=96.7 ± 3.5 nM, lacZ=76.2 ± 2.9 nM; unpaired *t*-tests with unequal variance; *, $p<0.001$). (*C*) Summary of average peak $[Ca^{2+}]_i$ responses elicited by KCl shows an increased maximum $[Ca^{2+}]_i$ achieved in capn-InsP$_3$R1 expressing neurons (capn-InsP$_3$R1=1540 ± 73 nM, lacZ=1035 ± 65 nM; unpaired *t*-tests with unequal variance; *, $p<0.001$).

Supplemental Figure 3.3

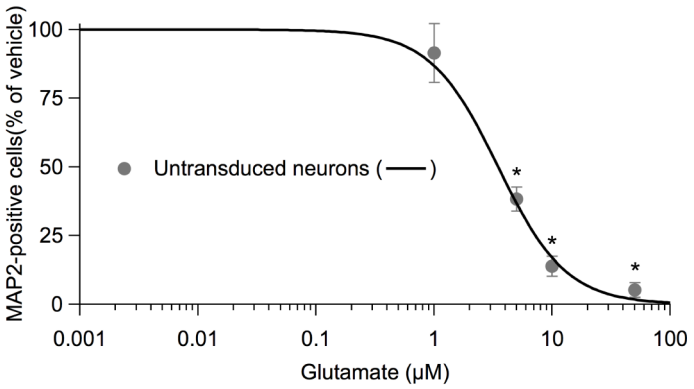

Supplemental Figure 3.3 Characterization of glutamate injury model

(*A*) Untransduced rat primary cortical cultures (14 DIV) were exposed to HBS vehicle or 1, 5, 10 or 50 μM glutamate. Twenty-four hours later, cultures were stained for MAP2 and percent neuronal survival quantified relative to vehicle treated controls. The percentage of surviving cells was significantly reduced in cultures treated with glutamate concentrations $\geq$ 5 μM (1 μM=91.5 ± 10.6 %, 5 μM=38.3 ± 4.4 %, 10μM=13.9 ± 3.7 %, 50μM=4.3 ± 2.6 %; one-way analysis of variance; *, $p<0.01$). LD_{50} for glutamate in these cultures is 3.49 ± 0.48 μM.

Supplemental Figure 3.4

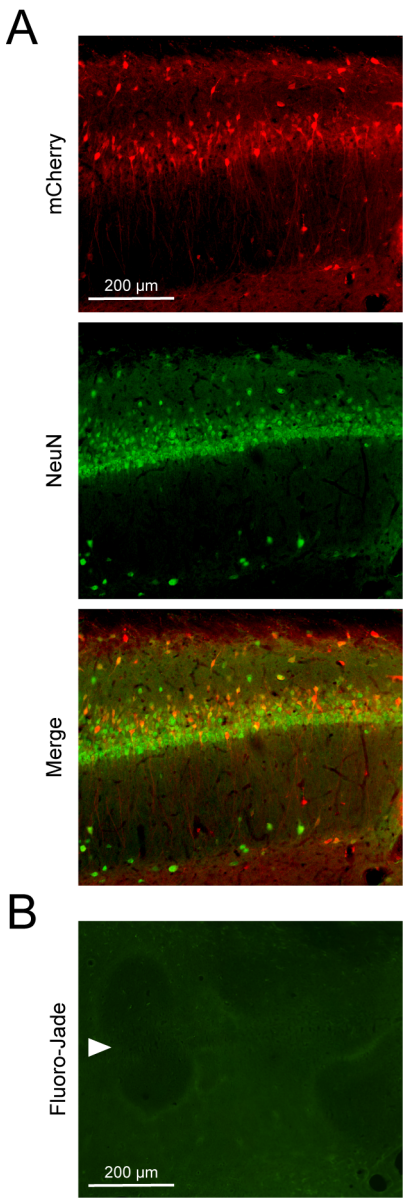

Supplemental Figure 3.4 CA1 neurons tolerate expression of capn-InsP$_3$R1

(*A*) Representative image (100X) of immunostained rat hippocampus 3 weeks after injection of AAV 2/1 vector expressing capn-InsP$_3$R1 and mCherry. CA1 pyramidal neurons were robustly transduced in this animal as evidenced by mCherry expression in the soma, and apical and basal dendrites (*top*). NeuN labeling (*center*) demonstrates healthy neurons in CA1 pyramidal layer. (*B*) Fluoro-Jade staining of an adjacent tissue section reveals no evidence of degeneration in CA1 pyramidal layer (*closed arrow*). These data provide evidence that expression of capn-InsP$_3$R1 is well tolerated by certain neuronal populations.

DISCUSSION

Ischemic brain injury resulting from cardiac arrest represents a major cause of severe cognitive impairment, disability and death. The molecular mechanisms of delayed neuronal death following ischemia-reperfusion remain incompletely understood. The work described in the previous chapters extends our understanding of how both calpain and disruption of neuronal Ca^{2+} homeostasis contribute to neuropathology resulting from ischemia. In this thesis, we present data that demonstrate calpain proteolysis of type 1 inositol 1,4,5-trisphosphate receptor ($InsP_3R1$) generates a leaky channel that impairs normal Ca^{2+} buffering by the endoplasmic reticulum (ER) and may contribute to neuronal death following ischemic brain injury. Specifically, in Chapter 2, we identified the precise cleavage site responsible for generating the stable carboxyl-terminal channel fragment of $InsP_3R1$, and determined that the cleaved channel has $InsP_3$-independent gating and constitutive activity. The calpain-cleaved form of $InsP_3R1$ decreased Ca^{2+} content of intracellular stores via increased ER Ca^{2+} leak. Importantly, we provided the first evidence of calpain-mediated proteolysis of $InsP_3R1$ *in vivo*, which we identified in selectively vulnerable cerebellar Purkinje neurons at early and late time points after cardiac arrest. Following these studies, we proceeded, in Chapter 3, to examine the functional consequences of calpain-cleaved $InsP_3R1$ on neuronal Ca^{2+} homeostasis and survival. We found that expression of truncated $InsP_3R1$ decreased neuronal viability in primary cultures, dramatically altered intracellular Ca^{2+} homeostasis, and increased sensitivity to excitotoxic injury. Finally, we began translation of these studies *in vivo*,

where we observed degeneration of CA2 hippocampal neurons induced by expression of calpain-cleaved $InsP_3R1$ without prior injury. Together, these findings support the novel role of $InsP_3R1$ proteolysis in post-ischemic neuronal death and expand our understanding of cell death pathways in neurodegenerative diseases associated with pathological protease activation and disruption in Ca^{2+} homeostasis.

Calcium Signaling Through Calpain-cleaved $InsP_3R1$

Our functional studies of calpain-cleaved $InsP_3R1$ raise important questions for future research into Ca^{2+} signaling through the proteolyzed channel. First, the $InsP_3$-independent gating of recombinant calpain-cleaved $InsP_3R1$ (capn-$InsP_3R1$; Chapter 2) suggests that proteolysis induces a shift in channel function from $InsP_3$-induced Ca^{2+} release (IICR) to Ca^{2+}-induced Ca^{2+} release (CICR). The combination of IICR and CICR through $InsP_3Rs$ normally coordinates propagation of Ca^{2+} signals by facilitating activation of neighboring clusters of $InsP_3Rs$ (Berridge, 1997; Foskett et al., 2007). Under physiological conditions, this Ca^{2+} signaling is regulated by 1) the $InsP_3$ requirement for channel gating, and 2) channel inactivation by high cytoplasmic free Ca^{2+} concentration ($[Ca^{2+}]_i$). In pathological states where calpain cleaves $InsP_3R1$, the truncated channel no longer depends on $InsP_3$ for activation, and while the biphasic Ca^{2+} regulation of the channel stills exists, this may not be enough to prevent aberrant CICR.

Cytoplasmic diffusion of Ca^{2+} released through $InsP_3R$ is typically spatially restricted, resulting in microdomains of elevated $[Ca^{2+}]_i$ that decrease with distance from the channel pore. $[Ca^{2+}]_i$ adjacent to an open $InsP_3R$ channel may reach 100 μM or more, whereas 1 or 2 μM from the pore, the concentration steeply decreases to only 1 μM

(Neher, 1998). Interestingly, high $[Ca^{2+}]_i$ (25 μM; Chapter 2) reduces capn-$InsP_3R1$ channel open probability (P_o), however $[Ca^{2+}]_i$ in the low micromolar range is, in fact, optimal for capn-$InsP_3R1$ gating (Chapter 2). Thus, $InsP_3R$ clustering and spatial organization of capn-$InsP_3R1$-mediated Ca^{2+} release may lead to continuous unregulated CICR. Additional experiments are required to characterize spatial domains of Ca^{2+} released by capn-$InsP_3R1$. Flash photolysis of caged Ca^{2+} provides a tool for uniformly elevating $[Ca^{2+}]_i$, which has been helpful in characterizing CICR properties of ryanodine receptors (RyR) (Shirokova and Niggli, 2008). This technique, in combination with dantrolene to block RyR-mediated Ca^{2+} release, could potentially elucidate the characteristics and global effects of CICR within neurons expressing capn-$InsP_3R1$.

In addition to causing a shift from IICR to CICR, calpain proteolysis of the amino-terminus of $InsP_3R1$ potentially alters normal receptor degradation pathways. $InsP_3R1$ expression can be down-regulated in an activity-dependent fashion by ubiquitination and proteasomal degradation (Wojcikiewicz, 2004). Chronic activation of G-protein coupled receptors linked with generation of $InsP_3$, as well as Ca^{2+} release through $InsP_3R1$ can cause ubiquitination of the channel (Alzayady and Wojcikiewicz, 2005; Bhanumathy et al., 2006). Thus, chronic Ca^{2+} release through calpain-cleaved $InsP_3R1$ may be a signal for ubiquitination. Recent data using mass spectrometric analysis has identified 11 lysine residues within $InsP_3R1$ that can be ubiquitinated (Sliter et al., 2008). Based on the $InsP_3R1$ cleavage site we identified (Chapter 2), calpain proteolysis of the channel removes 8 of the 11 potential sites for ubiquitination. Additionally, calpain proteolysis removes all of the polyubiquitination sites in the amino-

terminus of $InsP_3R1$ (Bhanumathy et al., 2006; Sliter et al., 2008), which are required for proteasomal degradation (Hicke, 2001; Ikeda and Dikic, 2008). While the functional significance of monoubiquitination of $InsP_3R1$ is unclear, these data suggest that calpain-cleaved $InsP_3R1$ cannot be targeted for proteasomal degradation, despite its constitutive activity. Thus, calpain cleavage of $InsP_3R1$ may be critical to executing cell death by removing activity dependent regulation of the channel thereby causing Ca^{2+} overload.

Our studies of calpain-cleaved $InsP_3R1$ that demonstrate disrupted intracellular Ca^{2+} homeostasis also raise questions about Ca^{2+}-induced remodeling of Ca^{2+} signaling. Ca^{2+} itself is a potent activator of gene transcription, and $InsP_3R$-mediated Ca^{2+} signaling is an important component of that process (Mellstrom and Naranjo, 2001; Berridge et al., 2003). Substantial evidence supports the role of Ca^{2+}-dependent transcription of Ca^{2+} regulatory proteins as a feedback mechanism for maintaining cellular Ca^{2+} homeostasis. Capn-$InsP_3R1$-mediated Ca^{2+} signaling may alter these pathways. Elevated resting $[Ca^{2+}]_i$, as seen in neurons expressing capn-$InsP_3R1$ (Chapter 3), is known to decrease neuronal excitability through Ca^{2+}-activated K^+ channels (Fakler and Adelman, 2008). However, previous data demonstrated that cultured neurons transfected with an inwardly rectifying K^+ channel eventually recover normal firing rates despite continued channel expression (Burrone et al., 2002). This suggests that compensatory alterations in expression of other genes occur to maintain an ideal level of neuronal excitability (Turrigiano, 2008). A similar compensatory mechanism may be activated by proteolyzed $InsP_3R1$, which could potentially lead to pathologically increased sensitivity to excitatory stimulation. Alternatively, Ca^{2+} signaling through calpain-cleaved $InsP_3R1$ may trigger

cell death if compensatory changes in other Ca^{2+} regulatory proteins are insufficient to restore normal spatiotemporal properties of neuronal Ca^{2+} signaling.

Future investigation of these Ca^{2+}-induced Ca^{2+} signaling remodeling processes may provide important insights into post-ischemic changes in gene expression in vulnerable neurons. Currently identified alterations in post-ischemic gene expression include changes in NMDA and AMPA glutamate receptor (Pellegrini-Giampietro et al., 1992; Pellegrini-Giampietro et al., 1994; Gorter et al., 1997; Zhang et al., 1997; Gascon et al., 2005; Liu et al., 2010), and voltage-gated Ca^{2+} channel expression (Chung et al., 2001a; Chung et al., 2001b). If these changes in expression are a downstream consequence of aberrant Ca^{2+} release through calpain-cleaved $InsP_3R1$, then blocking the truncated channel may prove to be neuroprotective.

How can Ca^{2+} release through calpain-cleaved $InsP_3R1$ be blocked? Heparin is an effective inhibitor of wild type (wt) $InsP_3R$ (Ghosh et al., 1988). However, it acts as a competitive inhibitor of $InsP_3$ binding, and therefore does not block capn-$InsP_3R1$ (Chapter 2). Another $InsP_3R$ antagonist is the membrane permeant 2-aminoethoxydiphenyl-borate (2-APB) (Maruyama et al., 1997; Bilmen and Michelangeli, 2002). Unlike heparin, 2-APB does not prevent $InsP_3$ binding to the receptor. Instead, it more likely acts as an allosteric inhibitor (Bilmen and Michelangeli, 2002) and may be able to block calpain-cleaved $InsP_3R1$. Unfortunately, 2-APB is not a specific inhibitor of $InsP_3R$, and has also been shown to target store operated channels (Bootman et al., 2002; Park et al., 2002), the sarcoplasmic/endoplasmic reticulum Ca^{2+}-ATPase (SERCA) (Bilmen et al., 2002; Peppiatt et al., 2003), and transient receptor potential channels (Hu

et al., 2004). Another potentially useful $InsP_3R$ blocker is xestospongin (Xe). Several forms of Xe have been used to specifically block Ca^{2+} release from $InsP_3R$ (Gafni et al., 1997). Their mechanism of action has not been definitively identified although it is speculated that XeB acts at an allosteric site on $InsP_3R$.[5] The potent inhibition of wt-$InsP_3R$-mediated Ca^{2+} release by XeB warrants examining the effects on calpain-cleaved $InsP_3R1$. Single-channel electrophysiology and single-cell Ca^{2+} imaging experiments using cultured cells expressing capn-$InsP_3R1$ provide useful models for determining whether XeB can effectively block the cleaved channel and restore Ca^{2+} homeostasis.

Defining the Role of $InsP_3R1$ Proteolysis in Cell Death Pathways

The work presented in this dissertation supports the causal role of calpain-cleaved $InsP_3R1$ in neurodegeneration and lays the framework for future investigations studying the cleaved channel in cell death pathways. An obvious question is, does blocking calpain proteolysis of $InsP_3R1$ prevent cell death? Unfortunately, this is experimentally difficult to answer as calpain sequentially cleaves $InsP_3R1$ into 200, 130 and 95 kDa carboxyl-terminal fragments (Magnusson et al., 1993; Igwe and Filla, 1997). Preventing calpain cleavage of the channel would require mutation of all 3 cleavage sites. However, only the site responsible for generating the 95 kDa fragment has been identified (Chapter 2). Investigations of the ~95 kDa caspase-3 cleaved form of $InsP_3R1$ could provide some insights. In one study, wt, caspase-cleaved, and caspase-resistant $InsP_3R1$ were expressed in $InsP_3R$ deficient B-lymphocytes to examine the impact of $InsP_3R1$ proteolysis on apoptotic cell death (Assefa et al., 2004). Expression of caspase-cleaved

[5] J. Molgo, via personal communication with G.E. Stutzmann, October 16, 2011

$InsP_3R1$ accelerated apoptosis in response to staurosporin and B-cell receptor stimulation compared with wt-$InsP_3R1$. In contrast, cleavage-resistant $InsP_3R1$ dramatically slowed apoptosis to levels observed in $InsP_3R$ deficient cells, and prevented Ca^{2+} overload and secondary necrosis. We speculate that calpain-resistant $InsP_3R1$ would afford similar protection against cell death. Since generating a calpain-resistant $InsP_3R1$ mutant is complicated at this time, future studies should focus on investigating the potentially protective effects of blocking Ca^{2+} release through the cleaved channel.

The proximal location of caspase and calpain cleavage sites within the primary amino acid sequence of $InsP_3R1$ further imply that proteolysis of $InsP_3R1$ is critical to cell death. This structural redundancy may be a fail-safe for cell death pathways, as there appear to be functional similarities between the caspase- and calpain-cleaved forms of $InsP_3R1$. The results presented in this dissertation regarding the effect of calpain-cleaved $InsP_3R1$ on Ca^{2+} homeostasis and cell death are similar to previously published studies of caspase-cleaved $InsP_3R1$ (Assefa et al., 2004; Verbert et al., 2008), suggesting that channel proteolysis by either caspase or calpain may produce a similar effect. Interestingly, $InsP_3R1$ digestion with caspase *in vitro* seems to prevent further proteolysis by calpain (unpublished observation). The implications of this are unclear, however it appears that $InsP_3R1$ proteolysis by either enzyme alone is sufficient for cell death. Importantly, both caspase (Haug et al., 2000) and calpain (Chapter 2) cleavage of $InsP_3R1$ are early steps in the molecular injury cascade suggesting a role for channel proteolysis in both the initiation and execution of cell death.

The idea that caspase- and calpain-proteolysis of $InsP_3R1$ provide a convergent pathway for cell death is further supported by evidence that there is considerable overlap between caspase and calpain proteolytic systems (Wang, 2000), and that calpain inhibition can shift cell death from calpain-mediated necrosis to caspase-mediated apoptosis (McGinnis et al., 1999; Zhu and Uckun, 2000; Neumar et al., 2003). Importantly, immunohistochemical staining for caspase- and calpain-specific substrate cleavage in ischemic brain tissue demonstrates distinct spatiotemporal patterns of activity for each enzyme (Zhang et al., 2002). Thus, $InsP_3R1$ proteolysis, by both caspase and calpain, may play a more diverse role in post-ischemic neurodegeneration than currently appreciated.

In ischemic brain injury, the effects of calpain-cleaved $InsP_3R1$ on impaired ER Ca^{2+} buffering (Chapters 2 and 3) may be compounded by proteolysis of other substrates. For example, calpain may further increase ER Ca^{2+} release by altering $InsP_3$ processing. Calpain cleavage of the B isoform of $InsP_3$ kinase prevents its localization to the ER membrane (Pattni et al., 2003), where it is responsible for converting $InsP_3$ into $InsP_4$ (Irvine et al., 1986), which cannot activate $InsP_3Rs$. Therefore, calpain proteolysis of $InsP_3$ kinase could reasonably increase the half-life of $InsP_3$ (Bevers and Neumar, 2008). This in turn would likely increase $InsP_3$ concentration, thereby activating more $InsP_3Rs$. Increased $InsP_3$ half-life also has interesting implications for the activity of heterotetrameric $InsP_3Rs$ with cleaved and full-length subunits following ischemia-reperfusion. We postulate that calpain proteolysis of individual subunits results in a gradual shift away from $InsP_3$-dependent Ca^{2+} activation. In the absence of $InsP_3$, this

means channel P_o increases with the number of subunits that are cleaved. In the presence of $InsP_3$, channels with non-cleaved subunits should have higher P_o. Although understanding the precise, complex function of heterotetrameric channels requires additional studies, based on this rationale, we predict that extended $InsP_3$ half-life resulting from calpain cleavage of $InsP_3$ kinase would result in a net increase in ER Ca^{2+} release over time. Additionally, proteolytic modification of SERCA could impair ER Ca^{2+} sequestration. While data demonstrating calpain-mediated cleavage of SERCA is tenuous, the predicted effect of proteolysis is a decrease in Ca^{2+} uptake into the ER (Parsons et al., 1999; Bevers and Neumar, 2008). Inhibition of ER Ca^{2+} store filling by impaired SERCA function can itself lead to depletion of lumenal ER $[Ca^{2+}]$ over time, and calpain-cleaved $InsP_3R1$ would certainly accelerate the effect. In our model expressing capn-$InsP_3R1$ in Neuro-2A cells, we observed slowed ER Ca^{2+} uptake, enhanced ER Ca^{2+} leak, and decreased steady-state ER $[Ca^{2+}]$ compared with controls (Chapter 2). In primary neuron culture, we observed increased resting $[Ca^{2+}]_i$ and impaired ER buffering of Ca^{2+} influx in neurons transduced with capn-$InsP_3R1$ (Chapter 3). These data indicate that, to a certain extent, the rate of Ca^{2+} leak through capn-$InsP_3R1$ is able to exceed the rate of Ca^{2+} uptake by functional SERCA. Under conditions in which calpain cleaves both $InsP_3R1$ and SERCA, the impact on intracellular Ca^{2+} homeostasis would likely be far more catastrophic. Together, these alterations in ER Ca^{2+} release and sequestration could represent an irreversible point of cellular injury, signaling post-ischemic neurodegeneration through cytoplasmic or mitochondrial Ca^{2+} overload. Better understanding of the sequence of these proteolytic and Ca^{2+} signaling

events, and identification of the calpain isoform(s) responsible may point to new targets for intervention in ischemic brain injury.

Implications for Therapeutic Intervention in Neurodegenerative Disease

The work presented in this thesis advances our understanding of the functional consequences of $InsP_3R1$ proteolysis and the broader role of the cleaved channel in neurodegeneration. Based on our results, we propose that blocking calpain-cleaved $InsP_3R1$ is a promising target for therapeutic intervention following ischemic brain injury. Moreover, calpain proteolysis of $InsP_3R1$ may be an important component of cell death pathways in a number of other neurodegenerative diseases characterized by disrupted Ca^{2+} signaling.

Translation of our investigation of calpain-cleaved $InsP_3R1$ into an *in vivo* system provides a potentially exciting and useful model for testing the neuroprotective efficacy of new therapeutic agents. Using intracranial injection and viral vector mediated gene delivery of capn-$InsP_3R1$, we successfully expressed the truncated channel in neurons in the adult brain, and observed degeneration of CA2 hippocampal neurons (Chapter 3). The selective vulnerability of this brain region lends itself to histological and stereological quantification of neuronal death. This in turn provides a simple, quantitative assay of neuroprotection afforded by potential therapeutic compounds. Limited neurodegeneration in this model also allows for studying compound effects in healthy, uninjured cells. Furthermore, using an *in vivo* system necessarily involves screening compounds for bioavailability in the brain, making results highly translatable.

Depending on results from *in vitro* experiments proposed above, XeB might provide a useful starting point for drug testing in our *in vivo* model.

Finally, our antibody directed against calpain-cleaved $InsP_3R1$ (Chapter 2) provides a valuable tool for examining $InsP_3R1$ proteolysis in other neurodegenerative diseases. Similar to data from ischemic brain injury, reductions in $InsP_3$-binding have been reported in brains from patients with Huntington's (Tanaka et al., 1993) and Alzheimer's diseases (Young et al., 1988; Garlind et al., 1995; Haug et al., 1996). Additionally, studies using animal models of excitotoxic injury (Haug et al., 1996) and prion disease (Lee et al., 2010) report decreased $InsP_3R$ expression, although Western blot analysis of $InsP_3R$ only examines the high molecular weight, full-length protein (260 kDa). Calpain proteolysis of $InsP_3R1$ could explain these results. Our cleavage specific antibody provides a sensitive way to detect calpain proteolysis of $InsP_3R1$ in brain homogenates and fixed tissue. Future investigators could utilize this antibody to screen animal and patient tissue for cleaved $InsP_3R1$. Regardless of which neurodegenerative diseases calpain-cleaved $InsP_3R1$ is identified in, these results will lay the groundwork for diverse future investigations of the broad neuropathologic role of $InsP_3R1$ proteolysis.

REFERENCES

Aarts M, Iihara K, Wei WL, Xiong ZG, Arundine M, Cerwinski W, MacDonald JF, Tymianski M (2003) A key role for TRPM7 channels in anoxic neuronal death. Cell 115:863-877.

Allen NJ, Attwell D (2002) Modulation of ASIC channels in rat cerebellar Purkinje neurons by ischaemia-related signals. J Physiol 543:521-529.

Alzayady KJ, Wojcikiewicz RJ (2005) The role of Ca^{2+} in triggering inositol 1,4,5-trisphosphate receptor ubiquitination. Biochem J 392:601-606.

Arai H, Passonneau JV, Lust WD (1986) Energy metabolism in delayed neuronal death of CA1 neurons of the hippocampus following transient ischemia in the gerbil. Metab Brain Dis 1:263-278.

Assefa Z, Bultynck G, Szlufcik K, Nadif Kasri N, Vermassen E, Goris J, Missiaen L, Callewaert G, Parys JB, De Smedt H (2004) Caspase-3-induced truncation of type 1 inositol trisphosphate receptor accelerates apoptotic cell death and induces inositol trisphosphate-independent calcium release during apoptosis. J Biol Chem 279:43227-43236.

Auriel E, Bornstein NM (2010) Neuroprotection in acute ischemic stroke--current status. J Cell Mol Med 14:2200-2202.

Bano D, Young KW, Guerin CJ, Lefeuvre R, Rothwell NJ, Naldini L, Rizzuto R, Carafoli E, Nicotera P (2005) Cleavage of the plasma membrane Na^{+}/Ca^{2+} exchanger in excitotoxicity. Cell 120:275-285.

Bardo S, Cavazzini MG, Emptage N (2006) The role of the endoplasmic reticulum Ca^{2+} store in the plasticity of central neurons. Trends Pharmacol Sci 27:78-84.

Bartus RT, Dean RL, Mennerick S, Eveleth D, Lynch G (1998) Temporal ordering of pathogenic events following transient global ischemia. Brain Res 790:1-13.

Beresewicz M, Kowalczyk JE, Zablocka B (2006) Cytochrome c binds to inositol (1,4,5) trisphosphate and ryanodine receptors in vivo after transient brain ischemia in gerbils. Neurochem Int 48:568-571.

Berridge MJ (1997) Elementary and global aspects of calcium signaling. J Physiol 499 (Pt 2):291-306.

Berridge MJ, Lipp P, Bootman MD (2000) The versatility and universality of calcium signalling. Nat Rev Mol Cell Biol 1:11-21.

Berridge MJ, Bootman MD, Roderick HL (2003) Calcium signaling: dynamics, homeostasis and remodelling. Nat Rev Mol Cell Biol 4:517-529.

Bevers MB, Neumar RW (2008) Mechanistic role of calpains in postischemic neurodegeneration. J Cereb Blood Flow Metab 28:655-673.

Bevers MB, Lawrence E, Maronski M, Starr N, Amesquita M, Neumar RW (2009) Knockdown of m-calpain increases survival of primary hippocampal neurons following NMDA excitotoxicity. J Neurochem 108:1237-1250.

Bevers MB, Ingleton LP, Che D, Cole JT, Li L, Da T, Kopil CM, Cohen AS, Neumar RW (2010) RNAi targeting micro-calpain increases neuron survival and preserves hippocampal function after global brain ischemia. Exp Neurol 224:170-177.

Bezprozvanny I (2005) The inositol 1,4,5-trisphosphate receptors. Cell Calcium 38:261-272.

Bhanumathy CD, Nakao SK, Joseph SK (2006) Mechanism of proteasomal degradation of inositol trisphosphate receptors in CHO-K1 cells. J Biol Chem 281:3722-3730.

Bilmen JG, Michelangeli F (2002) Inhibition of the type 1 inositol 1,4,5-trisphosphate receptor by 2-aminoethoxydiphenylborate. Cell Signal 14:955-960.

Bilmen JG, Wootton LL, Godfrey RE, Smart OS, Michelangeli F (2002) Inhibition of SERCA Ca^{2+} pumps by 2-aminoethoxydiphenyl borate (2-APB). 2-APB reduces both Ca^{2+} binding and phosphoryl transfer from ATP, by interfering with the pathway leading to the Ca^{2+}-binding sites. Eur J Biochem 269:3678-3687.

Boehning D, Joseph SK (2000) Functional properties of recombinant type I and type III inositol 1, 4,5-trisphosphate receptor isoforms expressed in COS-7 cells. J Biol Chem 275:21492-21499.

Boehning D, Mak DO, Foskett JK, Joseph SK (2001) Molecular determinants of ion permeation and selectivity in inositol 1,4,5-trisphosphate receptor Ca^{2+} channels. J Biol Chem 276:13509-13512.

Boehning D, Patterson RL, Sedaghat L, Glebova NO, Kurosaki T, Snyder SH (2003) Cytochrome c binds to inositol (1,4,5) trisphosphate receptors, amplifying calcium-dependent apoptosis. Nat Cell Biol 5:1051-1061.

Bootman MD, Collins TJ, Mackenzie L, Roderick HL, Berridge MJ, Peppiatt CM (2002) 2-aminoethoxydiphenyl borate (2-APB) is a reliable blocker of store-operated

Ca^{2+} entry but an inconsistent inhibitor of $InsP_3$-induced Ca^{2+} release. Faseb J 16:1145-1150.

BRCTIS Group (1991) A randomized clinical study of a calcium-entry blocker (lidoflazine) in the treatment of comatose survivors of cardiac arrest. Brain Resuscitation Clinical Trial II Study Group. N Engl J Med 324:1225-1231.

Burrone J, O'Byrne M, Murthy VN (2002) Multiple forms of synaptic plasticity triggered by selective suppression of activity in individual neurons. Nature 420:414-418.

Calle PA, Paridaens K, De Ridder LI, Buylaert WA (1993) Failure of nimodipine to prevent brain damage in a global brain ischemia model in the rat. Resuscitation 25:59-71.

Cardenas C, Miller RA, Smith I, Bui T, Molgo J, Muller M, Vais H, Cheung KH, Yang J, Parker I, Thompson CB, Birnbaum MJ, Hallows KR, Foskett JK (2010) Essential regulation of cell bioenergetics by constitutive $InsP_3$ receptor Ca^{2+} transfer to mitochondria. Cell 142:270-283.

CDC (2001) From the Centers for Disease Control and Prevention. Prevalence of disabilities and associated health conditions among adults--United States, 1999. Jama 285:1571-1572.

Chan J, Yamazaki H, Ishiyama N, Seo MD, Mal TK, Michikawa T, Mikoshiba K, Ikura M (2010) Structural studies of inositol 1,4,5-trisphosphate receptor: coupling ligand binding to channel gating. J Biol Chem 285:36092-36099.

Che D, Li L, Kopil CM, Liu Z, Guo W, Neumar RW (In Press) Impact of therapeutic hypothermia onset and duration on survival, neurologic function, and neurodegeneration after cardiac arrest. Crit Care Med.

Chen X, Kintner DB, Luo J, Baba A, Matsuda T, Sun D (2008) Endoplasmic reticulum Ca^{2+} dysregulation and endoplasmic reticulum stress following in vitro neuronal ischemia: role of Na+-K+-Cl- cotransporter. J Neurochem 106:1563-1576.

Cheung KH, Mei L, Mak DO, Hayashi I, Iwatsubo T, Kang DE, Foskett JK (2010) Gain-of-function enhancement of IP_3 receptor modal gating by familial Alzheimer's disease-linked presenilin mutants in human cells and mouse neurons. Sci Signal 3:ra22.

Cheung KH, Shineman D, Muller M, Cardenas C, Mei L, Yang J, Tomita T, Iwatsubo T, Lee VM, Foskett JK (2008) Mechanism of Ca^{2+} disruption in Alzheimer's disease by presenilin regulation of $InsP_3$ receptor channel gating. Neuron 58:871-883.

Chung YH, Shin CM, Kim MJ, Cha CI (2001a) Enhanced expression of L-type Ca^{2+} channels in reactive astrocytes after ischemic injury in rats. Neurosci Lett 302:93-96.

Chung YH, Shin CM, Kim MJ, Shin DH, Yoo YB, Cha CI (2001b) Spatial and temporal distribution of N-type Ca^{2+} channels in gerbil global cerebral ischemia. Brain Res 902:294-300.

Colbourne F, Sutherland GR, Auer RN (1996) An automated system for regulating brain temperature in awake and freely moving rodents. J Neurosci Methods 67:185-190.

Colegrove SL, Albrecht MA, Friel DD (2000) Quantitative analysis of mitochondrial Ca^{2+} uptake and release pathways in sympathetic neurons. Reconstruction of the recovery after depolarization-evoked [Ca2+]i elevations. J Gen Physiol 115:371-388.

Collins TJ, Lipp P, Berridge MJ, Bootman MD (2001) Mitochondrial Ca^{2+} uptake depends on the spatial and temporal profile of cytosolic Ca^{2+} signals. J Biol Chem 276:26411-26420.

Conn PJ, Pin JP (1997) Pharmacology and functions of metabotropic glutamate receptors. Annu Rev Pharmacol Toxicol 37:205-237.

Csordas G, Varnai P, Golenar T, Roy S, Purkins G, Schneider TG, Balla T, Hajnoczky G (2010) Imaging interorganelle contacts and local calcium dynamics at the ER-mitochondrial interface. Mol Cell 39:121-132.

Csordas G, Renken C, Varnai P, Walter L, Weaver D, Buttle KF, Balla T, Mannella CA, Hajnoczky G (2006) Structural and functional features and significance of the physical linkage between ER and mitochondria. J Cell Biol 174:915-921.

Cuerrier D, Moldoveanu T, Davies PL (2005) Determination of peptide substrate specificity for mu-calpain by a peptide library-based approach: the importance of primed side interactions. J Biol Chem 280:40632-40641.

Cummings DD, Wilcox KS, Dichter MA (1996) Calcium-dependent paired-pulse facilitation of miniature EPSC frequency accompanies depression of EPSCs at hippocampal synapses in culture. J Neurosci 16:5312-5323.

Dahl C, Haug LS, Spilsberg B, Johansen J, Ostvold AC, Diemer NH (2000) Reduced [^{3}H]IP_3 binding but unchanged IP_3 receptor levels in the rat hippocampus CA1 region following transient global ischemia and tolerance induction. Neurochem Int 36:379-388.

Davis RJ, Challiss J, Nahorski SR (1999) Enhanced purinoceptor-mediated Ca^{2+} signalling in L-fibroblasts overexpressing type 1 inositol 1,4,5-trisphosphate receptors. Biochem J 341 (Pt 3):813-820.

de Felipe P, Hughes LE, Ryan MD, Brown JD (2003) Co-translational, intraribosomal cleavage of polypeptides by the foot-and-mouth disease virus 2A peptide. J Biol Chem 278:11441-11448.

De Jongh KS, Colvin AA, Wang KK, Catterall WA (1994) Differential proteolysis of the full-length form of the L-type calcium channel alpha 1 subunit by calpain. J Neurochem 63:1558-1564.

Deshpande JK, Siesjo BK, Wieloch T (1987) Calcium accumulation and neuronal damage in the rat hippocampus following cerebral ischemia. J Cereb Blood Flow Metab 7:89-95.

Diaz F, Bourguignon LY (2000) Selective down-regulation of IP_3 receptor subtypes by caspases and calpain during TNF alpha -induced apoptosis of human T-lymphoma cells. Cell Calcium 27:315-328.

Dirnagl U, Iadecola C, Moskowitz MA (1999) Pathobiology of ischaemic stroke: an integrated view. Trends Neurosci 22:391-397.

Dong JY, Fan PD, Frizzell RA (1996) Quantitative analysis of the packaging capacity of recombinant adeno-associated virus. Hum Gene Ther 7:2101-2112.

Dong YN, Wu HY, Hsu FC, Coulter DA, Lynch DR (2006) Developmental and cell-selective variations in N-methyl-D-aspartate receptor degradation by calpain. J Neurochem 99:206-217.

Donnelly ML, Hughes LE, Luke G, Mendoza H, ten Dam E, Gani D, Ryan MD (2001) The 'cleavage' activities of foot-and-mouth disease virus 2A site-directed mutants and naturally occurring '2A-like' sequences. J Gen Virol 82:1027-1041.

Dux E, Mies G, Hossmann KA, Siklos L (1987) Calcium in the mitochondria following brief ischemia of gerbil brain. Neurosci Lett 78:295-300.

Erecinska M, Silver IA (1992) Relationship between ions and energy metabolism: cerebral calcium movements during ischaemia and subsequent recovery. Can J Physiol Pharmacol 70 Suppl:S190-193.

Fagni L, Chavis P, Ango F, Bockaert J (2000) Complex interactions between mGluRs, intracellular Ca^{2+} stores and ion channels in neurons. Trends Neurosci 23:80-88.

Fakler B, Adelman JP (2008) Control of K(Ca) channels by calcium nano/microdomains. Neuron 59:873-881.

Ferragamo MJ, Reinardy JL, Thayer SA (2009) Ca^{2+}-dependent, stimulus-specific modulation of the plasma membrane Ca^{2+} pump in hippocampal neurons. J Neurophysiol 101:2563-2571.

Fischer GA, Clementi E, Raichman M, Sudhof T, Ullrich A, Meldolesi J (1994) Stable expression of truncated inositol 1,4,5-trisphosphate receptor subunits in 3T3

fibroblasts. Coordinate signaling changes and differential suppression of cell growth and transformation. J Biol Chem 269:19216-19224.

Fisher KJ, Jooss K, Alston J, Yang Y, Haecker SE, High K, Pathak R, Raper SE, Wilson JM (1997) Recombinant adeno-associated virus for muscle directed gene therapy. Nat Med 3:306-312.

Fiskum G, Murphy AN, Beal MF (1999) Mitochondria in neurodegeneration: acute ischemia and chronic neurodegenerative diseases. J Cereb Blood Flow Metab 19:351-369.

Foskett JK (2010) Inositol trisphosphate receptor Ca^{2+} release channels in neurological diseases. Pflugers Arch 460:481-494.

Foskett JK, Mak DOD, Serysheva II (2010) Regulation of IP_3R Channel Gating by Ca^{2+} and Ca2+ Binding Proteins. In: Current Topics in Membranes, pp 235-272: Academic Press.

Foskett JK, White C, Cheung KH, Mak DO (2007) Inositol trisphosphate receptor Ca^{2+} release channels. Physiol Rev 87:593-658.

Frederick JR, Chen Z, Bevers MB, Ingleton LP, Ma M, Neumar RW (2008) Neuroprotection with delayed calpain inhibition after transient forebrain ischemia. Crit Care Med 36:S481-485.

French JP, Quindry JC, Falk DJ, Staib JL, Lee Y, Wang KK, Powers SK (2006) Ischemia-reperfusion-induced calpain activation and SERCA2a degradation are attenuated by exercise training and calpain inhibition. Am J Physiol Heart Circ Physiol 290:H128-136.

Furuichi T, Mikoshiba K (1995) Inositol 1, 4, 5-trisphosphate receptor-mediated Ca^{2+} signaling in the brain. J Neurochem 64:953-960.

Furuichi T, Simon-Chazottes D, Fujino I, Yamada N, Hasegawa M, Miyawaki A, Yoshikawa S, Guenet JL, Mikoshiba K (1993) Widespread expression of inositol 1,4,5-trisphosphate receptor type 1 gene (Insp3r1) in the mouse central nervous system. Receptors Channels 1:11-24.

Gafni J, Munsch JA, Lam TH, Catlin MC, Costa LG, Molinski TF, Pessah IN (1997) Xestospongins: potent membrane permeable blockers of the inositol 1,4,5-trisphosphate receptor. Neuron 19:723-733.

Galvan DL, Borrego-Diaz E, Perez PJ, Mignery GA (1999) Subunit oligomerization, and topology of the inositol 1,4, 5-trisphosphate receptor. J Biol Chem 274:29483-29492.

Gao L, Balshaw D, Xu L, Tripathy A, Xin C, Meissner G (2000) Evidence for a role of the lumenal M3-M4 loop in skeletal muscle Ca^{2+} release channel (ryanodine receptor) activity and conductance. Biophys J 79:828-840.

Garlind A, Cowburn RF, Forsell C, Ravid R, Winblad B, Fowler CJ (1995) Diminished [^{3}H]inositol(1,4,5)P_3 but not [^{3}H]inositol(1,3,4,5)P_4 binding in Alzheimer's disease brain. Brain Res 681:160-166.

Gascon S, Deogracias R, Sobrado M, Roda JM, Renart J, Rodriguez-Pena A, Diaz-Guerra M (2005) Transcription of the NR1 subunit of the N-methyl-D-aspartate receptor is down-regulated by excitotoxic stimulation and cerebral ischemia. J Biol Chem 280:35018-35027.

Ghosh TK, Eis PS, Mullaney JM, Ebert CL, Gill DL (1988) Competitive, reversible, and potent antagonism of inositol 1,4,5-trisphosphate-activated calcium release by heparin. J Biol Chem 263:11075-11079.

Gleichmann M, Mattson MP (2011) Neuronal calcium homeostasis and dysregulation. Antioxid Redox Signal 14:1261-1273.

Goll DE, Thompson VF, Li H, Wei W, Cong J (2003) The calpain system. Physiol Rev 83:731-801.

Gorter JA, Petrozzino JJ, Aronica EM, Rosenbaum DM, Opitz T, Bennett MV, Connor JA, Zukin RS (1997) Global ischemia induces downregulation of Glur2 mRNA and increases AMPA receptor-mediated Ca^{2+} influx in hippocampal CA1 neurons of gerbil. J Neurosci 17:6179-6188.

Guttmann RP, Sokol S, Baker DL, Simpkins KL, Dong Y, Lynch DR (2002) Proteolysis of the N-methyl-d-aspartate receptor by calpain in situ. J Pharmacol Exp Ther 302:1023-1030.

Hansen AJ (1985) Effect of anoxia on ion distribution in the brain. Physiol Rev 65:101-148.

Hara K, Yasuhara T, Matsukawa N, Maki M, Masuda T, Yu G, Xu L, Tambrallo L, Rodriguez NA, Stern DM, Kawase T, Yamashima T, Buccafusco JJ, Hess DC, Borlongan CV (2007) Hippocampal CA1 cell loss in a non-human primate model of transient global ischemia: a pilot study. Brain Res Bull 74:164-171.

Haug LS, Walaas SI, Ostvold AC (2000) Degradation of the type I inositol 1,4,5-trisphosphate receptor by caspase-3 in SH-SY5Y neuroblastoma cells undergoing apoptosis. J Neurochem 75:1852-1861.

Haug LS, Ostvold AC, Cowburn RF, Garlind A, Winblad B, Bogdanovich N, Walaas SI (1996) Decreased inositol (1,4,5)-trisphosphate receptor levels in Alzheimer's disease cerebral cortex: selectivity of changes and possible correlation to pathological severity. Neurodegeneration 5:169-176.

Hell JW, Westenbroek RE, Breeze LJ, Wang KK, Chavkin C, Catterall WA (1996) N-methyl-D-aspartate receptor-induced proteolytic conversion of postsynaptic class C L-type calcium channels in hippocampal neurons. Proc Natl Acad Sci U S A 93:3362-3367.

Hicke L (2001) Protein regulation by monoubiquitin. Nat Rev Mol Cell Biol 2:195-201.

Higo T, Hamada K, Hisatsune C, Nukina N, Hashikawa T, Hattori M, Nakamura T, Mikoshiba K (2010) Mechanism of ER stress-induced brain damage by IP_3 receptor. Neuron 68:865-878.

Higuchi M, Tomioka M, Takano J, Shirotani K, Iwata N, Masumoto H, Maki M, Itohara S, Saido TC (2005) Distinct mechanistic roles of calpain and caspase activation in neurodegeneration as revealed in mice overexpressing their specific inhibitors. J Biol Chem 280:15229-15237.

Hirota J, Furuichi T, Mikoshiba K (1999) Inositol 1,4,5-trisphosphate receptor type 1 is a substrate for caspase-3 and is cleaved during apoptosis in a caspase-3-dependent manner. J Biol Chem 274:34433-34437.

Hood JL, Brooks WH, Roszman TL (2004) Differential compartmentalization of the calpain/calpastatin network with the endoplasmic reticulum and Golgi apparatus. J Biol Chem 279:43126-43135.

Hood JL, Logan BB, Sinai AP, Brooks WH, Roszman TL (2003) Association of the calpain/calpastatin network with subcellular organelles. Biochem Biophys Res Commun 310:1200-1212.

Hu HZ, Gu Q, Wang C, Colton CK, Tang J, Kinoshita-Kawada M, Lee LY, Wood JD, Zhu MX (2004) 2-aminoethoxydiphenyl borate is a common activator of TRPV1, TRPV2, and TRPV3. J Biol Chem 279:35741-35748.

Igwe OJ, Filla MB (1997) Aging-related regulation of myo-inositol 1,4,5-trisphosphate signal transduction pathway in the rat striatum. Brain Res Mol Brain Res 46:39-53.

Ikeda F, Dikic I (2008) Atypical ubiquitin chains: new molecular signals. 'Protein Modifications: Beyond the Usual Suspects' review series. EMBO Rep 9:536-542.

Ionescu L, Cheung KH, Vais H, Mak DO, White C, Foskett JK (2006) Graded recruitment and inactivation of single $InsP_3$ receptor Ca^{2+}-release channels: implications for quantal [corrected] Ca^{2+} release. J Physiol 573:645-662.

Irvine RF, Letcher AJ, Heslop JP, Berridge MJ (1986) The inositol tris/tetrakisphosphate pathway--demonstration of $Ins(1,4,5)P_3$ 3-kinase activity in animal tissues. Nature 320:631-634.

Jayaraman T, Marks AR (1997) T cells deficient in inositol 1,4,5-trisphosphate receptor are resistant to apoptosis. Mol Cell Biol 17:3005-3012.

Jeffs GJ, Meloni BP, Bakker AJ, Knuckey NW (2007) The role of the Na^+/Ca^{2+} exchanger (NCX) in neurons following ischaemia. J Clin Neurosci 14:507-514.

Jorgensen MB, Jensen CV, Diemer NH (1991) Modification of [^{3}H]inositoltrisphosphate binding in kainic acid-lesioned and postischemic rat hippocampus. Brain Res 538:246-250.

Joseph SK, Samanta S (1993) Detergent solubility of the inositol trisphosphate receptor in rat brain membranes. Evidence for association of the receptor with ankyrin. J Biol Chem 268:6477-6486.

Joseph SK, Pierson S, Samanta S (1995) Trypsin digestion of the inositol trisphosphate receptor: implications for the conformation and domain organization of the protein. Biochem J 307 (Pt 3):859-865.

Katz L, Ebmeyer U, Safar P, Radovsky A, Neumar R (1995) Outcome model of asphyxial cardiac arrest in rats. J Cereb Blood Flow Metab 15:1032-1039.

Kirino T (1982) Delayed neuronal death in the gerbil hippocampus following ischemia. Brain Res 239:57-69.

Kirino T, Tamura A, Sano K (1984) Delayed neuronal death in the rat hippocampus following transient forebrain ischemia. Acta Neuropathol 64:139-147.

Kohno K, Higuchi T, Ohta S, Kohno K, Kumon Y, Sakaki S (1997) Neuroprotective nitric oxide synthase inhibitor reduces intracellular calcium accumulation following transient global ischemia in the gerbil. Neurosci Lett 224:17-20.

Kopil CM, Vais H, Cheung KH, Siebert AP, Mak DO, Foskett JK, Neumar RW (2011) Calpain-cleaved type 1 inositol 1,4,5-trisphosphate receptor ($InsP_3R1$) has

InsP(3)-independent gating and disrupts intracellular Ca^{2+} homeostasis. J Biol Chem 286:35998-36010.

Kristian T, Siesjo BK (1998) Calcium in ischemic cell death. Stroke 29:705-718.

Kumar K, Goosmann M, Krause GS, Nayini NR, Estrada R, Hoehner TJ, White BC, Koestner A (1987) Ultrastructural and ionic studies in global ischemic dog brain. Acta Neuropathol 73:393-399.

Lee HP, Choi JK, Shin HY, Jeon YC, Jeong BH, Lee HG, Kim JI, Choi EK, Carp RI, Kim YS (2010) Altered expression of type 1 inositol 1,4,5-trisphosphate receptor in the Ngsk Prnp deficient mice. Neuroscience 167:799-808.

Lee KS, Frank S, Vanderklish P, Arai A, Lynch G (1991) Inhibition of proteolysis protects hippocampal neurons from ischemia. Proc Natl Acad Sci U S A 88:7233-7237.

Lein ES, Zhao X, Gage FH (2004) Defining a molecular atlas of the hippocampus using DNA microarrays and high-throughput in situ hybridization. J Neurosci 24:3879-3889.

Lein ES, Hawrylycz MJ, Ao N, Ayres M, Bensinger A, Bernard A, Boe AF, Boguski MS, Brockway KS, Byrnes EJ, Chen L, Chen L, Chen TM, Chin MC, Chong J, Crook BE, Czaplinska A, Dang CN, Datta S, Dee NR, Desaki AL, Desta T, Diep E, Dolbeare TA, Donelan MJ, Dong HW, Dougherty JG, Duncan BJ, Ebbert AJ, Eichele G, Estin LK, Faber C, Facer BA, Fields R, Fischer SR, Fliss TP, Frensley C, Gates SN, Glattfelder KJ, Halverson KR, Hart MR, Hohmann JG, Howell MP, Jeung DP, Johnson RA, Karr PT, Kawal R, Kidney JM, Knapik RH, Kuan CL,

Lake JH, Laramee AR, Larsen KD, Lau C, Lemon TA, Liang AJ, Liu Y, Luong LT, Michaels J, Morgan JJ, Morgan RJ, Mortrud MT, Mosqueda NF, Ng LL, Ng R, Orta GJ, Overly CC, Pak TH, Parry SE, Pathak SD, Pearson OC, Puchalski RB, Riley ZL, Rockett HR, Rowland SA, Royall JJ, Ruiz MJ, Sarno NR, Schaffnit K, Shapovalova NV, Sivisay T, Slaughterbeck CR, Smith SC, Smith KA, Smith BI, Sodt AJ, Stewart NN, Stumpf KR, Sunkin SM, Sutram M, Tam A, Teemer CD, Thaller C, Thompson CL, Varnam LR, Visel A, Whitlock RM, Wohnoutka PE, Wolkey CK, Wong VY, et al. (2007) Genome-wide atlas of gene expression in the adult mouse brain. Nature 445:168-176.

Leissring MA, Parker I, LaFerla FM (1999a) Presenilin-2 mutations modulate amplitude and kinetics of inositol 1, 4,5-trisphosphate-mediated calcium signals. J Biol Chem 274:32535-32538.

Leissring MA, Paul BA, Parker I, Cotman CW, LaFerla FM (1999b) Alzheimer's presenilin-1 mutation potentiates inositol 1,4,5-trisphosphate-mediated calcium signaling in Xenopus oocytes. J Neurochem 72:1061-1068.

Leloup L, Shao H, Bae YH, Deasy B, Stolz D, Roy P, Wells A (2010) m-Calpain activation is regulated by its membrane localization and by its binding to phosphatidylinositol 4,5-bisphosphate. J Biol Chem 285:33549-33566.

Li C, Wang X, Vais H, Thompson CB, Foskett JK, White C (2007) Apoptosis regulation by Bcl-x(L) modulation of mammalian inositol 1,4,5-trisphosphate receptor channel isoform gating. Proc Natl Acad Sci U S A 104:12565-12570.

Li PA, Howlett W, He QP, Miyashita H, Siddiqui M, Shuaib A (1998) Postischemic treatment with calpain inhibitor MDL 28170 ameliorates brain damage in a gerbil model of global ischemia. Neurosci Lett 247:17-20.

Liu J, Tang TS, Tu H, Nelson O, Herndon E, Huynh DP, Pulst SM, Bezprozvanny I (2009) Deranged calcium signaling and neurodegeneration in spinocerebellar ataxia type 2. J Neurosci 29:9148-9162.

Liu Z, Zhao W, Xu T, Pei D, Peng Y (2010) Alterations of NMDA receptor subunits NR1, NR2A and NR2B mRNA expression and their relationship to apoptosis following transient forebrain ischemia. Brain Res 1361:133-139.

Lloyd-Jones D, Adams RJ, Brown TM, Carnethon M, Dai S, De Simone G, Ferguson TB, Ford E, Furie K, Gillespie C, Go A, Greenlund K, Haase N, Hailpern S, Ho PM, Howard V, Kissela B, Kittner S, Lackland D, Lisabeth L, Marelli A, McDermott MM, Meigs J, Mozaffarian D, Mussolino M, Nichol G, Roger VL, Rosamond W, Sacco R, Sorlie P, Roger VL, Thom T, Wasserthiel-Smoller S, Wong ND, Wylie-Rosett J (2010) Heart disease and stroke statistics--2010 update: a report from the American Heart Association. Circulation 121:e46-e215.

Mackrill JJ, Wilcox RA, Miyawaki A, Mikoshiba K, Nahorski SR, Challiss RA (1996) Stable overexpression of the type-1 inositol 1,4,5-trisphosphate receptor in L fibroblasts: subcellular distribution and functional consequences. Biochem J 318 (Pt 3):871-878.

Maeda E, Robinson HP, Kawana A (1995) The mechanisms of generation and propagation of synchronized bursting in developing networks of cortical neurons. J Neurosci 15:6834-6845.

Magnusson A, Haug LS, Walaas SI, Ostvold AC (1993) Calcium-induced degradation of the inositol (1,4,5)-trisphosphate receptor/Ca^{2+}-channel. FEBS Lett 323:229-232.

Martins E, Inamura K, Themner K, Malmqvist KG, Siesjo BK (1988) Accumulation of calcium and loss of potassium in the hippocampus following transient cerebral ischemia: a proton microprobe study. J Cereb Blood Flow Metab 8:531-538.

Maruyama T, Kanaji T, Nakade S, Kanno T, Mikoshiba K (1997) 2APB, 2-aminoethoxydiphenyl borate, a membrane-penetrable modulator of Ins(1,4,5)P_3-induced Ca2+ release. J Biochem 122:498-505.

Mattson MP (2007) Calcium and neurodegeneration. Aging Cell 6:337-350.

Mattson MP, LaFerla FM, Chan SL, Leissring MA, Shepel PN, Geiger JD (2000) Calcium signaling in the ER: its role in neuronal plasticity and neurodegenerative disorders. Trends Neurosci 23:222-229.

McGinnis KM, Wang KK, Gnegy ME (1999) Alterations of extracellular calcium elicit selective modes of cell death and protease activation in SH-SY5Y human neuroblastoma cells. J Neurochem 72:1853-1863.

Mellstrom B, Naranjo JR (2001) Mechanisms of Ca(2+)-dependent transcription. Curr Opin Neurobiol 11:312-319.

Michaelis EK (1998) Molecular biology of glutamate receptors in the central nervous system and their role in excitotoxicity, oxidative stress and aging. Prog Neurobiol 54:369-415.

Mignery GA, Sudhof TC (1990) The ligand binding site and transduction mechanism in the inositol-1,4,5-triphosphate receptor. Embo J 9:3893-3898.

Mitani A, Yanase H, Sakai K, Wake Y, Kataoka K (1993) Origin of intracellular Ca^{2+} elevation induced by in vitro ischemia-like condition in hippocampal slices. Brain Res 601:103-110.

Mongardon N, Dumas F, Ricome S, Grimaldi D, Hissem T, Pene F, Cariou A (2011) Postcardiac arrest syndrome: from immediate resuscitation to long-term outcome. Ann Intensive Care 1:45.

Murphy TH, Blatter LA, Wier WG, Baraban JM (1992) Spontaneous synchronous synaptic calcium transients in cultured cortical neurons. J Neurosci 12:4834-4845.

Nagasawa H, Kogure K (1991) Alterations of [^{3}H]inositol 1,4,5-trisphosphate binding in the postischemic rat brain. Neurosci Lett 133:129-132.

Nagata E, Tanaka K, Suzuki S, Dembo T, Fukuuchi Y, Futatsugi A, Mikoshiba K (1999) Selective inhibition of inositol 1,4,5-triphosphate-induced Ca^{2+} release in the CA1 region of the hippocampus in the ischemic gerbil. Neuroscience 93:995-1001.

Nakashima K, Todd MM, Warner DS (1995) The relation between cerebral metabolic rate and ischemic depolarization. A comparison of the effects of hypothermia, pentobarbital, and isoflurane. Anesthesiology 82:1199-1208.

Nakayama T, Hattori M, Uchida K, Nakamura T, Tateishi Y, Bannai H, Iwai M, Michikawa T, Inoue T, Mikoshiba K (2004) The regulatory domain of the inositol 1,4,5-trisphosphate receptor is necessary to keep the channel domain closed: possible physiological significance of specific cleavage by caspase 3. Biochem J 377:299-307.

Nakka VP, Gusain A, Mehta SL, Raghubir R (2008) Molecular mechanisms of apoptosis in cerebral ischemia: multiple neuroprotective opportunities. Mol Neurobiol 37:7-38.

Neher E (1998) Vesicle pools and Ca2+ microdomains: new tools for understanding their roles in neurotransmitter release. Neuron 20:389-399.

Neumar RW (2000) Molecular mechanisms of ischemic neuronal injury. Ann Emerg Med 36:483-506.

Neumar RW, Hagle SM, DeGracia DJ, Krause GS, White BC (1996) Brain mu-calpain autolysis during global cerebral ischemia. J Neurochem 66:421-424.

Neumar RW, Xu YA, Gada H, Guttmann RP, Siman R (2003) Cross-talk between calpain and caspase proteolytic systems during neuronal apoptosis. J Biol Chem 278:14162-14167.

Neumar RW, Meng FH, Mills AM, Xu YA, Zhang C, Welsh FA, Siman R (2001) Calpain activity in the rat brain after transient forebrain ischemia. Exp Neurol 170:27-35.

Neumar RW, Bircher NG, Sim KM, Xiao F, Zadach KS, Radovsky A, Katz L, Ebmeyer E, Safar P (1995) Epinephrine and sodium bicarbonate during CPR following asphyxial cardiac arrest in rats. Resuscitation 29:249-263.

Nicholls DG (1985) A role for the mitochondrion in the protection of cells against calcium overload? Prog Brain Res 63:97-106.

Nicholson C, Bruggencate GT, Steinberg R, Stockle H (1977) Calcium modulation in brain extracellular microenvironment demonstrated with ion-selective micropipette. Proc Natl Acad Sci U S A 74:1287-1290.

O'Donnell LA, Agrawal A, Jordan-Sciutto KL, Dichter MA, Lynch DR, Kolson DL (2006) Human immunodeficiency virus (HIV)-induced neurotoxicity: roles for the NMDA receptor subtypes. J Neurosci 26:981-990.

Orrenius S, Zhivotovsky B, Nicotera P (2003) Regulation of cell death: the calcium-apoptosis link. Nat Rev Mol Cell Biol 4:552-565.

Park MK, Lee KK, Uhm DY (2002) Slow depletion of endoplasmic reticulum Ca^{2+} stores and block of store-operated Ca^{2+} channels by 2-aminoethoxydiphenyl borate in mouse pancreatic acinar cells. Naunyn Schmiedebergs Arch Pharmacol 365:399-405.

Parker AK, Gergely FV, Taylor CW (2004) Targeting of inositol 1,4,5-trisphosphate receptors to the endoplasmic reticulum by multiple signals within their transmembrane domains. J Biol Chem 279:23797-23805.

Parsons JT, Churn SB, DeLorenzo RJ (1999) Global ischemia-induced inhibition of the coupling ratio of calcium uptake and ATP hydrolysis by rat whole brain microsomal Mg^{2+}/Ca^{2+} ATPase. Brain Res 834:32-41.

Paschen W, Mengesdorf T (2005) Endoplasmic reticulum stress response and neurodegeneration. Cell Calcium 38:409-415.

Pattni K, Millard TH, Banting G (2003) Calpain cleavage of the B isoform of Ins(1,4,5)P_3 3-kinase separates the catalytic domain from the membrane anchoring domain. Biochem J 375:643-651.

Pellegrini-Giampietro DE, Pulsinelli WA, Zukin RS (1994) NMDA and non-NMDA receptor gene expression following global brain ischemia in rats: effect of NMDA and non-NMDA receptor antagonists. J Neurochem 62:1067-1073.

Pellegrini-Giampietro DE, Zukin RS, Bennett MV, Cho S, Pulsinelli WA (1992) Switch in glutamate receptor subunit gene expression in CA1 subfield of hippocampus following global ischemia in rats. Proc Natl Acad Sci U S A 89:10499-10503.

Peppiatt CM, Collins TJ, Mackenzie L, Conway SJ, Holmes AB, Bootman MD, Berridge MJ, Seo JT, Roderick HL (2003) 2-Aminoethoxydiphenyl borate (2-APB) antagonises inositol 1,4,5-trisphosphate-induced calcium release, inhibits calcium pumps and has a use-dependent and slowly reversible action on store-operated calcium entry channels. Cell Calcium 34:97-108.

Pinton P, Giorgi C, Siviero R, Zecchini E, Rizzuto R (2008) Calcium and apoptosis: ER-mitochondria Ca^{2+} transfer in the control of apoptosis. Oncogene 27:6407-6418.

Pisani A, Bonsi P, Centonze D, Giacomini P, Calabresi P (2000) Involvement of intracellular calcium stores during oxygen/glucose deprivation in striatal large aspiny interneurons. J Cereb Blood Flow Metab 20:839-846.

Pottorf WJ, 2nd, Johanns TM, Derrington SM, Strehler EE, Enyedi A, Thayer SA (2006) Glutamate-induced protease-mediated loss of plasma membrane Ca^{2+} pump activity in rat hippocampal neurons. J Neurochem 98:1646-1656.

Pulsinelli WA (1985) Selective neuronal vulnerability: morphological and molecular characteristics. Prog Brain Res 63:29-37.

Pulsinelli WA, Brierley JB, Plum F (1982) Temporal profile of neuronal damage in a model of transient forebrain ischemia. Ann Neurol 11:491-498.

Rami A, Krieglstein J (1993) Protective effects of calpain inhibitors against neuronal damage caused by cytotoxic hypoxia in vitro and ischemia in vivo. Brain Res 609:67-70.

Ramos-Franco J, Galvan D, Mignery GA, Fill M (1999) Location of the permeation pathway in the recombinant type 1 inositol 1,4,5-trisphosphate receptor. J Gen Physiol 114:243-250.

Rao AM, Hatcher JF, Dempsey RJ (2000) Neuroprotection by group I metabotropic glutamate receptor antagonists in forebrain ischemia of gerbil. Neurosci Lett 293:1-4.

Rardon DP, Cefali DC, Mitchell RD, Seiler SM, Hathaway DR, Jones LR (1990) Digestion of cardiac and skeletal muscle junctional sarcoplasmic reticulum vesicles with calpain II. Effects on the Ca^{2+} release channel. Circ Res 67:84-96.

Roberts-Lewis JM, Savage MJ, Marcy VR, Pinsker LR, Siman R (1994) Immunolocalization of calpain I-mediated spectrin degradation to vulnerable neurons in the ischemic gerbil brain. J Neurosci 14:3934-3944.

Roine RO, Kaste M, Kinnunen A, Nikki P, Sarna S, Kajaste S (1990) Nimodipine after resuscitation from out-of-hospital ventricular fibrillation. A placebo-controlled, double-blind, randomized trial. Jama 264:3171-3177.

Royo NC, Vandenberghe LH, Ma JY, Hauspurg A, Yu L, Maronski M, Johnston J, Dichter MA, Wilson JM, Watson DJ (2008) Specific AAV serotypes stably transduce primary hippocampal and cortical cultures with high efficiency and low toxicity. Brain Res 1190:15-22.

Sahota P, Savitz SI (2011) Investigational therapies for ischemic stroke: neuroprotection and neurorecovery. Neurotherapeutics 8:434-451.

Saido TC, Yokota M, Nagao S, Yamaura I, Tani E, Tsuchiya T, Suzuki K, Kawashima S (1993) Spatial resolution of fodrin proteolysis in postischemic brain. J Biol Chem 268:25239-25243.

Samanta K, Kar P, Chakraborti T, Chakraborti S (2009) Calcium-dependent cleavage of the Na^{+}/Ca^{2+} exchanger by m-calpain in isolated endoplasmic reticulum. J Biochem 147:225-235.

Samanta K, Kar P, Ghosh B, Chakraborti T, Chakraborti S (2007) Localization of m-calpain and calpastatin and studies of their association in pulmonary smooth muscle endoplasmic reticulum. Biochim Biophys Acta 1770:1297-1307.

Sayers LG, Miyawaki A, Muto A, Takeshita H, Yamamoto A, Michikawa T, Furuichi T, Mikoshiba K (1997) Intracellular targeting and homotetramer formation of a truncated inositol 1,4,5-trisphosphate receptor-green fluorescent protein chimera in Xenopus laevis oocytes: evidence for the involvement of the transmembrane spanning domain in endoplasmic reticulum targeting and homotetramer complex formation. Biochem J 323 (Pt 1):273-280.

Schug ZT, Joseph SK (2006) The role of the S4-S5 linker and C-terminal tail in inositol 1,4,5-trisphosphate receptor function. J Biol Chem 281:24431-24440.

Sharp AH, McPherson PS, Dawson TM, Aoki C, Campbell KP, Snyder SH (1993) Differential immunohistochemical localization of inositol 1,4,5-trisphosphate- and ryanodine-sensitive Ca^{2+} release channels in rat brain. J Neurosci 13:3051-3063.

Shirokova N, Niggli E (2008) Studies of RyR function in situ. Methods 46:183-193.

Silver IA, Erecinska M (1990) Intracellular and extracellular changes of [Ca2+] in hypoxia and ischemia in rat brain in vivo. J Gen Physiol 95:837-866.

Silver IA, Erecinska M (1992) Ion homeostasis in rat brain in vivo: intra- and extracellular [Ca^{2+}] and [H^{+}] in the hippocampus during recovery from short-term, transient ischemia. J Cereb Blood Flow Metab 12:759-772.

Simon RP, Griffiths T, Evans MC, Swan JH, Meldrum BS (1984) Calcium overload in selectively vulnerable neurons of the hippocampus during and after ischemia: an electron microscopy study in the rat. J Cereb Blood Flow Metab 4:350-361.

Simpkins KL, Guttmann RP, Dong Y, Chen Z, Sokol S, Neumar RW, Lynch DR (2003) Selective activation induced cleavage of the NR2B subunit by calpain. J Neurosci 23:11322-11331.

Sims NR (1992) Energy metabolism and selective neuronal vulnerability following global cerebral ischemia. Neurochem Res 17:923-931.

Sirabella R, Secondo A, Pannaccione A, Scorziello A, Valsecchi V, Adornetto A, Bilo L, Di Renzo G, Annunziato L (2009) Anoxia-induced NF-kappaB-dependent upregulation of NCX1 contributes to Ca^{2+} refilling into endoplasmic reticulum in cortical neurons. Stroke 40:922-929.

Sliter DA, Kubota K, Kirkpatrick DS, Alzayady KJ, Gygi SP, Wojcikiewicz RJ (2008) Mass spectrometric analysis of type 1 inositol 1,4,5-trisphosphate receptor ubiquitination. J Biol Chem 283:35319-35328.

Smith ML, Auer RN, Siesjo BK (1984) The density and distribution of ischemic brain injury in the rat following 2-10 min of forebrain ischemia. Acta Neuropathol 64:319-332.

Starkov AA, Chinopoulos C, Fiskum G (2004) Mitochondrial calcium and oxidative stress as mediators of ischemic brain injury. Cell Calcium 36:257-264.

Streb H, Irvine RF, Berridge MJ, Schulz I (1983) Release of Ca^{2+} from a nonmitochondrial intracellular store in pancreatic acinar cells by inositol-1,4,5-trisphosphate. Nature 306:67-69.

Stutzmann GE, Mattson MP (2011) Endoplasmic reticulum Ca^{2+} handling in excitable cells in health and disease. Pharmacol Rev 63:700-727.

Stutzmann GE, Caccamo A, LaFerla FM, Parker I (2004) Dysregulated IP_3 signaling in cortical neurons of knock-in mice expressing an Alzheimer's-linked mutation in presenilin1 results in exaggerated Ca^{2+} signals and altered membrane excitability. J Neurosci 24:508-513.

Sugawara H, Kurosaki M, Takata M, Kurosaki T (1997) Genetic evidence for involvement of type 1, type 2 and type 3 inositol 1,4,5-trisphosphate receptors in signal transduction through the B-cell antigen receptor. Embo J 16:3078-3088.

Szydlowska K, Tymianski M (2010) Calcium, ischemia and excitotoxicity. Cell Calcium 47:122-129.

Szymczak AL, Workman CJ, Wang Y, Vignali KM, Dilioglou S, Vanin EF, Vignali DA (2004) Correction of multi-gene deficiency in vivo using a single 'self-cleaving' 2A peptide-based retroviral vector. Nat Biotechnol 22:589-594.

Tanaka C, Nishino N, Hashimoto T, Kitamura N, Yoshihara C, Saito N (1993) Second messenger systems in brains of patients with Parkinson's or Huntington's disease. Adv Neurol 60:175-180.

Tang TS, Tu H, Chan EY, Maximov A, Wang Z, Wellington CL, Hayden MR, Bezprozvanny I (2003) Huntingtin and huntingtin-associated protein 1 influence neuronal calcium signaling mediated by inositol-(1,4,5) triphosphate receptor type 1. Neuron 39:227-239.

Tang TS, Slow E, Lupu V, Stavrovskaya IG, Sugimori M, Llinas R, Kristal BS, Hayden MR, Bezprozvanny I (2005) Disturbed Ca^{2+} signaling and apoptosis of medium spiny neurons in Huntington's disease. Proc Natl Acad Sci U S A 102:2602-2607.

Taylor CW, da Fonseca PC, Morris EP (2004) IP_3 receptors: the search for structure. Trends Biochem Sci 29:210-219.

Taylor RC, Cullen SP, Martin SJ (2008) Apoptosis: controlled demolition at the cellular level. Nat Rev Mol Cell Biol 9:231-241.

Tompa P, Buzder-Lantos P, Tantos A, Farkas A, Szilagyi A, Banoczi Z, Hudecz F, Friedrich P (2004) On the sequential determinants of calpain cleavage. J Biol Chem 279:20775-20785.

Turrigiano GG (2008) The self-tuning neuron: synaptic scaling of excitatory synapses. Cell 135:422-435.

Verbert L, Lee B, Kocks SL, Assefa Z, Parys JB, Missiaen L, Callewaert G, Fissore RA, De Smedt H, Bultynck G (2008) Caspase-3-truncated type 1 inositol 1,4,5-trisphosphate receptor enhances intracellular Ca^{2+} leak and disturbs Ca^{2+} signalling. Biol Cell 100:39-49.

Verkhratsky A, Toescu EC (2003) Endoplasmic reticulum Ca^{2+} homeostasis and neuronal death. J Cell Mol Med 7:351-361.

Vosler PS, Brennan CS, Chen J (2008) Calpain-mediated signaling mechanisms in neuronal injury and neurodegeneration. Mol Neurobiol 38:78-100.

Wang KK (2000) Calpain and caspase: can you tell the difference? Trends Neurosci 23:20-26.

Wang Y, Xu L, Pasek DA, Gillespie D, Meissner G (2005) Probing the role of negatively charged amino acid residues in ion permeation of skeletal muscle ryanodine receptor. Biophys J 89:256-265.

Wei H, Perry DC (1996) Dantrolene is cytoprotective in two models of neuronal cell death. J Neurochem 67:2390-2398.

Wei X, Neely A, Lacerda AE, Olcese R, Stefani E, Perez-Reyes E, Birnbaumer L (1994) Modification of Ca^{2+} channel activity by deletions at the carboxyl terminus of the cardiac alpha 1 subunit. J Biol Chem 269:1635-1640.

White C, Li C, Yang J, Petrenko NB, Madesh M, Thompson CB, Foskett JK (2005) The endoplasmic reticulum gateway to apoptosis by Bcl-X(L) modulation of the $InsP_3R$. Nat Cell Biol 7:1021-1028.

Wojcikiewicz RJ (2004) Regulated ubiquitination of proteins in GPCR-initiated signaling pathways. Trends Pharmacol Sci 25:35-41.

Wojcikiewicz RJ, Oberdorf JA (1996) Degradation of inositol 1,4,5-trisphosphate receptors during cell stimulation is a specific process mediated by cysteine protease activity. J Biol Chem 271:16652-16655.

Xing H, Azimi-Zonooz A, Shuttleworth CW, Connor JA (2004) Caffeine releasable stores of Ca^{2+} show depletion prior to the final steps in delayed CA1 neuronal death. J Neurophysiol 92:2960-2967.

Xiong ZG, Zhu XM, Chu XP, Minami M, Hey J, Wei WL, MacDonald JF, Wemmie JA, Price MP, Welsh MJ, Simon RP (2004) Neuroprotection in ischemia: blocking calcium-permeable acid-sensing ion channels. Cell 118:687-698.

Yamashima T, Tonchev AB, Tsukada T, Saido TC, Imajoh-Ohmi S, Momoi T, Kominami E (2003) Sustained calpain activation associated with lysosomal

rupture executes necrosis of the postischemic CA1 neurons in primates. Hippocampus 13:791-800.

Yamashima T, Saido TC, Takita M, Miyazawa A, Yamano J, Miyakawa A, Nishijyo H, Yamashita J, Kawashima S, Ono T, Yoshioka T (1996) Transient brain ischaemia provokes Ca^{2+}, PIP2 and calpain responses prior to delayed neuronal death in monkeys. Eur J Neurosci 8:1932-1944.

Yamazaki H, Chan J, Ikura M, Michikawa T, Mikoshiba K (2010) Tyr-167/Trp-168 in type 1/3 inositol 1,4,5-trisphosphate receptor mediates functional coupling between ligand binding and channel opening. J Biol Chem 285:36081-36091.

Yokota M, Tani E, Tsubuki S, Yamaura I, Nakagaki I, Hori S, Saido TC (1999) Calpain inhibitor entrapped in liposome rescues ischemic neuronal damage. Brain Res 819:8-14.

Yoshikawa F, Iwasaki H, Michikawa T, Furuichi T, Mikoshiba K (1999) Trypsinized cerebellar inositol 1,4,5-trisphosphate receptor. Structural and functional coupling of cleaved ligand binding and channel domains. J Biol Chem 274:316-327.

Young LT, Kish SJ, Li PP, Warsh JJ (1988) Decreased brain [^{3}H]inositol 1,4,5-trisphosphate binding in Alzheimer's disease. Neurosci Lett 94:198-202.

Zaidan E, Sims NR (1994) The calcium content of mitochondria from brain subregions following short-term forebrain ischemia and recirculation in the rat. J Neurochem 63:1812-1819.

Zhang C, Siman R, Xu YA, Mills AM, Frederick JR, Neumar RW (2002) Comparison of calpain and caspase activities in the adult rat brain after transient forebrain ischemia. Neurobiol Dis 10:289-205.

Zhang L, Hsu JC, Takagi N, Gurd JW, Wallace MC, Eubanks JH (1997) Transient global ischemia alters NMDA receptor expression in rat hippocampus: correlation with decreased immunoreactive protein levels of the NR2A/2B subunits, and an altered NMDA receptor functionality. J Neurochem 69:1983-1994.

Zhao X, Lein ES, He A, Smith SC, Aston C, Gage FH (2001) Transcriptional profiling reveals strict boundaries between hippocampal subregions. J Comp Neurol 441:187-196.

Zhivotovsky B, Orrenius S (2011) Calcium and cell death mechanisms: a perspective from the cell death community. Cell Calcium 50:211-221.

Zhu DM, Uckun FM (2000) Calpain inhibitor II induces caspase-dependent apoptosis in human acute lymphoblastic leukemia and non-Hodgkin's lymphoma cells as well as some solid tumor cells. Clin Cancer Res 6:2456-2463.

Zipp F, Aktas O (2006) The brain as a target of inflammation: common pathways link inflammatory and neurodegenerative diseases. Trends Neurosci 29:518-527.